INVESTIGATION OF STABILIZED BEREA RED SOIL WITH EMPHASIS ON TENSILE AND CYCLIC TRIAXIAL TESTS

RUSSELL ADRIAN CLAYTON

A THESIS SUBMITTED AS PARTIAL FULFILLMENT OF THE COURSE REQUIREMENTS FOR THE MASTERS DEGREE OF SCIENCE.

CAPE TOWN 1989

ABSTRACT

This dissertation investigates the soil mechanical properties of a sample of Berea Red soil and the most suitable methods of treatment to improve it. Special attention has been paid to lime stabilization and different curing techniques.

Gradings, special indicators and California Bearing Ratios were determined on both natural and lime stabilized Berea Red soil. Consolidometer tests were performed on natural and lime or cement stabilized soil at various densities to establish the compressibility and collapse potential.

A computer controlled Indirect Tensile Testing apparatus with data logging facilities was developed in order that some of the soil mechanical properties of Berea Red soil may be determined.

Natural and stabilized Berea Red soil was tested in a monotonic and cyclic triaxial apparatus to determine the short and long stress strain characteristics.

A correlation between soil mechanical properties of a soil derived from indirect tensile and monotonic and cyclic triaxial tests was investigated in order that a simpler test method may be used to determine Youngs modulus and Poisson's ratio.

DECLARATION

I declare that this dissertation is my own, unaided work. It is being submitted for the degree of Master of Science in the University of Cape Town, Cape Town. It has not been submitted before for any degree or examination in any other University.

Signed by candidate

29..day of September 1989.

ACKNOWLEDGEMENTS

The author wishes to express his thanks to

Dr F Scheele, Senior Lecturer and supervisor
for his assistance and encouragement that he offered during the course of this research.

Prof. J B Martin:
for the opportunity he afforded me to undertake and complete a post-graduate degree.

Mr A Burgers:
for his wealth of information, encouragement and understanding.

Mr D F Wright and the Directors of Ninham Shand (Cape) Inc:
for the provision of up-to-date test equipment and financial assistance that was made available.

The Directors of the Council for Scientific and Industrial Research:
for the generous post-graduate bursary that was granted for the two years of study.

Family and friends (especially my mother, father and wife, Maeve):
for their help, understanding and tolerance during the frustrating moments.

The author is very appreciative for the encouragement, advice and criticism given by the above without whom this research would not have been possible.

TABLE OF CONTENTS

LIST OF FIGURES

LIST OF TABLES

1. INTRODUCTION

A road pavement is built to carry a design capacity of traffic safely and efficiently with minimum delays or inconvenience.

The highest traffic capacity that a roadway can accomodate is influenced by many factors, most of which can be allowed for during the design stages.

Quality of the ride which is a function of the quality of the pavement is a major design aim. However, with time and use, pavements deteriorate due to many reasons, one being rutting. Rutting is best described as a permanent depression of the pavement in the wheel path. Rutting of the wheel paths of a pavement is one of the major causes of reduced service life and is cause for much concern to transportation engineers in most countries.

One of the most severe consequences of pavement rutting is that water will remain in puddles on the roadway, resulting in the loss of vehicle control due to excess water between the tyres of the vehicle and the pavement. This phenomena is called hyrdoplaning.

Rutting of the wheel paths is due to densification and settlement of one or more of the underlying pavement layers as a result of repeated wheel loadings, especially the heavier loads of the multiaxle and multiwheel vehicles.

Vibrations due to traffic and excessive wheel load stresses are transmitted through the pavement layers, into the underlying layers resulting in the material being overstressed.

Failure of the pavement can be identified as excessive deformation and rutting. In most pavement design procedures protection of the subgrade from excessive stress caused by traffic loading is a major consideration. If the mechanical properties of each layer can be determined with confidence, then it is a relatively easy procedure to design adequate layer thicknesses to prevent the weaker underlying subgrade layer from being overstressed, which results in poor performance of the layer.

The cyclically loaded soil mechanical properties of a pavement layer play an important role in the successful design of a pavement. Excessive deflection due to a highly resilient underlying layer could easily cause the cemented upper layers to crack, resulting in failure of the water-proofing layer and total failure of the entire pavement structure with time. To adequately understand the stress-strain characteristics of a material it is required that the resilient modulus and permanent strain be evaluated whilst the pavement material is undergoing cyclic loading and unloading in both the field and the laboratory. With the successful determination of the material properties one can apply computer aided structural analyses.

Structural analyses procedures of pavements as layered systems are becoming increasingly a part of a regular design practice. This is largely due to the efficiency with which such analyses can be done by readily available computer programmes and the ease of interpreting the results.

There has been good correlation with the results of these analyses which have been directly related to observed field performance and also using heavy vehicle simulators for simulated field performance on existing pavements. The material properties needed for these structural analyses must come from laboratory and field measurements and tests requiring great accuracy and care to obtain

meaningful and reliable results. Computers can assist in the data-logging, operational control and the testing of soil specimens.

Materials testing technology in the pavement field has, for good reason, been largely built on an empirical and comparative basis, using index type tests. Such index testing is useful for comparison of the same types of materials, but is often inadequate for comparison between different material types, especially when modified or non-standard materials are considered. In addition, they do not provide material properties needed for a reliable structural analysis.

These mechanical properties may be evaluated in a number of different ways, both in the field, and in the laboratory. Since field testing for road pavements is time consuming, usually very expensive and not always practical, laboratory methods have gained considerable popularity. However, even though a specific property is being tested for, different types of tests can give widely different results. Similarly, the pavement response can vary widely, depending on the test results used.

The reliability of a test method is best determined by the repeatability of the test result for an essentially identical specimen. Attempts have been made to use empirical tests to estimate mechanical properties using indicator tests such as California Bearing Ratio (CBR), and Unconfined Compression Strength tests (UCS) to evaluate elastic moduli and tensile strengths of the material in order that soil mechanical properties may be simply determined. These correlation attempts are avoided by most engineers as they are usually only very approximate, and apply to one type of material.

Over the years, a wide variety of laboratory and field tests have been developed to evaluate the mechanical characteristics of a soil. Many of the tests have been considered unsuitable, but some tests have remained in use for over 60 years, for example the CBR test.

The laboratory tests of interest for the structural design of pavements are:

(a) Triaxial (Static and Cyclic)

(b) Indirect Tensile (Static and Cyclic)

(c) One dimensional consolidation testing.

With reference to modern day needs of pavements, it has become obvious that scientific testing procedures should be investigated and developed, which are lacking in commercial soils laboratories in South Africa.

With the obvious lack of facilities for materials characterization, a decision was made to develop and improve locally available test equipment, which included cyclic indirect tensile strength and cyclic triaxial test apparatus, to be able to characterise materials that did not comply to normal road material requirements.

In the Province of Natal in South Africa a material which is in great abundance in the coastal zone commonly known as Berea Red soil exists. This fine grained silty-clayey sand has been used with considerable success in low volume secondary roads in rural areas where traffic loads are not considered exceptionally high.

Financial implications of importing suitable materials for high load-bearing primary and major roads has been the major factor that has influenced an investigation into determining a suitable means of modifing or stabilizing Berea Red soil in order that it may be used as a suitable subbase or selected subgrade. With the above requirement an investigation was initiated to characterize the soil mechanical properties of a typical Berea Red soil, which, if treated correctly, could produce a reliable and economic substitute.

2. RESEARCH OBJECTIVES AND WORK PROGRAM

This research work was initiated by the Department of Transport to investigate the feasability of using Berea Red soil as a selected subgrade or as a stabilized subbase in a road pavement design.

The question of implementing a "non standard" fine grained pavement material such as Berea Red soil in a road structure raises a variety of issues to be addressed. Some of which would be considered in this research.

Road pavement design incorporates the identification of the physical properties and the characterization of the mechanical behaviour of the material. In order that adequate pavement layer depths may be determined an analysis of the stresses and deformations are needed. The complexity of road pavement design, considering the material in question, along with the aspects of construction, maintenance and rehabilitation as a function of the long-term performance could be considered.

To limit the wide-spanned field of topics needed in this study, it was decided to concentrate on the investigation of the soil mechanical properties of Berea Red soil and of its characteristics under static and cyclic loading in the light of its possible use as a pavement material. Particular emphasis will be placed on laboratory tests, and innovative testing techniques wherever required.

A literature review in geotechnical applications on Berea Red soil with emphasis on road pavements will be necessary to set out the research program.

As chemical stabilization would play an important role in the characterization of treated Berea Red soil, an in-depth study would be necessary on the behaviour and effects of various pozzolanic stabilisers. Three soil stabilizing agents were envisaged, namely cement, lime and lime-slagment at various percentages of the dry mass of the material.

An attempt to correlate the soil mechanical properties to the empirical and mechanistic design procedures derived from traditional road pavement laboratory tests would be investigated.

Road pavement materials experience tensile stresses during normal operational use. It is therefore important that the tensile properties of stabilized Berea Red soil be investigated.

An Indirect Tensile Strength (ITS) test apparatus, only available at specialized research centres, would have to be developed.

Based on the relatively straight forward ITS tests one could expect to establish a bench-mark with respect to material qualities.

Advanced testing, namely standard (static) and cyclic triaxial tests would follow, to determine the stress strain relationships of Berea Red soil, both in its natural and treated form.

Representative traffic loading may be realistically simulated in a cyclic triaxial test apparatus. Resilient properties and permanent strain predictions of the material can be derived from the test data. It is envisaged to carry out the tests in a fully automated (personal computer controlled) standard and cyclic triaxial apparatus incorporating the Bishop-Wesley stress path cell.

A simple elastic analysis of a road pavement cross-section would be undertaken to establish a stress pattern in the structure providing guidance for the applied stresses in the triaxial cell.

Since the general procedures for cyclic triaxial testing are not applicable for problematical materials, a literature review will be required with the aim of establishing the best possible testing approach.

On the basis of the above findings a test program would be drawn up which is presented in Table 1.

A comparison of material properties determined from traditional road pavement tests, material properties from ITS tests, standard and cyclic triaxial tests would be made to establish if any relationship exists between the various test techniques.

It was with the above research objectives in mind that the investigation of stabilized Berea Red soil was undertaken with the added hope that the work program would cover all aspects sufficiently to be able to address the question with confidence, give guidance for further work and thus provide a procedure for similar investigations.

WORK PROGRAM OF TESTS PERFORMED ON BEREA RED SOIL DURING THE INVESTIGATION

TEST DESCRIPTION	REFERENCE PROCEDURE	MATERIAL TREATMENT (and days curing)									
		NATURAL MATERIAL	2% LIME(3)	4% LIME	6% LIME	8% LIME	2% LIME-SLAG	4% LIME-SLAG	2% CEMENT	4% CEMENT	6% CEMENT
Grading & Indicators	TMH1(56)	-	-	-	-	-	-	-	-	-	
Moisture Density Relationships	TMH1(56)	-	-	-	-	-	-	-	-	-	
California Bearing Ratio	*(1) TMH1 (56)	-	3, 7, 28 days curing	3, 7, 28 days curing	-	-	-	-	-	-	
Consolidation Tests	*(2) HEAD(83)	3 @ 90, 95, 100% mod(1,2) 2 collapse potential	1 @ 10 days 2 @ 18 days	2 @ 10 days 1 @ 18 days	-	-	-	-	-	-	
Unconfined Compression Tests	TMH1(56)	-	2 @ 7, 28, 90 days & RC(4)	2 @ 7, 28, 90 days & RC	-	2 @ 7,28, 90 days & RC	2 @ 7,28, 90 days & RC	2 @ 7,28, 90 days & RC	2 @ 7,28, 90 days & RC	2 @ 7,28, 90 days & RC	-
Indirect Tensile Strength	many authors	4 @ 99% mod 4 @ 100% mod	4 @ 7 days 4 @ 28 days	4 @ 7 days 4 @ 28 days	4 @ 28 days	4 @ 28 days	-	-	4 @ 28 days	4 @ 28 days	4 @ 28 days
Direct Shear Tests	HEAD(83)	3 Points	-	-	-	-	-	-	-	-	-
Saturated Consolidated Undrained Triaxial Tests	HEAD(67)	3 cells @ 95% mod 3 cells @ 100% mod	3 Cells	3 Cells	-	-	-	-	-	-	-
Saturated Consolidated Undrained Cyclic Triaxial Tests (No. of cycles)	many authors	1 @ (2500)	1 @ 28 days (5000) 1 @ 170 days (5000)	1 @ 28 days 1 (5000)	-	-	-	-	1 @ 28 days (5000)	1 @ 28 days 1 (5000)	-
Partially Saturated Undrained Cyclic Triaxial Tests (No. of cycles)		1 @ (3000)	1 @ 28 days (3000)	1 @ 28 days 1 (3000)	-	-	-	-	-	-	-
Saturated Consolidated Drained Cyclic Triaxial Tests (No. of cycles)		1 @ (2500)	1 @ 28 days 1 @ 120 days (17000) 1 @ RC (8000)	1 @ 28 days 1 @ RC (8000)	-	-	-	-	-	-	-

(1) unless otherwise stated, specimens were moulded @ 100% mod
(2) % mod is an abbreviation for % mod AASHTO density
(3) % additive by dry mass

3. REPORTED AND OBSERVED SOIL PROPERTIES OF BEREA RED SOIL

3.1 Origin and Distribution of Berea Formations

Berea formations are found along most of the present coastline and inland of the sea. They can be placed in general sequence of increasing geological age away from the coast and on the basis of colouring and pedogenism (Webb(61)).

The Berea formation occurs as a narrow belt along almost the entire coast of Natal and sporadically along the Transkei coast to the north of East London. The properties of the material vary laterally and vertically in relation to clay content, moisture content, and colour.

Berea Red soils attracted interest from a geotechnical point of view since it is was identified as a collapsible material in its in situ undisturbed state (Schwartz(81)).

A collapsible soil can be described as a material which can withstand a considerably high stress level in its dry state, but experiences large volume decreases if the moisture content is increased or is subjected to excessive vibrations, as in a pavement subgrade. These changes in behaviour can be attributed to a radical rearrangement of particles within the matrix or the breaking of colloidial or other bonds due to particle coating.

Collapsing soils are geologically young and are formed by either aeolian, colluvial or alluvial deposition. A collapsible soil is generally described as an open textured silty sandy soil with a high void ratio which has undergone chemical weathering to produce an intensively leached residual soil.

Brink(80) reports that distribution of the Berea Red soil does not occur below the 8,5m mean sea level, unless it was redistributed during Pleistocene times. The formations of the aeolianite, of which the Berea Red soil is a weathering product, are soft and porous. It has been decalcified and weathered almost completely, and is found nearly 100 metres thick in places. Samples taken from deep borings frequently indicate a white or yellowish coloured zone near the basal boulder bed, where concentrations of ground water have caused more intensive leaching and reduction of ferruginous material. In some areas intense tropical weathering has brought about the formation of silicious sand zones probably as a result of perched water tables due to underlying clay.

Although termed a sand, the Berea Red soil has been reported by Brink(80) to contain appreciable amounts of clay. As these sands were transported by wind one would expect the grain size to be single sized. The clay is a product of in situ weathering of the feldspars. The clay minerals are mainly kaolinite with some illite and geothite, and a hydrated red oxide whose colour may vary from yellow to brown red to black, mainly due to ferrous oxide coating of the quatz grains.

Boniface et al(79) reported that a variation in colour and clay content were found while profiling, along with isolated boulders and zones of irregular shaped masses of leached calcerous sandstone. Occasional layers of soft sand with scattered calcareous nodules were observed.

Podsolic formations have been reported in some locations as evaporation exceeds the annual precipitation of 750 to 1000mm.

3.2 Reported Soil Mechanical properties of Berea Red Soil

3.2.1 Grading and Index Tests

Wide variations of the soil can be encountered on one single site. This is reflected by the variations with depth of the natural water content P.I. and percentage material finer than 0.075 mm as reported by Webb & Hall(61) and Boniface et al(79).

In many similar texts which authors have published on Berea Red soils, they have paid special attention to its in situ and undisturbed properties, of which its load bearing behaviour of foundations was of most interest.

Berea Red soil moulded and compacted to 100 percent mod AASHTO dry density and used as a pavement material has not been well documented in the literature.

Boniface et al(79) performed many in situ and undisturbed tests on Berea Red soil during the exploratory and construction phases of the Glenwood Tunnel in Natal which were sampled in both horizontal and vertical borings. The results of the above exploratory test programme revealed clay contents of up to 30% with little or no plasticity, and with an average relative density of 2.67. The in situ bulk and dry densities were reported to increase with depth (z) and for design purposes $1450+6(z)kg/m^3$ for dry density and $1810+4.5(z)kg/m^3$ for bulk density was used for ranges of z from 0 to 60m. The corresponding void ratios e ranged from 0.9 to 0.4. In situ moisture contents were reported to be between 17% and 23% with corresponding degrees of saturation of 75% - 87%.

Undisturbed Elastic Moduli E were determined using five varying techniques, namely triaxial, consolidation, pressuremeter, standard penetration and Terzaghi's empirical formula. The range of moduli values ranged from 18 to 40 MPa from cored samples. No mention was made whether the increase in modulus was due to increased confining stress.

Webb and Hall's(61) discussion of recorded properties reveals similar values, but they reclassified Berea Red soil into two categories, based on the percentage clay content (<0,002 mm) below 5% and above 30% (see Table 3.1).

Table 3.1 - REPORTED INDEX PROPERTIES OF BEREA RED SOIL

Clay content	2 - 40%	< 0,002 mm
Liquid Limit	0 - 40% and shown to be more	
Plasticity Index	0 - 20%	

With a clay content <5%
In situ bulk density 1600 - 1750 kg/m³ (undrained conditions) $\phi' = 30° - 33°; c' = 0$ kPa mod AASHTO dry density 1790 - 2010 kg/m³ at w_{opt} = 11,2% to 13,2%

With a clay content >30%
In situ bulk density = 1550 - 1700 kg/m³ $\phi' = 27° - 30°; c' = 10 - 15$ kPa

3.2.2 Triaxial testing of Berea Red soil

To the writer's knowledge no triaxial testing of Berea Red soil at 100% mod AASHTO density has been published. The only reported consolidated undrained triaxial tests performed on Berea Red soil were by Boniface and Olivier(79).

The undisturbed samples were obtained and tested from the Glenwood Tunnel, Durban, while construction was in progress. The stress strain curves were reported to lack uniformity, due to possible disturbance. Young's Modulus values obtained from the above tests ranged from 10 to 52 MPa with an average effective angle of shear resistance of 34^{o}.

3.2.3 Stabilization and California Bearing Ratio Response

The only reports of Berea Red soils stabilized with lime and CBR's determined were by Webb and Hall(61) in which they reported that clayey sands respond well to stabilization with lime at 4% by mass. The CBR value of 95% mod AASHTO density increases from 5% to 95% and drying was often required to obtain optimum moisture content.

The Natal Roads Department confirmed the above data collected from road construction sites in which Berea Red soil was stabilized with lime and used successfully as a pavement on low volume roads.

3.2.4 Stability of Berea Red soil

Berea Red soils are particularly prone to erosional effects. Both the clay and the water content effects its shear strength. As previously mentioned the natural moisture content of most Berea Red soils are rarely below optimum and its use as a subbase material may necessitate expensive drying out operations. Maximum compacted densities increase markably with reduced water content.

Moisture induced cohesion is often present in highly clayey materials and could provide temporary stability to steep cut slopes.

The permeability of Berea Red soil is high and it is seldom saturated under natural conditions, unless underlain by a low permeability material.

SPT N values range from loose to very dense. Both shear strength and coefficient of compressibility are sensitive to changes in moisture content.

Excessive settlement in the sands and clayey sands of the formation, in the generally loose, soft and highly compressible superficial horizons, have been recorded.

A bearing pressure of 200 kPa can normally safely be applied at a depth of 2.5 - 3 m below ground level. Two major high rise buildings on the Berea formation in Durban were founded on recompacted material 2-5 m thick and showed maximum settlement of 13 mm.

In less clayey zones of Berea Red soils, vibroflotation has been successfully used as an alternative to piling. Even with clay contents of up to 30%, vibroflotation was used along with crushed stone backfill to improve the material. The amount of compaction achieved was checked using a cone penetrometer. Settlements estimated from these were found to be twice those actually encountered.

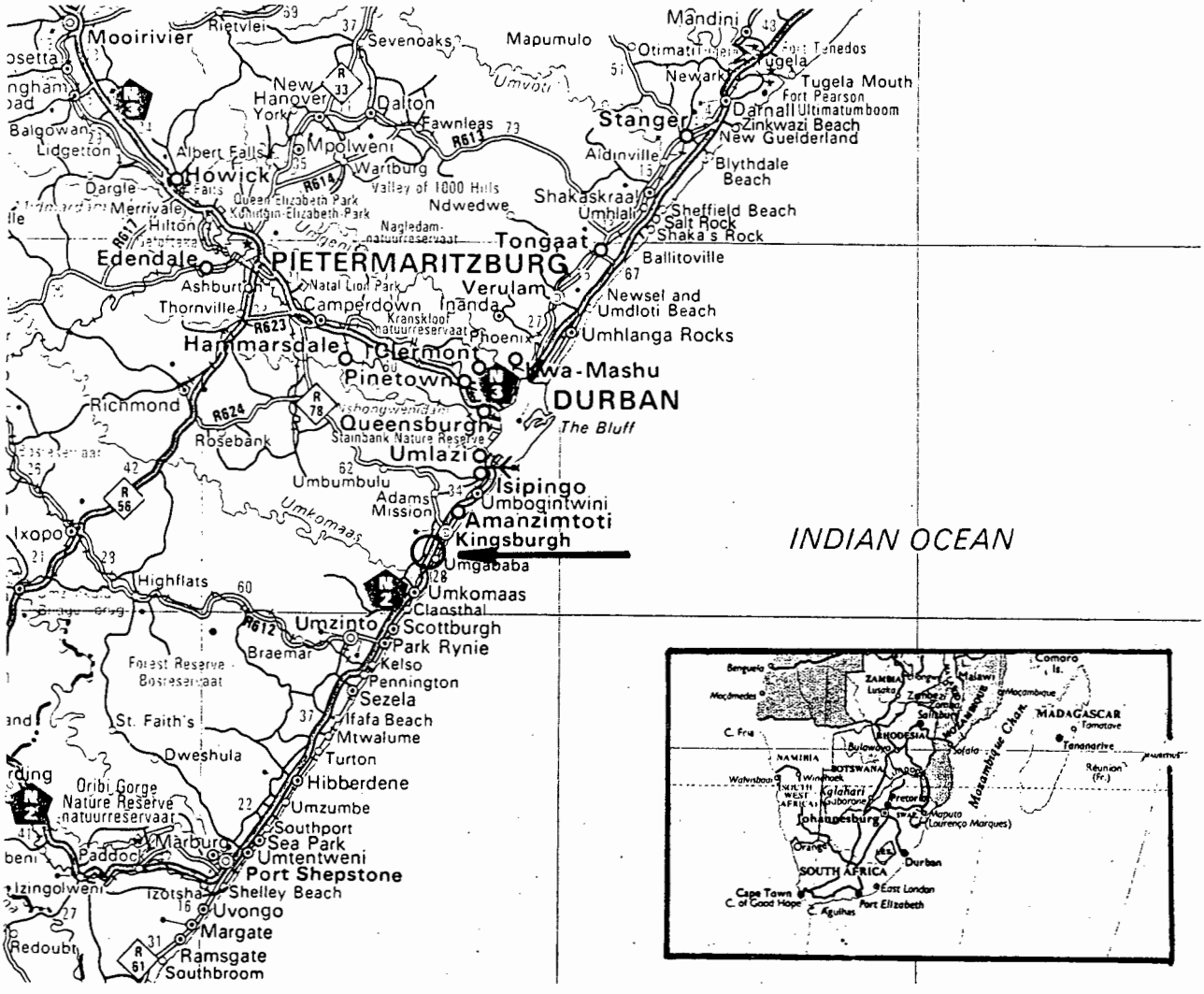

Fig. 3.1 Site Location of sampled Berea Red soil.

3.3 Range of Soil Mechanical Properties of Test Material Determined from Natural Remoulded Berea Red Soil

To determine the range of soil mechanical properties of the naturally occurring Berea Red soil the following results of laboratory indicator tests are presented.

3.3.1 Natural Berea Red soil properties

The Berea Red soil used for characterization was sampled from a fresh cut face on a section of the National Route N2 which was under construction in 1986. Sampling was carried out at various points along the cut face between a depth of approximately 2 to 6 metres below the original ground level. These samples were then mixed together to form one large sample which was air dried and placed in canvas bags for transportation by rail. Fig.3.1 shows the location of the site with respect to Southern Africa.

The results of the experiments performed on the natural Berea Red soil are covered in this chapter, and the stabilized Berea Red soil is covered in the following chapter.

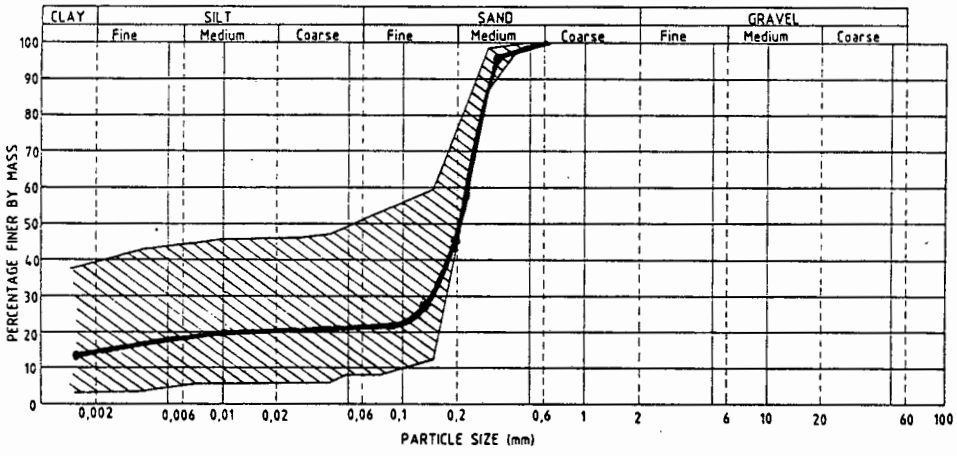

Fig. 3.2 Grading of natural Berea Red soil sample within the range of the Berea Red soil grading

3.3.2 Soil classification

Grading of the natural material shows that all particles pass the 1,18mm sieve and are classed as a poorly graded sand clay-silt. The grading curve of naturally occurring Berea Red soil fits well within the grading envelope presented by Webb(80) (See Fig.3.2). Examination of the grading envelope shows two significant features compatible with the soil formation processes:

(1) The material consists of a mixture of fine sand and clay, the intermediate range of silt size particles being negligible, which indicates a likelihood of structural instability.

(2) The clay content of Berea Red soil is reported to vary from 5% to 40% and was found to be 15% in the samples used.

Particle size analysis discloses very little about the engineering properties of fine grained soils in which a percentage of clay is present. These physical limits are known as the Atterberg limits and are shown in Table 3.2.

Table 3.2 Atterberg Limits of Berea Red soil

Liquid Limit	= 20%
Plastic Limit	= 13%
Plasticity Index	= 7%
Linear Shrinkage	= 2,0%

These values were considered rather low, as the grading curve reveals a moderate percentage of material passing the 0,075mm sieve.

Therefore "modified" Atterberg limits tests were performed using material that passed the 0,075mm sieve. The apparent values were:

Table 3.3 Modified Atterberg Limits of Berea Red soil

Liquid Limit	= 63%
Plastic Limit	= 23%
Plasticity Index	= 40%
Linear Shrinkage	= 16,0%

From the above test data it can be concluded that the mechanical behaviour of the clay fractions is masked by the sand size particles present in the soil matrix.

The activity of the soil fraction is given by

$$\frac{\text{Plastic Index}}{\text{\% by weight finer than 0,002mm}}$$

for the Berea Red soil sample tested, the activity was determined to be 0,50, which falls between the activities of illite and kaolinite as derived by Skempton(19) shown in Fig. 3.3.

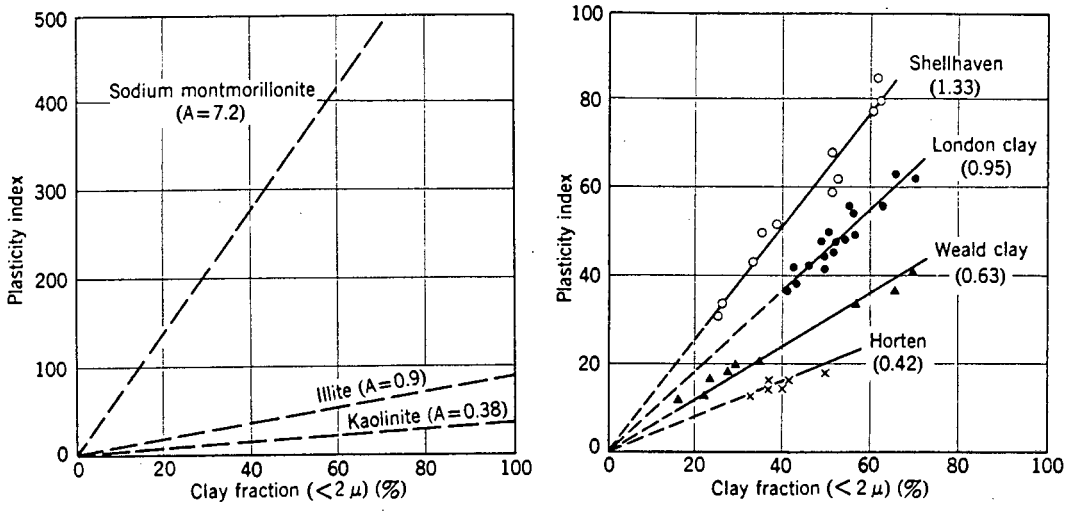

Fig.3.3 Relationship between plasticity index and clay fraction (Lambe and Whitman(68)).

which agrees well with Webb and Hall's(61) findings that the clay minerals are mainly kaolinite, illite, and geothite. A differential thermal analysis (DTA) to determine the mineral content of the Berea Red soil samples was not undertaken.

3.4 Maximum dry density and optimum moisture content

Maximum compaction is measured as the maximum dry density for a certain compactive energy applied. The modified AASHTO density determined was 1960kg/m^3 at an optimum moisture content of 10,4%, which falls within Wilson(80) and Webb and Hall's(61) findings of 1700-2025kg/m^3. The void ratio (e) was 0,36 and a degree of saturation (S_r) of 77% based on a relative density of 2.68 were the relative density is understood to be the ratio of the mass in a given volume of a material at a stated temperature to the mass in air of an equal volume of distilled water at the same temperature. As the degree of saturation was above Errera's(73) threshold value of S_r=69%, collapse behaviour was not expected in the soil.

3.5 Consolidation Properties

The consolidation and collapse behaviour of Berea Red soil was investigated by performing a series of consolidation tests based on the following facts:

1. If Berea Red soil was used as a fill material, it would not be known what the settlement potential was after compaction and additional overburden load had been applied.

2. Undisturbed in situ Berea Red soil possesses a collapse potential, and could be hazardous to road pavements.

3.5.1 Collapse phenomenon

Berea Red soil is classified as a "collapsible material". Collapsible soils can withstand relatively large imposed vertical stresses at low moisture contents. However, upon wetting, the material exhibits a decrease in volume and settlement (which sometimes can be quite large), with no additional increase in applied stress. This decrease in volume leads to a collapse of the soil structure.

Typically, the compression curves of a soil with a collapsible fabric, having different moisture contents, are quite different. It implies that the lower the in situ moisture content, the higher the bearing capacity, and lower the compressibility.

Alternatively, if the moisture content is increased the bearing capacity decreases.

Errera(73) reported that Berea Red soils with 25% fines less than 0,075 mm diameter should not experience collapse potential problems if the degree of saturation exceeds 69%. Jennings and Knight(74) identified a procedure to determine a collapse potential of a doubtful soil by defining the collapse potential $\%CP = \Delta e/(1+e_o)*100$ where e_o was the initial void ratio of the sample at the beginning of the oedometer test and Δe was the change in void ratio when the unsoaked soil was loaded to 200 kPa and then soaked.

Research work has shown that in South Africa a collapsible in situ soil has to be subjected to a pressure greater than the overburden pressure before collapse will occur. This was described by Jennings & Knight(74) as the stable soil surface condition.

Collapse will only occur if there is an increase in moisture content, as the bridging colloidal material undergoes a loss of strength, and the soil grains are forced into a denser state of packing which is equivalent to a reduction of void volume.

3.5.2 Collapsible soils in road construction

It is apparent that a collapsible material is not suitable as an in situ subgrade material for road construction. Knight and Dehlen(75) reported that collapse settlement extended to a depth of about two metres on the Witbank-Springs road in the Transvaal. It was observed that, on certain sections of the road, there were settlements of up to 150mm due to the collapse of the subgrade material.

Investigation has shown that densification can reduce the potential for collapse. Jennings & Knight(74) indicate that the depth to which densification is necessary has not been successfully established.

It has been recommended Knight et al(75) that if collapsing soils are present, the road bed below the subbase should be compacted so as to achieve 90% mod AASHTO density from 0 to 0,5 metres and 85% mod AASHTO density from 0,5 to 1,0 metres. These recommendations appear to apply to roads with very heavy traffic loads. Van Alphen(78) indicated that even under light traffic, collapse could occur to a depth of 700 mm. Application of a high compactive effort to the subgrade should alleviate the collapsible nature of the soil.

3.5.3 Consolidometer testing

Standard consolidation testing was performed according to the procedure outlined by Head(83). Collapse potential testing was performed according to the procedure outlined by Schwartz(81).

3.5.4 Consolidation test results

To evaluate and characterize the compressibility and consolidation of Berea Red soil, a series of specimens with densities ranging from 90% to 100% mod AASHTO were investigated. Fig.3.4 shows the effect of density on the log pressure versus void ratio curve.

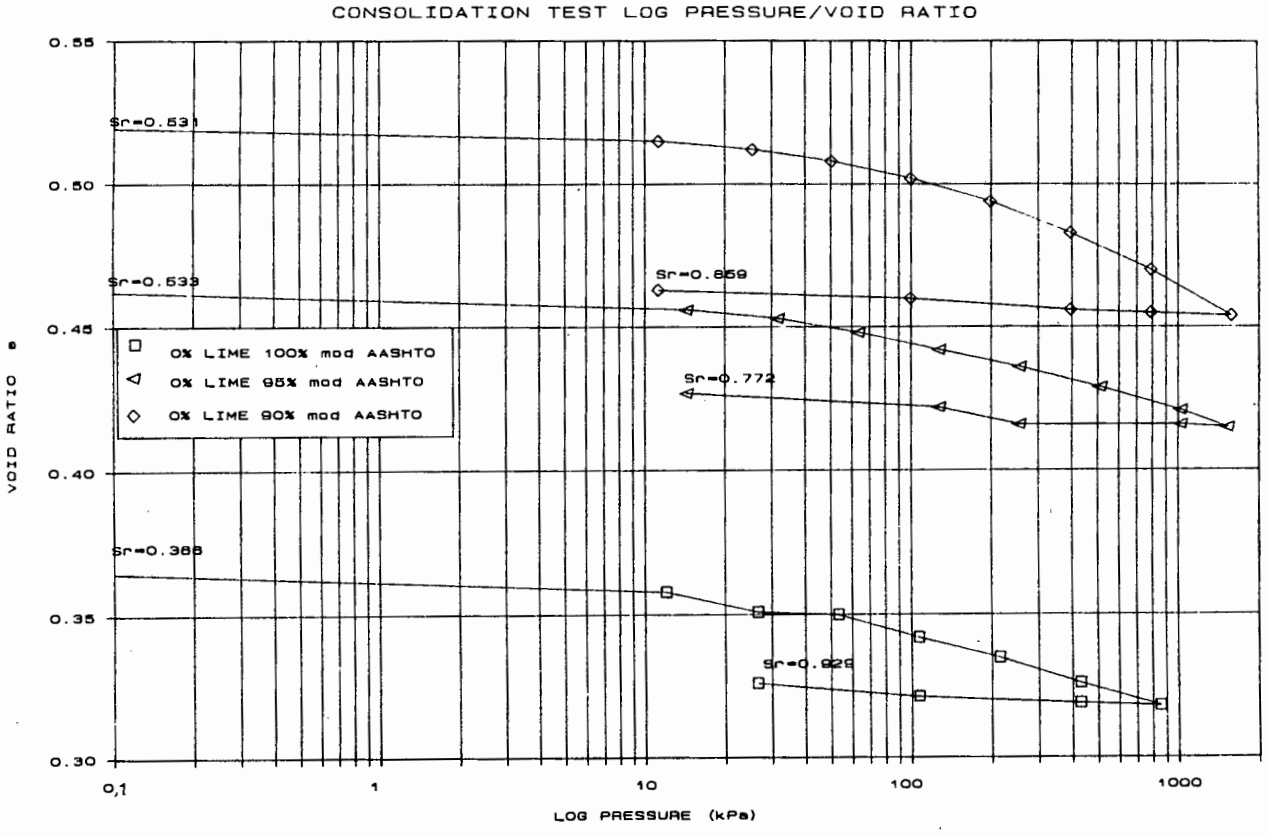

Fig. 3.4 Log Pressure versus void ratio of natural Berea Red soil.

To characterize the above relationship the compression index C_c is used. Table 3.4 indicates the ranges of C_c for natural recompacted Berea Red soil. The void ratio at any pressure greater than the existing pressure (P_c) can be expressed as

$$e = e_o - C_c \log ((P_c + \Delta P)/P_c)$$

where e_o is the initial void ratio, ΔP is the increase in pressure and P_c is the effective preconsolidation pressure.

TABLE 3.4 CONSOLIDATION PROPERTIES OF NATURAL RECOMPACTED BEREA RED SOIL TESTED IN OEDOMETRES

% Mod AASHTO density	w(%)	Dry Density	e_o	P_c (kPa)	C_c
99,6	10,2	1962	0,366	14	0,025
97,8	10,2	1927	0,390	16	0,027
98,4	10,3	1938	0,383	12	0,021
100,3	11,4	1976	0,356	4	0,025
93,0	9,2	1832	0,463	21	0,025
93,9	9,5	1849	0,449	1	0,024
89,5	10,3	1763	0,520	52	0,042
89,7	9,7	1768	0,516	35	0,037

%w = moisture content.
Max Dry Density 1970 kg/m^3

3.5.5 Collapse settlement of Berea Red soil

The collapse potential properties of natural Berea Red soil recompacted to 90% and 95% mod AASHTO are presented in this section. The log pressure versus void ratio curves show that remoulded natural Berea Red soils display no collapse potential when in a saturated state. However, soil compacted to 90% or 95% mod. AASHTO loaded to 214 kPa or 390kPa, respectively while partially saturated and then saturated, show a small percentage of collapse potential. The applied stresses are typical stresses experienced in the pavement layer at these densities as shown by Schwartz(81) Fig.3.5 is a summary of the two collapse tests performed according to the procedure described by Jennings & Knight(74).

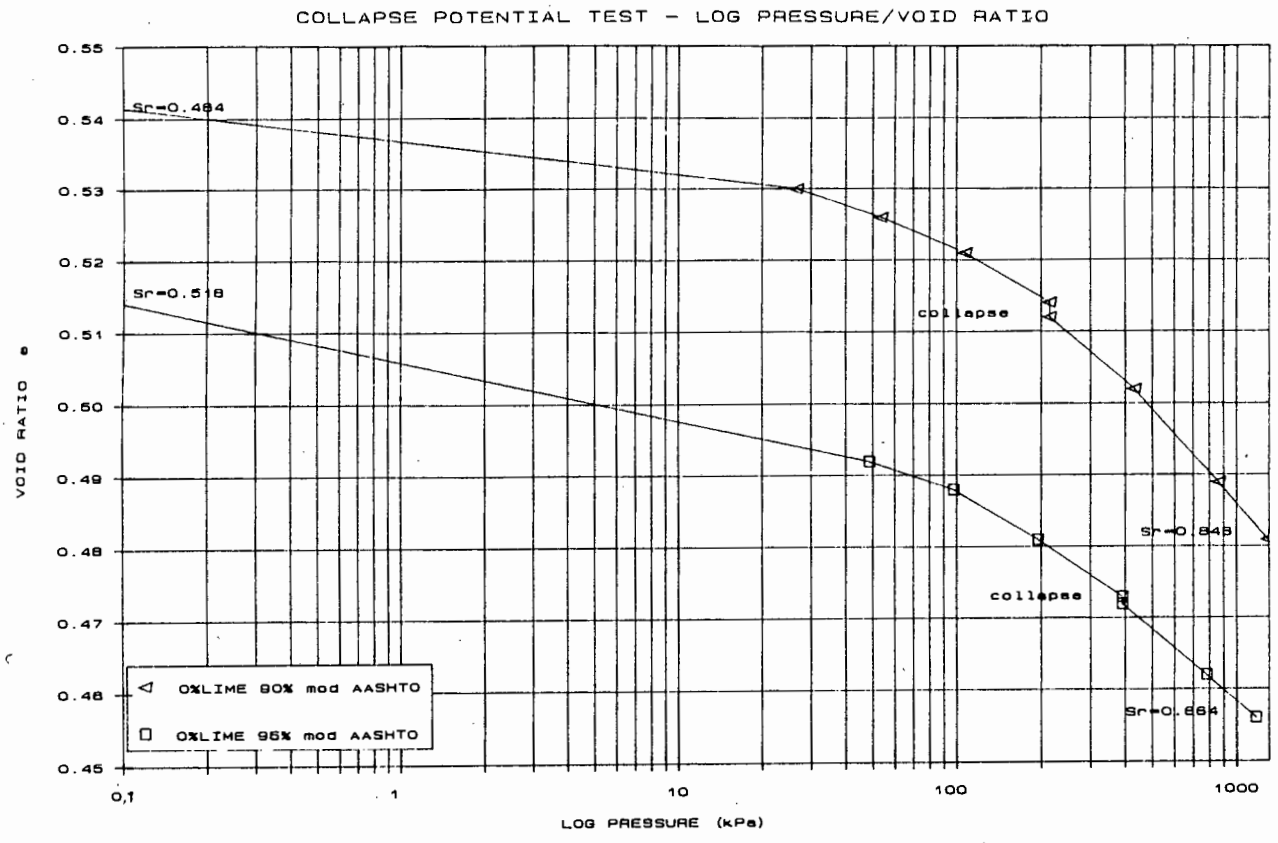

Fig. 3.5 Log pressure versus void ratio illustrating the collapse potential of natural Berea Red soil.

The % collapse potential based on the equation Schwartz(81)

$$CP[\%] = \Delta e/(1+e_o) * 100$$

was found to be 0,37% and 0,19% for material moulded at 90% and 95% of mod AASHTO density, respectively, at OMC

Jennings & Knight(74) report that a collapsible potential between 0% and 1% presents no problem with respect to the foundations of a structure.

3.5.6 Interpretation of the collapse potential of Berea Red soil

Schwartz(81) expressed concern about the manner in which the Jennings & Knight's collapse potential was being interpreted by some engineers.

The trend has been to test a sample at a moisture content W_1 and to produce a plot of log pressure versus void ratio that shows a change in volume on soaking, indicating collapse potential. The same soil has also been tested at a higher moisture content and loaded up to 200kPa and soaked, only to find the wetter sample shows no collapse potential as normal consolidation has taken place (see Fig. 3.6).

If a road or structure were built on a soil, say with a moisture content of W_1, very little compression may take place. However, if wetting took place severe distress could occur due to collapse. Any road or structure founded on the soil at a higher moisture content W_2 could be subjected to severe distress due to normal consolidation, but not collapse.

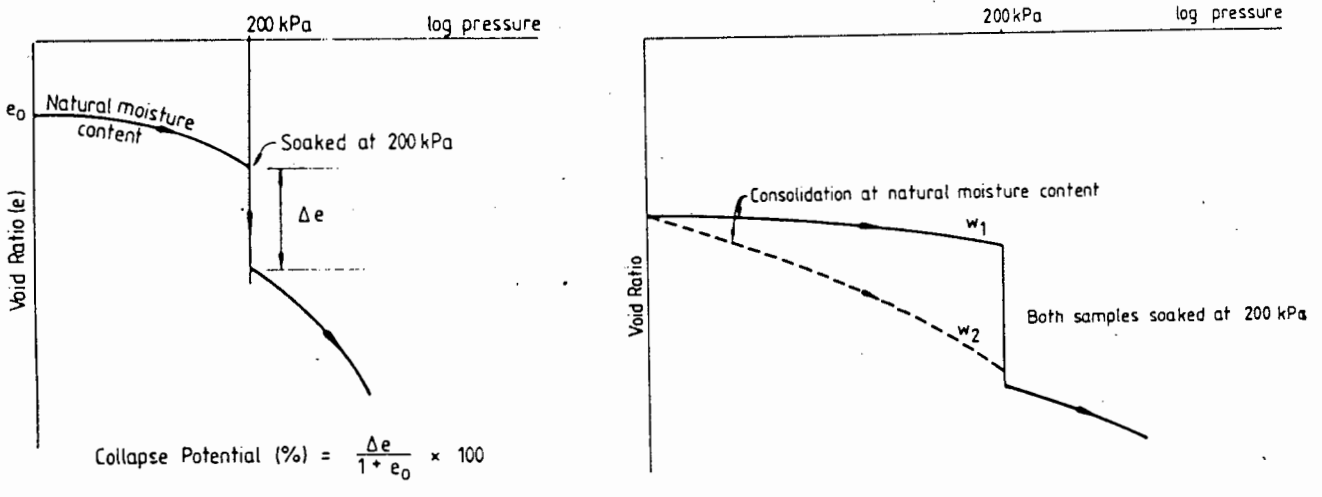

Fig. 3.6 Illustration of problems associated with the interpretation of the collapse potential test. Schwartz(81)

It was envisaged that the above situation would not occur in road pavements, as the OMC of Berea Red soil is quite low (11 to 13%) and it is seldom that the subgrade layer on site would be compacted drier than 2% OMC (lower optimum moisture contents can be used for compactors with compactive efforts greater than the mod AASHTO compactive effort) as the in situ Berea Red soil generally has a natural moisture content higher than the OMC at 100% mod AASHTO density.

3.6 California Bearing Ratio (CBR)

A CBR test was performed on natural recompacted Berea Red soil and was found to be 87% at 100% mod AASHTO density.

The relationship between CBR and % mod AASHTO compaction is illustrated in Fig.3.7. The exceptionally high CBR at 100% mod AASHTO compaction and the lack of swelling when soaked were verified by a second set of tests.

This condition can be attributed to the rather high density achieved during compaction of this material, and grading. It is highly possible that any swelling that may have occurred within the sample was contained by the voids around the larger sand particles and the friction created by the particle interlock.

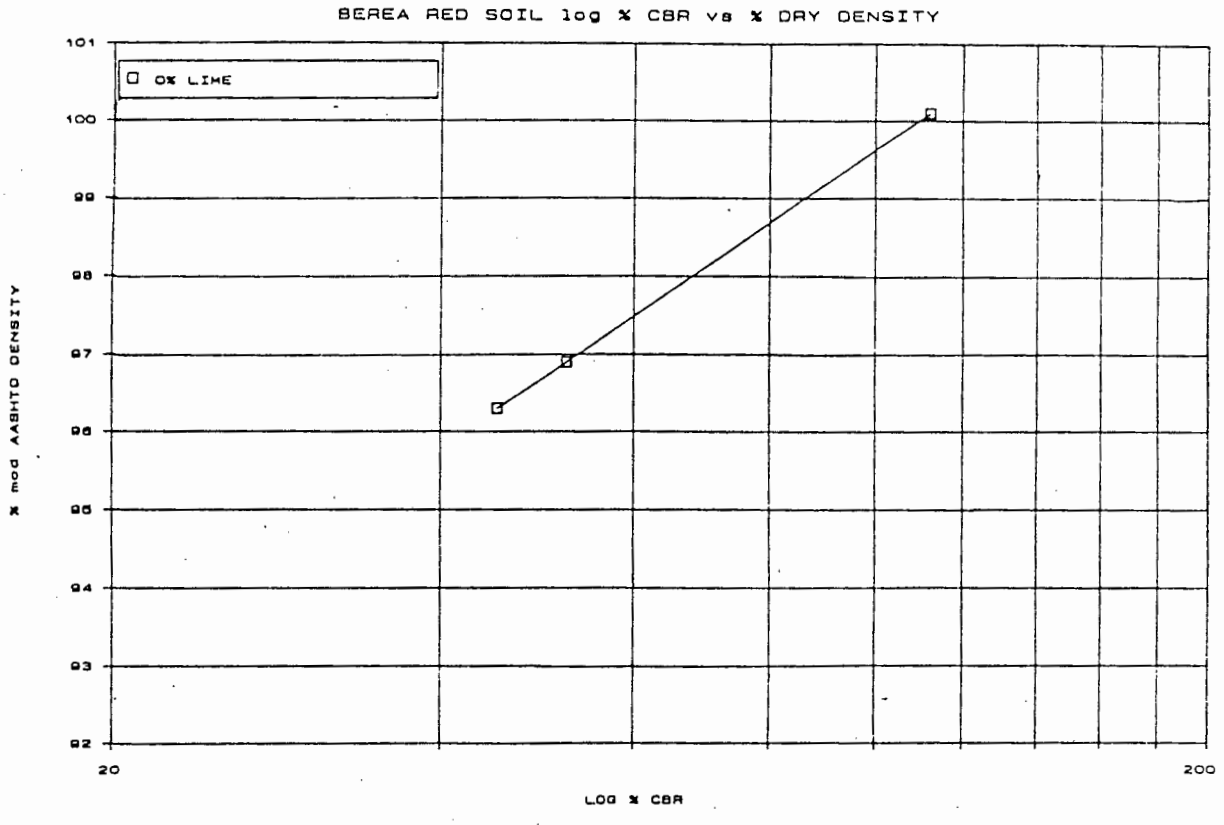

Fig.3.7 Log CBR versus % mod AASHTO compaction of Berea Red soil.

3.7 Unconfined Compression Strength Testing (UCS)

UCS tests were attempted on the natural Berea Red soil in order to determine the improvement lime may have on its unconfined strength. The specimen disintegrated on immersion for the required four hour soaking period. Unsoaked specimens were tested and revealed an average value of 0,5MPa at failure.

3.8 Direct Shear Properties of Natural Berea Red Soil

The specimens were compacted to 100% mod AASHTO density at the optimum moisture content in a proctor mould. The samples were then extruded, cut and trimmed using a shearbox cutter/trimmer. Each specimen was transferred and installed into the shearbox to be tested.

Three normal stresses of 100kPa, 200kPa and 300kPa was chosen equal to those to be used during standard triaxial testing. A strain rate of 3% per hour was used.

The specimen was allowed to stand for an hour to dissipate any excess pore pressure built up during loading.The effective shear diagram revealed an effective apparent cohesion to be 33kN/m^2 with an effective internal angle of friction of 42°. Fig. 3.8 shows the stress strain relationships of natural recompacted Berea Red soil as well as the Coulomb envelope and initial tangent modulus values. Strain at failure was found to be 10%

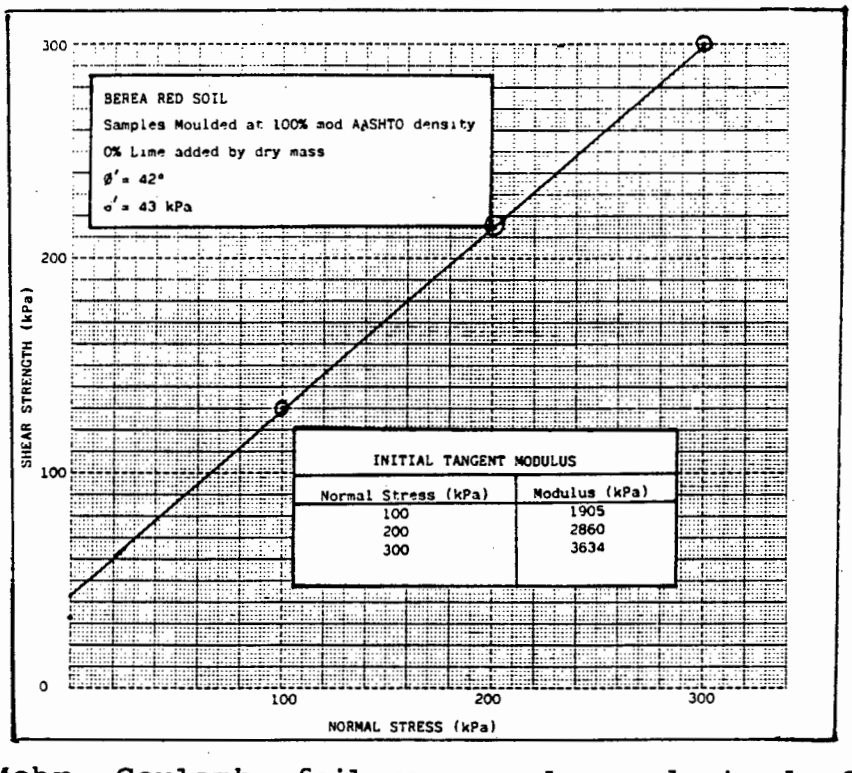

Fig. 3.8 Mohr – Coulomb failure envelope derived from direct shearbox tests

4. LIME STABILIZATION WITH SPECIAL REFERENCE TO BEREA RED SOIL

Three methods by which problematical soils can be overcome are: a) to avoid the soil b) adapt the design to tolerate the soil or c) improve it by soil stabilization.

Soil stabilization is broadly defined as the alteration of any of the soils properties, in order to improve the engineering performance. Engineering performance may include increased strength, reduced compressibility and reduced permeability. The most popular type of stabilizer used of the hydraulic cements, which, as the name implies, reacts with water to improve the soil properties with time.

X-Ray defraction and electron microscope studies made on lime-soil stabilization have indicated that pozzolanic reaction can be described as a slow and continuous reaction in the presence of $Ca(OH)_2$ soluable silica and alumina.

4.1 Soil Stabilization using Hydraulic Cements

Hydraulic cements are mineral compositions that under correct conditions may react with water to form strong cementing complex compounds. The common hydraulic cements are mixtures of calcium silicates and aluminates which include the portland, natural, slagment and high alumina cements.

The varying hydraulic cement compositions are according to Winterkorn(59) SiO_2; CaO; $Al_2O_3+Fe_2O_3$ which are shown in Fig. 4.1.

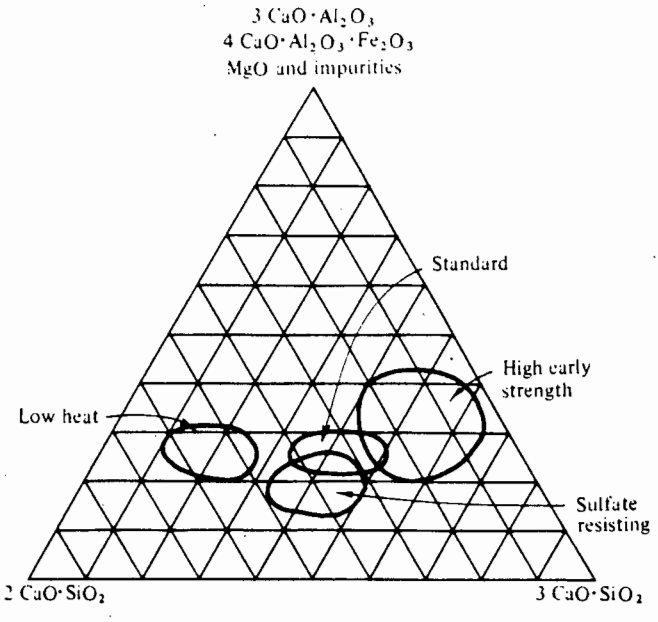

Fig. 4.1 Compositional relationships of hydraulic cements (Winterkorn(59))

The figure shows the relative relationships of quick lime, hydraulic lime, and pozzolan cement. From the location of their respective compositional ranges in Fig. 4.1, one could conclude that portland cement could be produced from hydraulic lime and a pozzolan. Given sufficient time, the hydration products of portland cement may be duplicated by combining, at normal environmental temperature, two or more of the primary components i.e., calcium oxides CaO, SiO2, and A1203(Fe203) (Winterkorn(59)) in the correct proportions in an aqueous system. Most soils requiring stabilization contain silica and alumino-silicates, simple addition of quick or hydrated lime and water may suffice to establish an hydraulic cement.

The critical question is whether the rate of reaction will be rapid enough that the cementing compounds will be formed within a reasonable time period.

TABLE 4.1 TYPES AND GRADES OF LIME (after Winterkorn(59)

TYPE	CHEMICAL COMPOSITION
Calcia (high calcium quicklime)	CaO
Hydrated high-calcium lime	$Ca(OH)_2$
Dolomitic lime	CaO+MgO
Normal Hydrated or Monohydrated dolomitic lime	$Ca(OH)_2$+MgO
Pressure hydrated or di-hydrated dolomitic lime	$Ca(OH)_2$+Mg(OH)

4.1.1 Soil and lime reactions

The effect of lime and soil being mixed is described by most authors as a two stage reaction, namely:

(i) Immediate modification, known as flocculation and agglomeration due to cation exchange.

(ii) Pozzolanic cementing reaction.

4.1.1.1 Modification: cation exchange and flocculation agglomeration

When fine grained soils are treated with lime they usually display rapid cation exchange and flocculation agglomeration reactions. Cation exchange is best explained in the state-of-the-art report on lime stabilization (TRB(60)) which states that if the soil has fairly equal proportions of Na+, K+, Ca++ and Mg++ in the preceeding order with the preferential adsorbtion of cations, beginning with sodium,then the cations will tend to replace cations to the left in the above series.

Monovalent cations are usually replaced with multivalent cations. The addition of lime creates a condition in the soil in the presence of water that produces a Ca++ concentration that will replace dissimilar adsorbed cations on the colloidal surface. In some natural soils the condition may exist that an abundance of Ca++ ions exist before lime is added. Addition of lime increases the pH which in turn increases the cation exchange potential. When soil is subjected to lime the texture of the fine particles change, which is caused by flocculation and agglomeration. This is the process in which the clay minerals clump together to form flocs or larger sized aggregates which is caused by the increase in electrolyte concentration of the pore water and clay surface absorbtion of calcium. Close inspection of the grading curves for Berea Red soil illustrates that this condition probably occurs.

It is well documented (TRB(60),Winterkorn(59)) that the rapid formation of calcium aluminate hydrate cementing materials are responsible for strength development.

4.1.1.2 Soil lime pozzolanic reaction

A pozzolan is defined as a siliceous or siliceous aluminous material which has little or no cementation value. For the pozzolanic reactions to take place with the added lime, soil silica (as mentioned in section 4.1) and alumina minerals are needed. The source of these minerals include clay minerals, quartz, feldspars, micas, and similar silicate products. When a significant quantity of lime is added to a soil, the pH of the soil-lime increases to a value of 12,4 which is the pH of lime saturated water. The increase in pH greatly enhances the solubility of silica and alumina.

For the cementing process to begin it must be assured that the (initial consumption of lime) "ICL" of the soil has been satisfied and that there is still sufficient free lime available for cementation.

The cementation process as with cement is permanent and can be inhibited by the presence of organic material and iron. Twenty percent (by mass) of organic material is the maximum that lime as a pozzolan can tolerate (Moore(62)).

The higher the magnesium content of the quick or hydrated lime, the less the water affinity and heat development on mixing with water, causing pozzolanic reaction to be reduced. Quick and hydrated lime absorb and react with carbon dioxide from the air and form $CaCO_3$ which would not perform as a hydraulic cement. This process is known as carbonation, which should be avoided by properly expedited and sequenced construction procedures. Isolation of the soil-lime specimens from carbon dioxide is ensured by placing them in air tight plastic bags and expelling any excess air before sealing them. When cementation takes place, calcium aluminate and calcium silicate hydrates are formed. In the concrete industry calcium silicate hydrate is known as a tobermorite gel which is understood to be the first poorly crystalline colloidal substance to form during cementation Shen and Li (59).

A simplified qualitative view of some typical soil-lime reactions are described in the state-of-the-art report (TRB(60)).

$$Ca[OH] - Ca^{++} + 2[OH]$$

$$Ca^{++} + 2[OH]^- + SiO(\text{Clay Silica}) \rightarrow CSH$$

$$Ca^{++} + 2[OH]^- + AlO(\text{Clay Alumina}) \rightarrow CAH$$

The use of lime on Berea Red soil revealed a 100% increase in the CBR of natural material, which was thought to indicate that the lime was reacting with the soil.

4.1.2 Compositional requirements for lime stabilization

Soils will not stabilize effectively if they do not possess finely subdivided, highly siliceous minerals that are capable of reacting with lime. If this condition occurs a siliceous material can be added in the form of diatomaceous earth or highly siliceous fly ash to produce an end product of tobermorite.

A literary minerology investigation of Berea Red soil was undertaken to establish whether silica was present in sufficient quantity to react with lime.

Webb(61) indicated that deep borings had been made and at the basal boulder bed a white, or yellowish coloured zone was apparent. This is due to the intensive leaching and reduction of ferruginous material. Hence, the presence of siliceous materials was confirmed by the presence of feldspar in the soil. As Berea Red soil is a wind blown sand, it would be expected that the particle size would be single sized. The presence of clay indicates that in situ weathering has taken place. Webb(61) postulates that feldspar in the aeolian sand was the probable source of the now present Kaolinite, Illite, and Geothite minerals, as the present Natal beach sands contain a high percentage of feldspar.

The presence of hydrated ferric oxide has already been noted, and it is a coating on the quartz grains, which is presumed to be the weathering of the ferro magnesium minerals, which were derived from the igneous formations inland, namely Pyroxenes [(MgFe)SiO3] and Amphiboles [(CaMgFeNaAl3)-(AlSi)O11(OH)].

4.1.3 Reaction of lime with iron

It is a well known fact that iron oxides do not respond well with lime, as in the case of the Cape Peninsula's ferricretes. Studies done by Moore et al's(62) on the activity of 40 Illonois soils has revealed that in poorly drained soils the pH and oxidation potential of the environment can be such that most of the iron can be reduced to the Fe++ valence state which will readily dissolve in water and become quite mobile. Some of the iron is moved a short distance to a location where the micro-environment is favourable to oxidation and a concentration in these areas occurs while some iron may be totally leached out of the soil. In better drained soils, the undissolved iron is moved across microscopically small distances. It is usual that the pH and oxidation potential does not favour the further oxidation of the iron and macroscopic relocation is not possible. Thus, secondary iron minerals in various states of hydration occur in microaggregation with a nett positive surface charge. The situation tends to cause the minerals to disperse evenly throughout the soil mass. It is possible that the clay fraction of soil may lose the properties of cation exchange resulting in an insoluble and chemically stable iron coated aggregation.

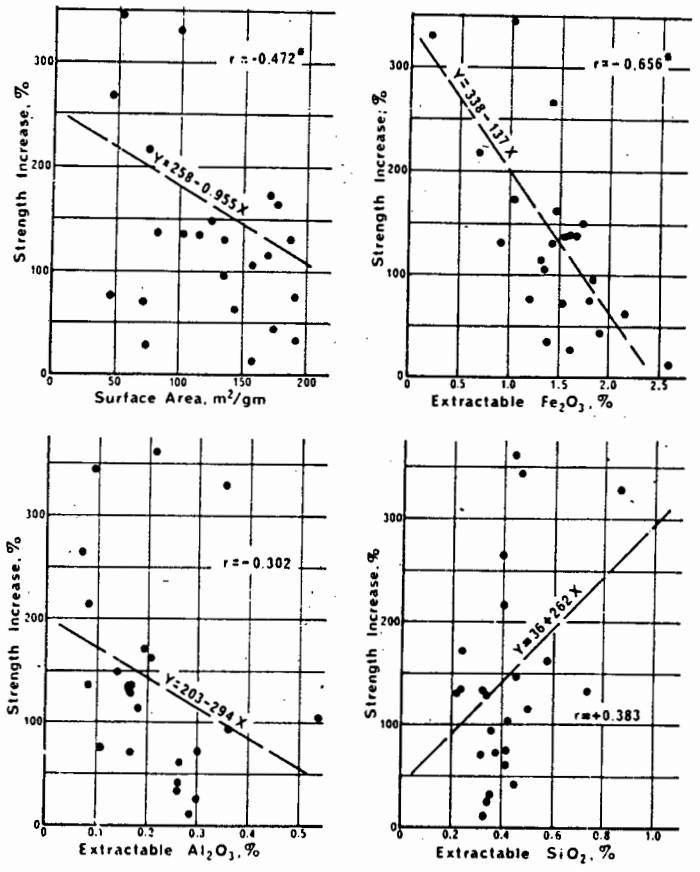

Fig. 4.2 Relationship between increase in compressive strength with lime treatment and several physicochemical properties of 24 Illinois soils (Moore et al(62)).

The contrast in iron distribution between poorly drained and well drained soils is reflected in soil colour. The subsoil of a typically well drained soil profile is usually a uniform yellow-brown colour indicating that the iron is well scattered over the entire soil mass.

Imperfectly drained soils reveal a colour distribution with light and dark concretations, as discussed in Section 3.2.

Moore et al(62) in his literature study found that the form in which the iron exists is of most concern with respect to lime stabilization than the total amount present. It appears that the iron that exists in the form of coatings on individual particles is in the form of magnetic oxide which can be detected by magnetic susceptability. Another form is concretionary iron which is predominantly geothite, is far less magnetic. Moore et al(62) reports that the primary sources of iron as with Berea Red soils are oxides (principally magnetite and ilenite) and silicates (including amphiboles and pyroxenes).

It is also reported that there is a good correlation between measurable iron content of the soils and increase in strength of the soils with lime treatment (See Fig. 4.2)

To investigate and confirm that the iron oxide that was present in the soil was bonded to the clay particles, Desphande et al(63) performed a series of tests on red tropical soils with a grain size not greater than 2mm. The origin of the soils ranged from North and South of Australia and India. It is interesting to note that the above geographical areas were on essentially the same latitude as part of the Gondwanaland in carboniferrous times. Desphande et al's(63) tests involved precipitating the iron out of the soil which amounted to between 2 and 15% dry mass, and then comparing the properties before and after precipitation. The most important fact that was established from the testing was that when the results were expressed on the basis of the original weight of untreated soil, decreases in the proportion of clay were observed corresponding to the amount of iron oxide removed. This seems to clearly support Moore's theory, that the presence of iron oxide coatings prevents and retards cementation.

It seems from Moore et al's(62) report that successful lime stabilization is favoured in the absence of finely divided iron oxyhydroxides associated with the clay fraction. However, on the other hand one should not expect poorly drained soils to stabilize well, as a high organic and carbon content could also be present.

It would appear that Berea Red soils could suffer from the same high iron oxide content as with the Illinois soils.

4.1.4 Soil Activity Index

Research work performed by Cabrera et al(64) and Nwakanma et al(65) showed that the activity of red tropical soils is directly related to the clay fraction present in the soil, where the activity index of a soil is defined as the ability of some of the components of the soil to react with lime to produce cementitious material. Cabrera et al(64) is in agreement with most other authors when addressing the question of which constituents react with lime. He did, however, note that during the electron microscope scans which they performed, 92% of the lime used, up to and including the 28 day period, was consumed during the first seven days during which the clay fraction was the most responsive. This is an indication that the initial rapid uptake of lime after the first seven day period is very slow and limited in quantity. Therefore, it appears that the increase in strength of a soil-lime system beyond the seven day period cannot be explained in terms of the generation of pozzolanic reaction products.

This seems to suggest that the increase in strength shown by Berea Red soil in Fig.4.7, beyond seven days is mainly due to the changes which take place in the structure of the cementitious products, which is analogus to that of concrete made with portland cement i.e., continuing hydration and increase in crystallinity of the reaction products.

An empirical relationship of activity index (Ai) versus confined compressive strength (UCS) was proposed by Thomson(64):

$$UCS = 1{,}639\ Ai + 0{,}0135\ Ai^2 - 0{,}0276\ Ai^3 + 0{,}33$$

where UCS = unconfined compressive strength of the soil-lime mixture in MPa

Ai = Activity Index x 10E-4 per day

and Cabreras et al(64) lime reactivity parameter was proposed and equated to Ai as

$$LR = 0{,}72\ Ai + 0{,}278$$

where LR = Lime Reactivity parameter in MN/m^2

The UCS values of Berea Red soil were calculated and are shown in Table 4.2

TABLE 4.2 LIME REACTIVITY AND ACTIVITY INDEX OF BEREA RED SOIL

% LIME CONTENT BY MASS	2%	4%
Ai	0,66	0,90
LR (MN/m^2)	0,75	0,92
UCS (MN/m^2)	0,96	1,51

The values obtained in Table 4.2 from the Berea Red soil were compared to those of Cabrera et al's(64) soils with similar activity indeces. It is of interest to note that Cabrerea et al's soils had high percentages of FeO. The silicon and aluminiuum oxides of these soils were neither abnormally high nor low when compared to materials with high and low activity indeces. As previously discussed, clay is essentially responsible for the cementation of material with lime. Yet Cabrera et al's(64) materials which had low activity indexes had high clay contents (30% of dry mass).

In conclusion, the activity index proposed by Cabrera et al(64) & Nwakanma (65) appears to be a very good parameter to measure the pozzolanic activity of red tropical soils.

The amount of lime reacting with a soil does not correlate with strength and lime reactivity and is thus a poor indicator of pozzolanic activity. This implies that the method such as the Eades and Grim lime consumption test Winterkorn(59) does not necessarily hold for Berea Red soils.

The Eades and Grim test requires incremental percentages of lime to be added and the pH to be measured after a period of time for each increment. The required percentage to satisfy the soil consumption is reached when the pH of 12.4 is maintained. It appears that materials with low clay content and high iron content offer the least response to lime stabilization, as with the case of Berea Red soils.

4.2 Lime Type Selection

A commercial grade calcium type hydrated lime was used during the lime modified specimen production.

4.2.1 Lime Specification

The following specifications apply to the lime used as supplied by the producer. (Macquet Bros. of Pinetown, Natal)

Nature of test

% retained in the sieves	850 microns	0.1%
	600 microns	2.5%
	75 microns	30%

Soundness factor	1
Calcium Oxide and Magnesium Oxide by % mass	>90%
Carbide dioxide content % by mass	1%
Free water content	1%
Available lime content by mass	>60%

The above specification of the lime complied with all the requirements of SABS 824/1967 except for the fraction retained on the 850 micron sieve.

The subject of lime treatment can be considered from two view points: lime modification and lime stabilization, the difference being based on the quantity of lime added to the soil. Lime modification for silty and clayey soils generally requires the additional of 1% to 4% by mass of lime.

The addition of a low percentage of lime usually induces quick changes in some physical properties, particularly consistency limits, but little strength is gained. This is verified with Berea soils where the P I of 7% was reduced to a non-plastic state.

On the other hand, however, lime stabilization requires a greater percentage of lime in the range of 4% to 10% to cause substantial gain in strength as a result of the formation of cement compounds while curing.

The lime treatment used in this investigation was carried out on the level of soil modification and not stabilization, even though some stabilization occurs at low percentages of lime by mass.

4.2.2 Selection of lime quantity

The literature indicates that the design lime content for lime modification is based on an analysis of the effect of the percentage of lime on either the plasticity properties or pH of the soil, whereas the design lime content for stabilization is based on evaluation of the relationship between the lime content and the unconfined compressive strength for a given curing condition. Thus, in this study, the percentage of lime used in the modification process was chosen based on the results of the plasticity index and unconfined compression tests.

4.2.3 Atterberg limits

The required percentage of lime for soil modification can be determined by the method suggested by Hilt & Davidson(57) in which the "lime-fixation capacity" is obtained for that soil, that is, the lime percentage above which change in the plastic limit is minimal. Generally, if the amount of lime used is below the percentage needed for fixation, the soil will merely be modified. This means that its plastic behaviour will be altered but that no substantial strength development will take place.

The liquid limit and plastic limit for three percentages of hydrated lime were determined according to TMH1(56) methods A2 and A3. The variation of consistency limits were determined for 0%,2% and 4% lime by dry mass, and are summarized in Table 4.3

The liquid limit decreased with increasing lime content. The largest decrease occurred between 2% and 4% when the material became non-plastic.

Therefore, addition of 4% lime could be considered the optimum percentage needed for lime modification.

With reference to the trend in the change in consistency limits, the decrease in liquid limit may be considered normal. Alfi(57) reported that conflicting data on the effect of lime on the liquid limit has been published. Decreases in the liquid limit on the addition of lime as well as increases in the liquid limit have been reported.

The results obviously depend on the type of soil being tested.

It is well known that regardless of whether the liquid limit decreases or increases along with either a decrease or increase in the plastic limit, the plasticity index is usually reduced with the addition of a small amount of lime.

The changes which occurred in the Berea Red soil with the addition of hydrated lime are explained below.

4.2.4 The effect of lime on liquid limit

The liquid limit is defined as the water content at which the water films become so thick that cohesion between particles is decreased and the soil mass becomes viscous and flows under an applied force, the observed decrease in the liquid limit due to the addition of lime may be attributed to an immediate flocculation and agglomeration.

The immediate effect in terms of compaction characteristics following the addition of lime will be discussed in the next Section.

The amount of water necessary to thicken the water films surrounding soil particles to the point of flow under an applied force, as in the liquid limit test, depends on the amount of surface associated with water and consequently the size of the particles. As flocculation and agglomeration of the fine soil particles decrease the total surface area, the amount of water which is required to satisfy the surface behaviour would be lowered and the liquid limit decreased.

4.2.5 The effect of lime on the plastic limit

The plastic limit may be defined as the lowest moisture content of the soils plastic range. The plastic limit depends on the amount and nature of the clayey material present in the soil. At the plastic limit moisture content the clay particles are supposed to be covered with enough water so that the soil particles are orientated in such a way that they can slide over each other when pressure is applied. The increase in the plastic limit is due to the addition of lime, which possesses high water absorption capacity within the soil mixture, as well as to immediately impliment flocculation and agglomeration within the soil.

When the soil particles are flocculated and agglomerated, water is held between the particles in aggregate formation as well as around the individual particles. The retained water in the soil aggregates increases the total amount of water required to supply the degree of lubrication of the soil mixture indicated by the test of plastic limit.

As the degree of plasticity increases with increasing lime, the plastic limit of the soil mixture also increases up to the optimum lime content where flocculation and agglomeration reach their maximum.

The strength increase has been attributed to the degree of accomplishment of lime soil reactions, namely cation exchange, flocculation, carbonation, and pozzolanic reaction. The last reaction is considered to be primarily responsible for the long term strength increase in lime-soil mixtures, as discussed previously.

It is interesting to note that most work done in lime stabilization specifies the amount of lime added to the mixture as a percentage of either the total weight or total volume of the soil mixture. However, it is generally recognized that lime reacts primarily with the fine grain fraction (passing No. 200 sieve) of the soil mixture. It is Shen and Li's(58) opinion that it would be worthwhile to specify the lime content for stabilization on the basis of the fine-grained fraction.

4.3 Soil Mechanical Properties of Lime Stabilized Berea Red soil

A series of indicator tests were performed to evaluate the reaction of Berea Red soil to the addition of various percentages of lime.

The remoulding and indicator tests were undertaken four hours after the lime and water was added to the soil to facilitate proper moisture distribution and simulate site conditions. Testing was performed using lime, lime-slagment and cement as stabilizers.

4.3.1 Soil classification

Grading curves were produced for (2% and 4% lime) stabilized Berea Red soil and compared to the curves of natural material. Lime stabilized material was obtained from CBR samples which had been cured and tested. The material was extruded, broken into small lumps, and sieved through sieves with smaller openings until all material passed the 1,18mm sieve. The natural Berea Red soil used had a maximum partical size of 1,18mm.

Grading curves of the modified and natural materials are presented in Fig.4.2. The effect lime modification has on the material is illustrated by the reduction of finer particle sizes.

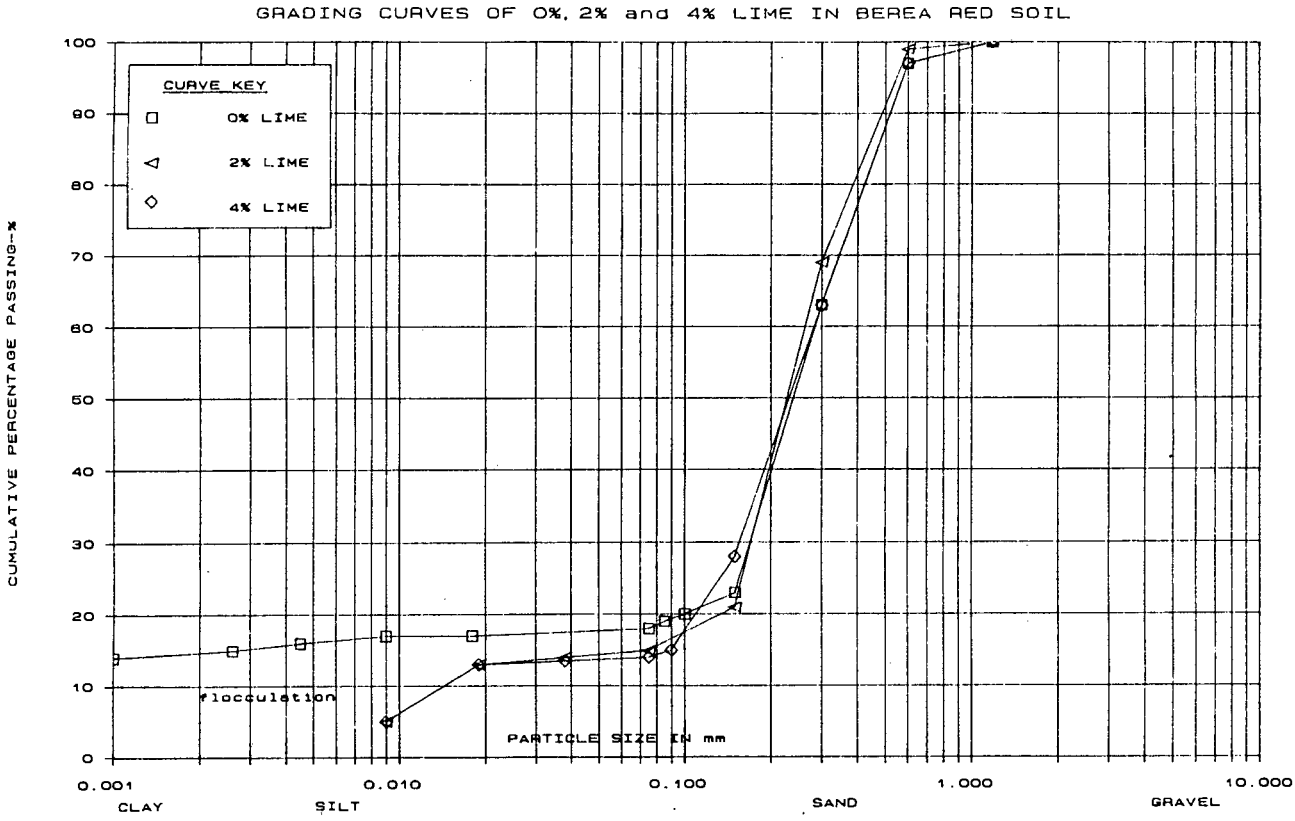

Fig. 4.2 Grading curves of Berea Red soil with 0%, 2% and 4% Lime by dry mass

The following reasons may explain the variation in grading curves:

i) Mechanical compaction may have broken down some sand sized particles, resulting in marginally less material in the larger sand fraction.

ii) Cementation has bonded silt and clay, resulting in larger particles, hence a coarser grading.

iii) Flocculation of clay particles occurred.

The Atterberg limits for lime modified soil are presented in Table 4.3.

TABLE 4.3 SUMMARY OF ATTERBERG LIMITS OF BEREA RED SOIL MODIFIED WITH LIME

LIME CONTENT	DESCRIPTION	LL	PI	LS
0%	Passing 0,425 mm	20	7	2,0
	*Passing 0,075 mm	63	40	16,0
2%	Passing 0,425 mm	19	2	1,0
	*Passing 0,075 mm	73	32	14,0
4%	Passing 0,425 mm	-	**SP	0,5
	*Passing 0,075 mm	65	26	11,5

* Although material used for the Apparent Atterberg Limits (passing 0,075mm) does not represent true Atterberg limits, inclusion in the above table is for comparative purposes only.

** Slightly plastic

The PI of unmodified soil is lowered from 7 to 2 by the addition of 2% lime and no PI was recorded with the addition of 4% lime.

A similar trend of reducing the apparent PI is noticeable in the modified test (performed on material passing 0,075mm sieve).

Linear shrinkage is reduced with the addition of lime on all samples tested.

The relative density was determined and is understood to be the ratio of the mass in a given volume of a material at a stated temperature to the mass in air of an equal volume of distilled water at the same temperature.

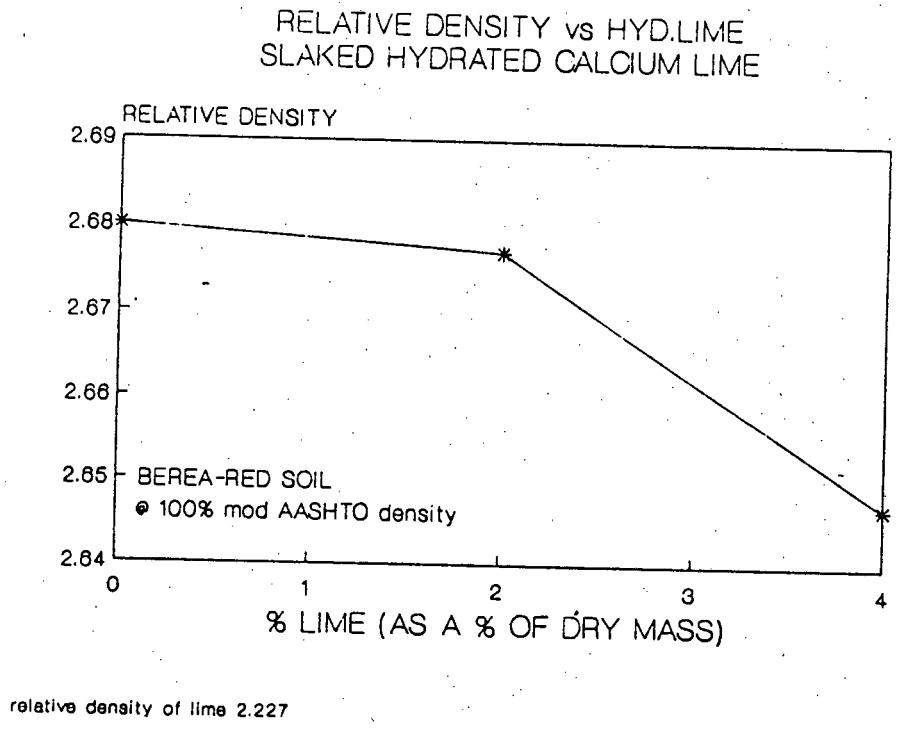

relative density of lime 2.227

Fig.4.3 Relative density of Berea Red soil as a function of the % of lime content

The effect lime has on reducing the relative density of a modified soil is illustrated in Fig.4.3. This can be attributed to the fact that lime itself has a low relative density which, when flocculated with clay, has an overall reducing effect.

4.4 Maximum Dry Density and Optimum Moisture Content

The dry density versus moisture content curves were obtained by using the mod AASHTO compactive effort and are summarized in Table 4.4

TABLE 4.4 MAXIMUM DRY DENSITY AND OPTIMUM MOISTURE CONTENT

MATERIAL	DRY DENSITY kg/m³	w%	e	S_r
Berea Red with 0% lime	1970	10,4	0,36	0,77
Berea Red with 2% lime	2000	9,9	0,34	0,78
Berea Red with 4% lime	2006	10,0	0,32	0,83

A summary of the moisture density relationships appear in Appendix A. The overall effect of the addition of lime is to reduce the OMC of the material needed to achieve the desired compaction. The increase in lime increase the maximum dry density.

4.5 Consolidation behaviour of Lime Stabilized Berea Red Soil

Consolidometer tests were performed on Berea Red soil in order to evaluate the effect in consolidation behaviour due to the addition of lime and curing.

Curing periods of 10 to 18 days were chosen to avoid monitoring the test during weekends. Collapse potential testing on lime modified specimens was not investigated as the natural material indicated a collapse potential of 1% (see Section 3.5.5). It was envisaged that in the case of lime modified specimens it would be lower due to the higher densities and cementation that could be achieved. The effect of lime stabilization on the log pressure versus void ratio curves is illustrated in Fig.4.4.

Inspection of identical specimens which have been cured for different time periods (10 and 18 days) reveal that the compression index (C_C) (see Table 4.5) is slightly lower for the longer curing period, indicating greater stiffness and resistance to consolidation. This could be attributed to a possible crystaline growth of lime cementitious compounds.

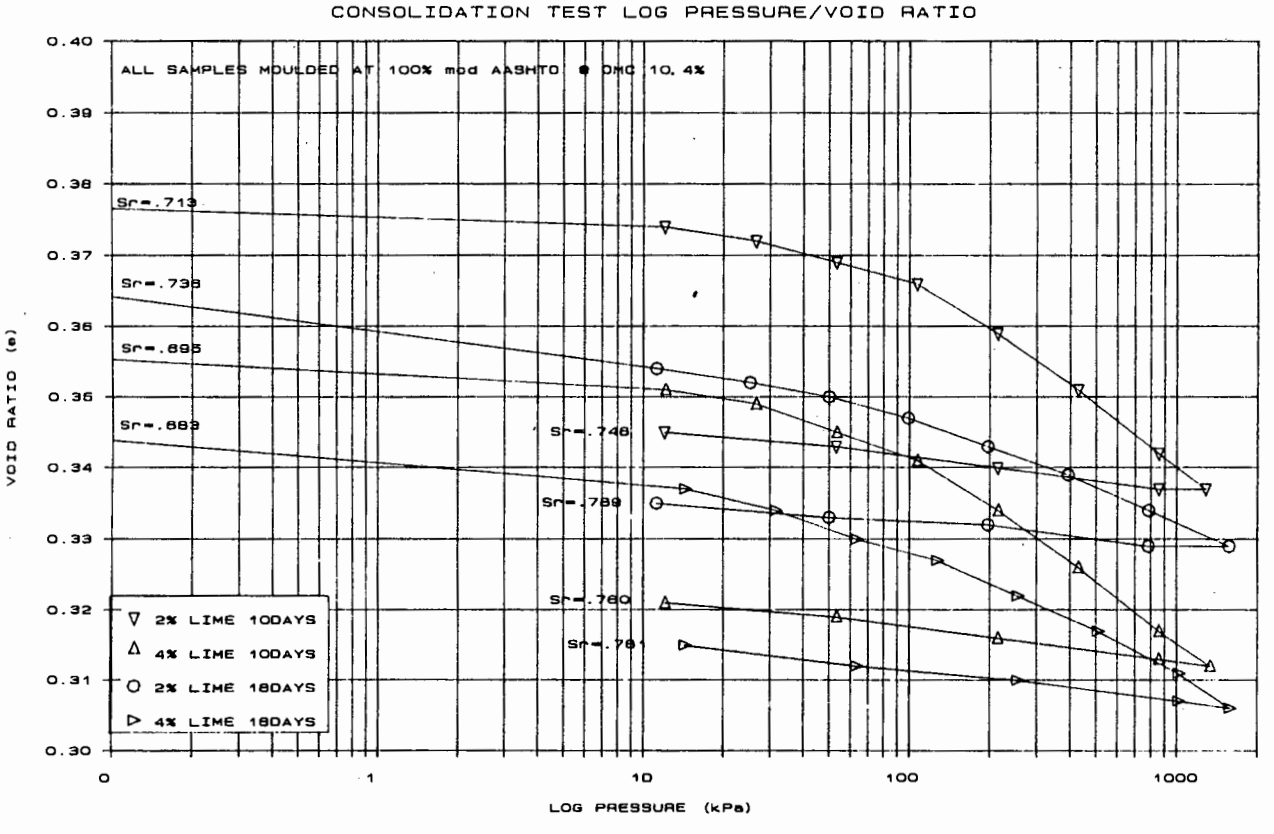

Fig.4.4 Log Pressure versus Void Ratio of Lime Stabilized Berea Red soil.

TABLE 4.5 PROPERTIES OF LIME STABILIZED BEREA RED SOIL TESTED IN OEDOMETERS

Tested after 10 days curing

% mod AASHTO density	% LIME by dry mass	Dry Density kg/m³	%w	e_o	P_c(kPa)	C_c
97,3	2	1945	9,9	0,377	50	0,029
97,4	4	1953	9,9	0,356	35	0,028
98,6	4	1978	9,7	0,338	35	0,025

Tested after 18 days of curing

% mod AASHTO density	% LIME by dry mass	Dry Density kg/m³	%w	e_o	P_c(kPa)	C_c
98,1	4	1968	8,9	0,345	22	0,016
98,8	4	1981	8,3	0,336	80	0,018
98,0	2	1960	9,5	0,366	12	0,017

where P_c is an effective preconsolidation pressure.

4.6 California Bearing Ratio

The CBR's of lime modified Berea Red soil 2% and 4% lime by dry mass at 3, 7 and 28 days were evaluated. The CBR increases by 20% from 3 days to 7 days curing for 2% lime, but negligible increase was detected for 4% lime specimens. However, the change from 3 days curing of both 2% and 4% specimens at 28 days is negligible (illustrated in Fig.4.5). This indicates, as discussed previously, that the modification process is immediate and occurs well within a 3 day period, thereafter the improvement is extremely slow due to cementation. This highlights the discussions that evaluation of lime stabilization of a material cemented with lime after 28 days is not correct. The effect of the two percentages of lime at 3, 7 and 28 days curing has on the log CBR is illustrated in Fig 4.6.

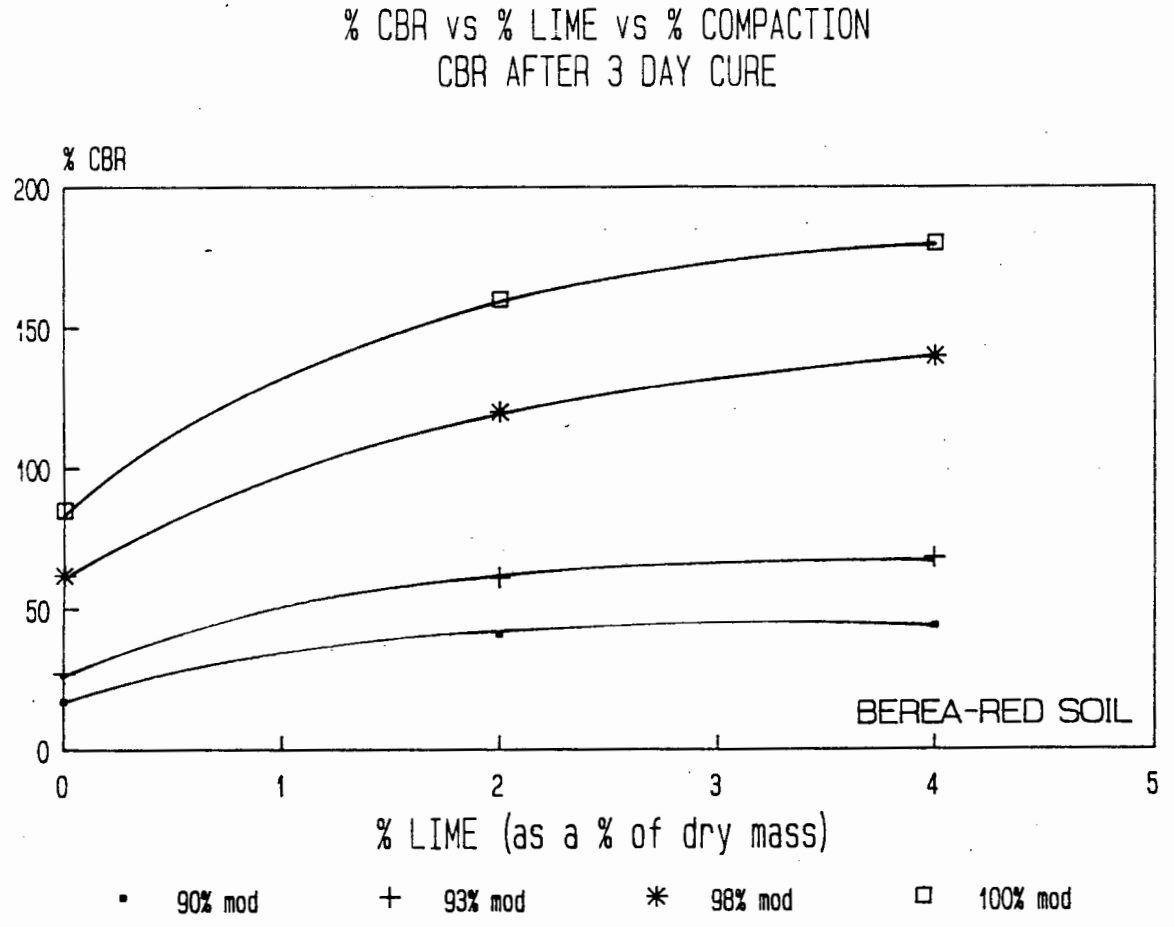

Fig.4.5 a. % CBR vs % Lime vs % mod AASHTO compaction of Berea Red soil tested after various periods of curing

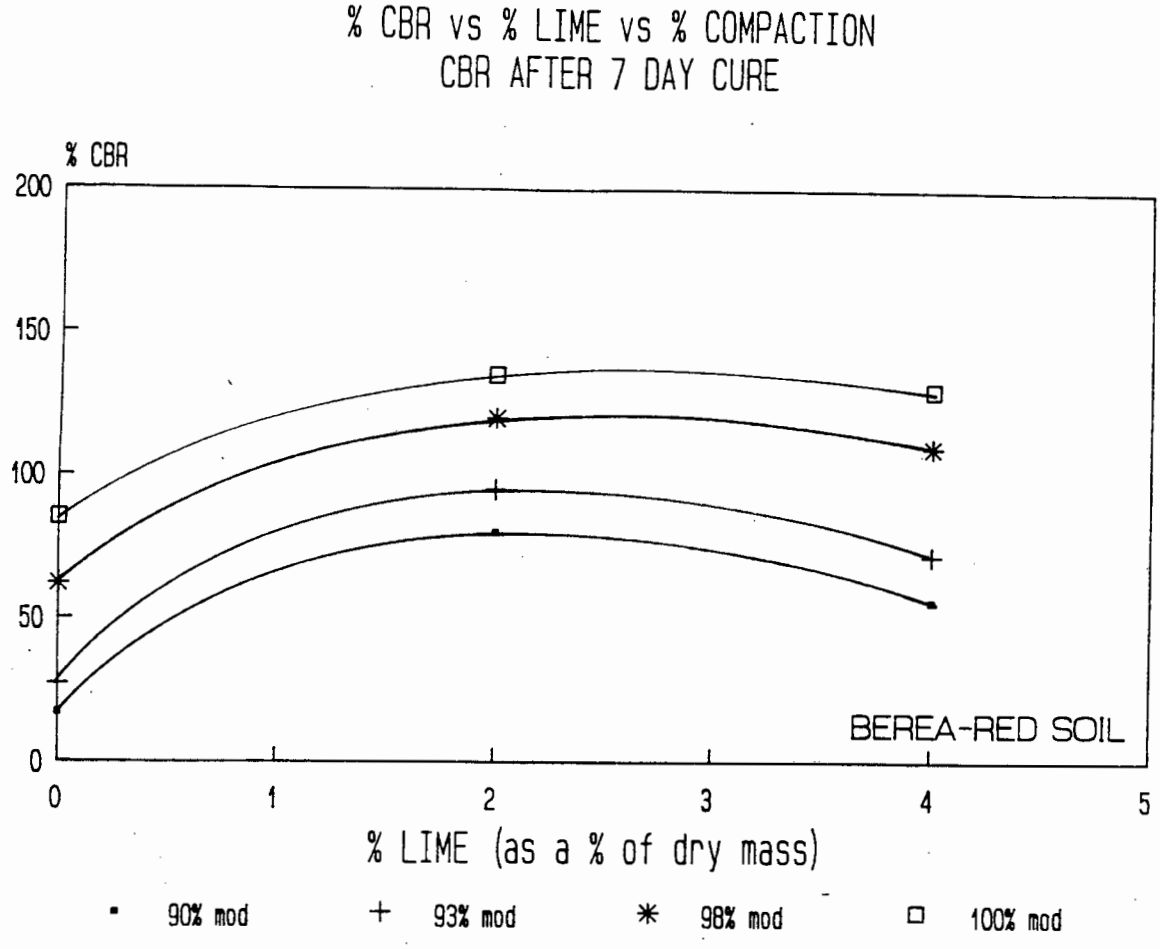

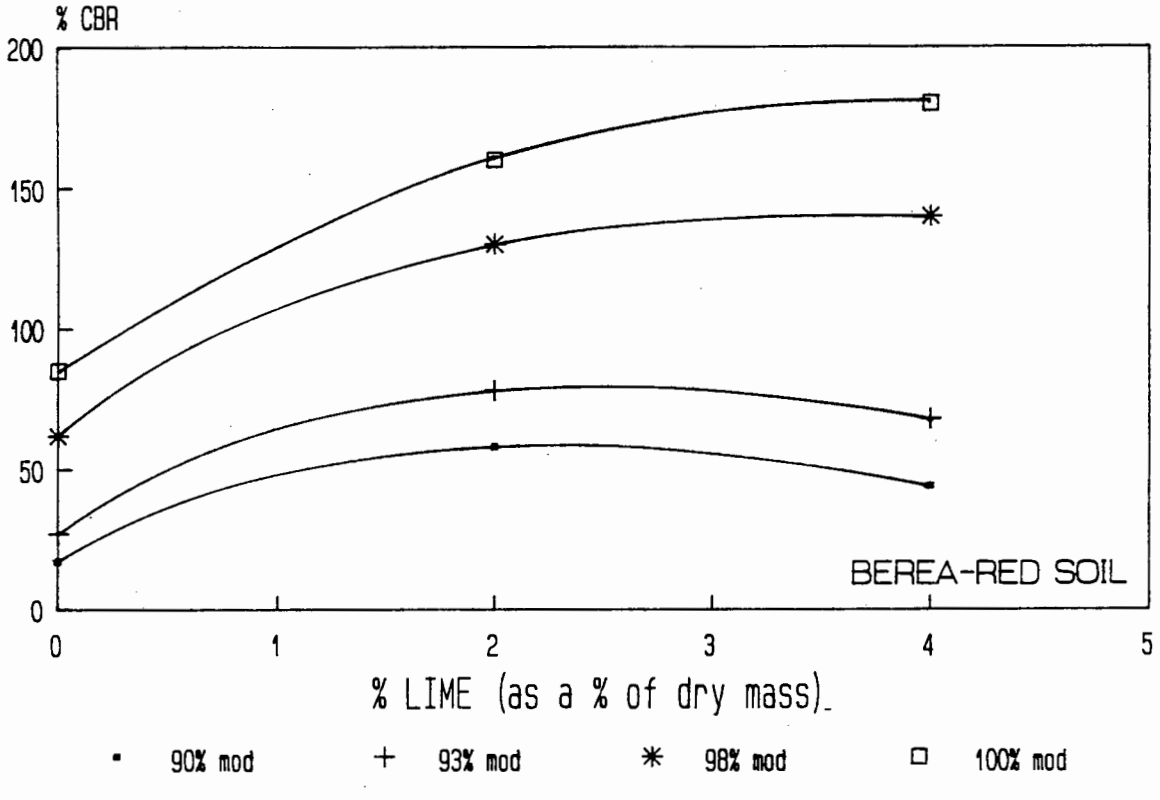

Fig.4.5 b&c **% CBR vs % Lime vs % mod AASHTO compaction of Berea Red soil tested after various periods of curing**

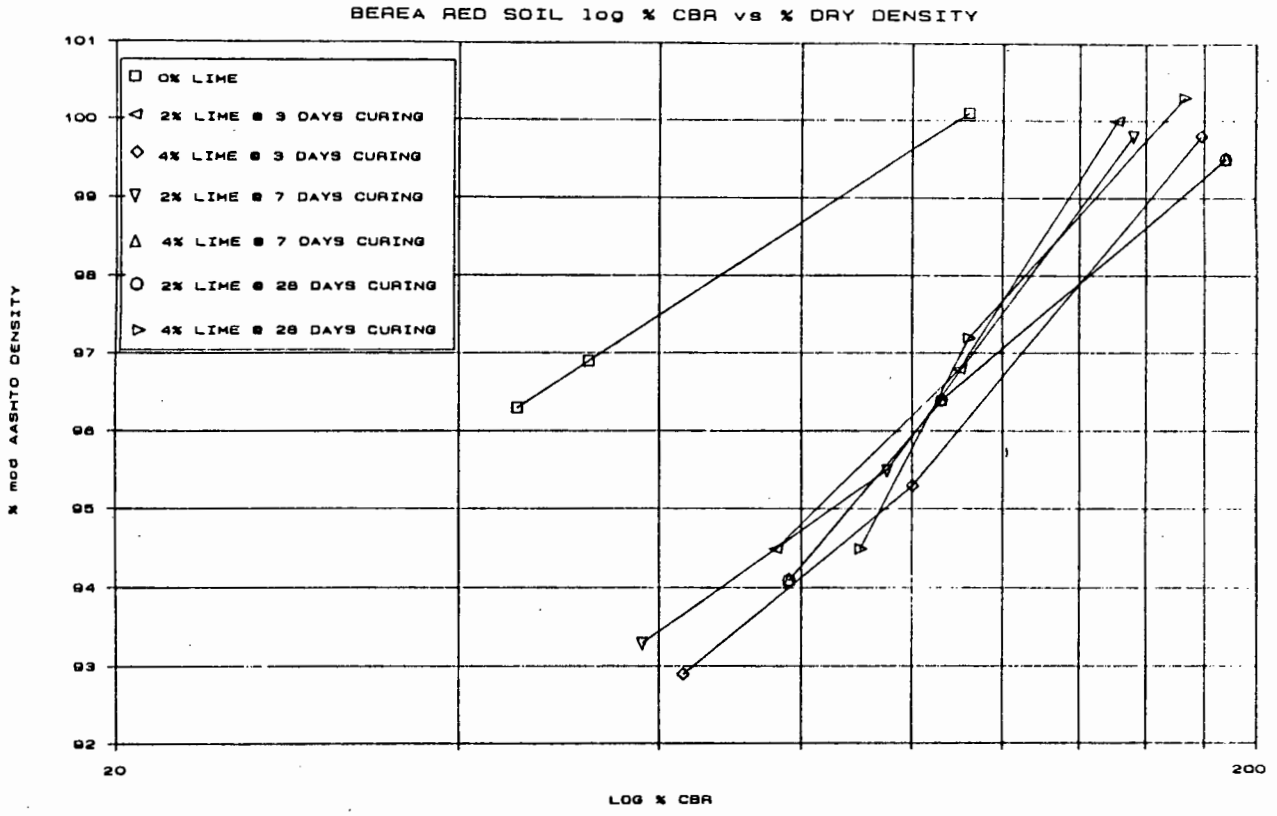

Fig.4.6 Log % CBR vs Dry Density of Lime modified Berea Red soil

4.7 Unconfined Compression Strength Testing

In pavement construction UCS tests are a good means of initial estimation of a soils reaction to stabilization. In order to evaluate the compressive strength properties of Berea Red soil to lime, cement and lime-slagment stabilization, a series of UCS tests were performed.

The following types of popular stabilizers used in the investigation are listed in Table 4.6.

TABLE 4.6 Stabilizing Agents and Percentages used on Berea Red Soil

AGENT	% OF DRY MASS
Cement (OPC)	2% and 4%
Lime	2% and 4%
Lime Slagment	1% Lime + 1% Slagment
	2% Lime + 2% Slagment

Specimens were prepared and moulded in proctor sized moulds and were sealed in plastic bags and placed in a bucket which was immersed in a temperature controlled waterbath of between 22° to 25° C.The specimens were cured for 7 and 28 days.

The effects rapid curing had on the degree of stabilization were investigated, to determine the results of elevated high curing temperatures on the unconfined compression failure strength in order to project the long term strength of the material.

Rapid curing of cement specimens was achieved by placing the extruded specimen in a plastic bag and placing them in an oven (set at a temperature of 70° C) for 24 hours and then loading them to failure at a stress rate of 140kPa/s.

The preparation and testing procedure of rapid cured lime and lime-slagment specimens was similar to that of rapid cured cement specimens. Curing was performed at a temperature of 60° C for a time period of 45 hours.

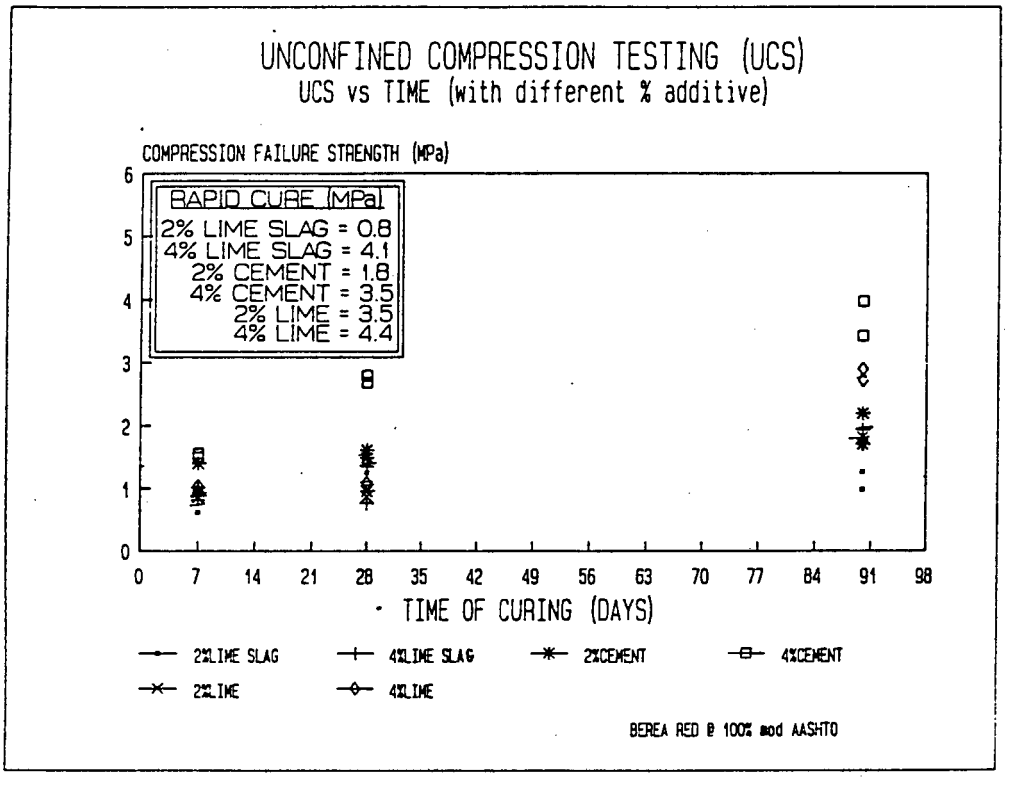

Fig. 4.7 Unconfined Compression Strength versus Time of Stabilized Berea Red soil

The rate of strength gain for lime stabilized specimens is slow from 0 to 28 days, yet the rapid cured lime specimens are comparable to those of cement which were rapid cured (See Fig.4.7).

However, the 2% cement showed very little improvement in strength from 7 to 28 days. As only two specimens per variable were moulded due to limited material, it is difficult to evaluate the cause. Possible damage or poor mixing could be attributed to the poor response of cement stabilized specimens.

From the results of rapid cured UCS samples it is quite obvious that the choice of 2% or 4% lime, 4% lime slagment or 4% cement would be satisfactory. However, the lime or lime slagment would be the obvious choices as they allow the pavement builder a grace period with respect to time if the lime stabilized compacted layer had to be ripped and recompacted. As the pozzolanic reaction of lime is quite slow, disturbance may be allowed in the first 48 hours of it being mixed with the soil.(as discussed in section 4.1)

Cement on the otherhand is not as forgiving and should be compacted within 4 to 6 hours after mixing and cannot be disturbed as cementation occurs rapidly.

An indication of the improvement that lime makes is indicated by:

1) The high erosion properties of a soaked natural Berea Red soil specimen can be controlled with the addition of lime.

2) The unconfined failure strength is improved two fold by the addition of a stabilizer.

5. INDIRECT TENSILE TESTING

The uniaxial tensile strength test of soil is seldom carried out due to the practical problems of applying tensile force to a soil specimen. Ajaz et al(11) have indicated that in material testing the uniaxial tensile strength test is determined from "dog bone" shaped specimens. In soils these are difficult to mould, and the test results are not reliable. Prior to the acceptance of the Brazilian splitting test, as a means of determining the indirect tensile strength of soil, various tests had been employed and have been unsuccessful for soils testing.

(1) The Rotary Tension soil test.

(2) Direct tension test on briquettes and cylindrical soil specimens, which have steel plates "glued" to them.

(3) Direct long tension tests on large (1.32 m long) specimens which have been placed on frictionless supports and pulled (this was reported by Ajaz et al (11) as an unacceptable and impractical test).

(4) Mercury bed test in which long square cross sectioned specimens are supported on mercury and pulled from enlarged ends. (Most tests failed at the point of embedment)

Thus, the Brazilian test became more acceptable. The indirect tensile strength test (ITS) is understood to be the loading of a cylindrical soil specimen with compressive forces applied through knife edges diametrically opposite each other along the length of the specimen.

Tensile normal stresses are generated within the specimen causing it to split in two, so that the direction of maximum tensile stress is roughly normal to the fracture surface.

The analysis assumes that the soil is linear elastic and homogeneous and isotropic. The equations for the maximum tensile stress is described as a function of the magnitude of the loading force and the geometry of the soil specimen.

In all cases, at least one other normal stress at the point where the maximum tensile stress occurs is found to be compressive and the absolute value of this compressive stress is at least three times larger than that of the maximum tensile stress. Ajaz et al(11) indicates that ITS tests reveal lower tensile failure values than uniaxial tensile failure values. This is due to the large compressive stresses acting perpendicular to the tensile stresses.

5.1 Review of Specific ITS Results with respect to Berea Red soil testing

5.1.1 Change in the tensile strength as a result of a change in the moisture content

Tests performed by Krishnayya et al(7) on glacial till PI=3,5 and maximum dry density 2110kg/m^3 at a moisture content of 9,2% (similar values to that of Berea Red soil) indicate that the ITS decreased with an increase in water content above the optimum moisture content at proctor compaction. It was also observed that the increase in strain became disproportionately higher with increased water content.

Krishnayya et al(7) noted that if the stiffness was regarded as a ratio of the tensile failure stress to tensile strain, it decreased with an increase in water content.

Fang et al(17) verified the above by studying three types of stabilizing agent at different percentages of dry mass and varying moisture contents. It was found that with all the additives the tensile strength increased with decreasing water content which generally occurred on the dry side of optimum. However, a minimum water content was achieved after which shrinkage cracking of the soil occurred causing a reduction in tensile strength.

The explanation by Ajaz et al(11) for the reduction of the tensile strength in soils on the wet side of optimum was approached from a theoretical elastic analysis point of view. Ajaz et al(11) concluded that 55% of the "tensile strain" is due to compressive stress. Therefore the steep increase in tensile failure strain with moisture content may be due to the increase in Poisson's ratio as the degree of saturation increases in ITS tests.(Reference to the theoretical analysis in Section 5.2 highlights the above statement.)

5.1.2 Variation of tensile strength due to stress or strain rate on compacted soil specimens

A study on the effect of loading rate was done by Fang et al(17) and it was found that there is no definite trend in tensile strength variation or deformation at failure when the loading rate varies from 0,76 mm/min (0,03"/min) to 50,8 mm/min (2"/min).

However, Krishnayya et al(7) noted that the effect of rate of loading on the tensile strength and observed tensile strain at water contents from 9% to 10,4%, both attain minimum values at an undisclosed predetermined rate of loading. A decrease in tensile strength and strain at failure is achieved with a slower test rate. The time to failure ranged from 5 minutes to 430 minutes. Notably neither fall within the time to failure of this research. However, the relationship between tensile strength and the soil in question is a complex one, as the soil matrix and water content has to be considered before the critical rate of loading at which minimum tensile strength is mobilized can be determined.

Krishnayya et al(7) concluded that the critical rate of loading is influenced by the water content, and therefore leads one to realise that the pore pressure has an effect.

Urial et al's(8) discussions highlight the problem, concluding that normally, if no thixotropy is present, the strength should be lower for slow tests. The tendency for lower tensile failure stress at lower strain rates is due to the different levels of effective stress that exist inside partially saturated specimens.

Urial et al(8) showed that two zones exist inside the specimens whose boundaries are not well defined, but their states of stress are clearly different from each other.

In the area of the load plattens, two plastic areas exist that are under compression, hence a positive pore pressure due to the reduction in volume would take place, thereby reducing the effective stress.

On the other hand the center of the cylinder which is under tension would undergo a positive volume change (dilation), causing a negative pore pressure.

Uriel et al(8) argue that the slower test allows the compression zone pore water pressure to dissipate thus increasing its strength while simultaneously allowing the dilating central zone to only partially rearrange its menisci (due to void changes) and result in an overall higher ultimate load. The above statement seems somewhat contradictory, as the assumption that the positive pore water pressure in the compression zone can dissipate, while the negative porewater pressure can only rearrange the menisci assumes the air voids in the centre will not allow negative pore pressure dissipation, while in the compression zone the positive pore pressure may. As the original assumption is that the tensile failure stress occurs at the centre of the specimen, the increased compression strength in the compression zones should have little effect at all.

In order to determine the effect of incresed density and moisture content Krishnayya et al(7) modified a tillite by adding 6% bentonite, the effect was an increase in OMC by 1,6%, and the plasticity index and liquid limit by 23,8% and 17,3%, respectively. The dry density was increased by 96 kg/m^3. An additional increase in water content above the optimum with bentonite is to decrease the tensile failure stress extremely quickly during cyclic loading, but under static loading the effect was to increase the tensile failure stress. The loading rates in both cyclic and static tests were the same, i.e. 0,13 mm/min. An explanation for this behaviour was not put forward, but one would expect the pore pressure to build up more rapidly in a cyclicly loaded specimen than a statically loaded specimen and so increase the tensile failure stress.

Hadley et al(22) suggests a strain rate of 50,4 mm/min with no supporting explanation why this load rate was chosen. TRB162(6) advise the above strain rate as well to simulate rapidly applied pavement loadings, but both authorities suggest the same loading apparatus, which implies that Hadley et al's work has been accepted as the norm.

The author felt that applying one single static load "to simulate rapid pavement loading" is unrealistic, as the material is not expected to fail on the first application in the road pavement, however, the use of rapid cyclic ITS loading should simulate the tensile stresses that occur during the loading of the layers.

5.2 Determination of Soil Mechanical Properties using ITS Testing Procedures

The theoretical analysis of a cylinder or disc with loads applied through knife edged strips applied along the length has been investigated and discussed by Hondros(1), Timoshenko(2), Wright(3), Sokolnikoff(4) and Muskhelishvili(5).

Approaches to the analyses have included geometrical and linear elastic procedures. When the body forces of the specimen are neglected the plane stress and plane strain solution to the problem is identical. The following equations were derived by Wright(3), Fainhurst(13) and Hondros(1). The orientation of the stresses is illustrated in Fig. 5.1.

(a) Stresses along the vertical diameter (OY)

$$\sigma_{\theta y} = \frac{+2p}{\pi}\left\{\frac{(1-\frac{r^2}{R^2})\sin 2\alpha}{(\frac{1-2r^2}{R^2})\cos 2\alpha + \frac{r^4}{R^4})} - \arctan\frac{(\frac{1+r^2}{R^2})}{(\frac{1-r^2}{R^2})}\tan\alpha\right\}$$

$$\sigma_{ry} = \frac{-2p}{\pi}\left\{\frac{(1-\frac{r^2}{R^2})\sin 2\alpha}{(\frac{1-2r^2}{R^2}cos2\alpha + \frac{r^4}{R^4})} + \arctan\frac{(\frac{1+r^2}{R^2})}{(\frac{1-r^2}{R^2})}\tan\alpha\right\}$$

(b) Stresses along the horizontal diameter (OX)

$$\sigma_{\theta x} = \frac{-2p}{\pi}\left\{\frac{(1-\frac{r^2}{R^2})\sin 2\alpha}{\frac{1+2r^2}{R^2}\cos 2\alpha + \frac{r^4}{R^4}} - \arctan\frac{(\frac{1-r^2}{R^2})}{\frac{1+r^2}{R^2}}\tan\alpha\right\}$$

$$\sigma_{rx} = \frac{+2p}{\pi}\left\{\frac{(1-\frac{r^2}{R^2})\sin 2\alpha}{\frac{1+2r^2}{R^2}\cos 2\alpha + \frac{r^4}{R^4}} - \arctan\frac{(\frac{1-r^2}{R^2})}{\frac{1+r^2}{R^2}}\tan\alpha\right\}$$

Resulting in the following theoretical stress distribution shown in Fig.5.1.

where: a = Projected width of the loaded section on the rim

t = Length of the specimen

P = Applied load

p = P/at load per unit area

2α = Angle subtended at the center of the disc by the loaded section of the rim

r = Radial distance of a point from the center of a disc

R = Radius of the disc

An indepth discussion on the derivation of the above formula is presented in Appendix B.

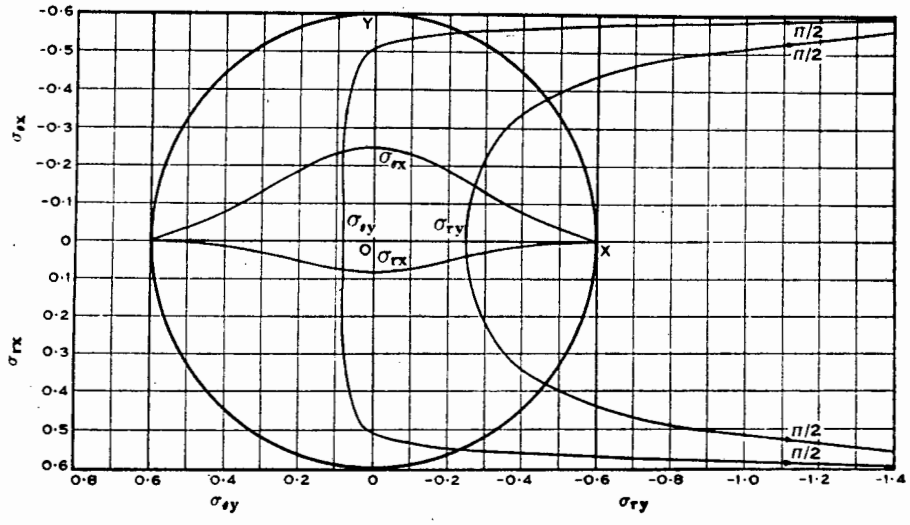

Fig. 5.1 Theoretical stress distribution along vertical and horizontal diameters (after Wright(3)).

5.3 Development of the Indirect Tensile Strength Test Apparatus

The following section discusses the development and use of an ITS test apparatus. The general principle is based on work done by Hadley et al(22).

A brief description of the components that make up the ITS apparatus are described below.

1. G.D.S 1000 cc/2000 kPa digital controller was used for the pressure source/pump
2. An hydraulic jack was designed and built to produce the force.
3. (i) A redundant CBR load frame was used to mount and test the specimens
   (ii) The configuration of the loading strips and guide posts was manufactured in accordance with that described in the tentative method for the determination of the ITS of stabilized materials (Method A16T) of TMH1 (56)

The accuracy of the GDS activator is presented in Appendix B. A maximum stress and strain rate of 30kPa and 8mm/min can be achieved.

5.3.2 Jack design

The jack cylinder comprised of a spun glass reinforced polyester (G.R.P.) with a mica type finish in the bore. This material is inert to most solutions and has a high abrasion resistance.

The top and bottom plattens of the cylinder were machined from aluminium with the inlet and outlet pressure supply entering the jack in the centre. This was done so that the plattens could easily be machined to accommodate smaller diameter cylinders if the need arose. Grooves were cut to accommodate a sealing O-ring and align the cylinder, which was held together with M10 studs.

The piston used was an ex-stock 100mm diameter double acting rubber encased steel plunger. The safe maximum pneumatic operating pressure was 15 bar but an hydraulic pressure could be increased to 20 bar.

As an experiment to check the reliability of the piston seals, a pressure of 19 bar was applied, which resulted in a loss of 0,79% over 60 hours which was considered very acceptable.

The force produced by the jack was transferred via a 20 mm diameter stainless steel rod which was guided through a nylon bush in the top platten of the cylinder.

Deairing the cylinder cavity was done by repeatedly extending and retracting the piston with the outlet immersed in deaired water.

Friction in the apparatus was allowed for in the software by providing a routine which checks, reads and corrects for it. The friction in the cylinder, and load plattens, was found to be about 20kPa.

5.3.3 Design and modification of load frame and load plattens

The load frame used was a redundant portable manual CBR load apparatus. The 4mm square thread on the rod suffered from a seating error (due to slack) when loading was taking place, causing a considerable jump in the vertical strain. Slack in the reaction rod thread was overcome by machining a knurled lock nut to prevent any movement. The load apparatus had already been built according to the TMH1(56) testing manual. The ITS apparatus was mounted on top of the jack so that the load was applied from the bottom and the reaction was provided by the adjustable reaction rod at the top of the specimen(see Fig.5.2 and Fig.5.3). As 100 mm proctor specimens had been chosen, the 19 mm wide load plattens had to be modified to 12 mm. This was achieved by machining a 50 mm hollow face radius in 12 mm plattens and bolting them on to the old 19 mm plattens with cap screws.

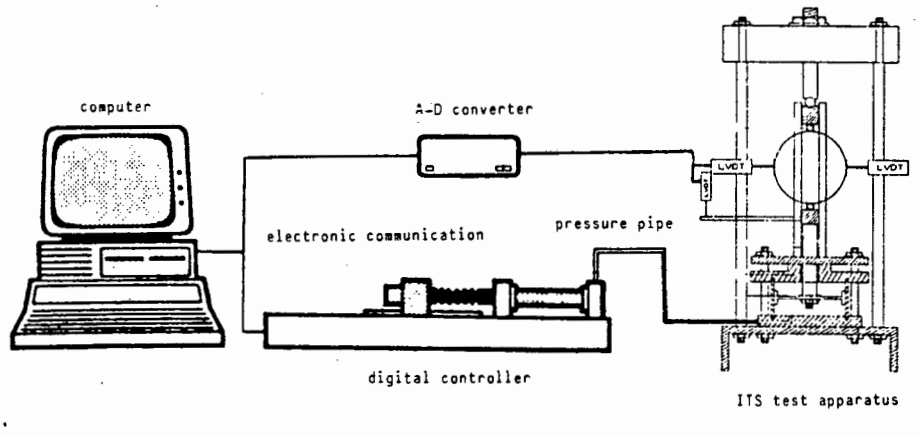

Fig. 5.3 Diagramatic layout of the ITS test apparatus and peripherals

5.3.4 Strain measurement

Strain was measured using NOVOTECHNIK LINEAR VARIABLE DISPLACEMENT TRANSDUCERS (LVDT), which works on the principle that as the reaction head moves through its operating stroke it varies the output voltage linearly. The success of the LVDT's in this project application was due to the bearings at either end of the body. The bearings held the core centrally as side forces were experienced during horizontal strain.

All electrical connections, where possible, were soldered and individually insulated with heat-shrink to prevent interference. This was verified by stretching, bending and knocking the cable in a no-strain situation to see if a scatter of readings occurred. No drift was experienced if a specimen of readings were taken for a continuous period of 15 minutes. This time period was deemed satisfactory for static tests. One vertical and two horizontal LVDT's diametrically opposite each other were located around the specimen. The advantage of two horizontal LVDT's is that the horizontal diametrical strain is summed and if side ways movement were to occur it would be accounted for. The gauging head on the LVDT's are standard with hardened roller-ball points which penetrate into the material when used as horizontal displacement transducers.

To alleviate this problem 15mm x 7mm x 1mm stainless steel skid plates were made, so that the extreme position would always be measured. The success of these plates depended entirely on the squareness of the plate with respect to the LVDT shaft. For monitoring extreme diametrical displacement after many trials, it was found that these were responsible for varying vertical as well as horizontal strain ratios.

Absolute rigidity was achieved by mounting of the LVDT's on 50 x 8mm plate held together with 5mm cap screws.

Calibration was achieved by manufacturing a calibration apparatus which consists of a clamping device which rigidly clamped an LVDT in place while the gauging head was butted against a micrometer which could measure repeatably to 0,001mm over a range of 25mm. The resolution achieved was 0,002mm.

A summary of problems encountered while developing the strain measurement equipment is presented in Appendix B.

5.3.5 Power Supplies

The main incoming power supply was smoothed with a voltage stabilizer which guaranteed no fluctuation exceeding 1% at 250 volts. Each individual LVDT was supplied with a 10volt DC supply of high stability.

5.3.6 Software

The software was written for a Hewlett Packard 86B micro computer. The software consists of three programmes as follows:

Calib 4 which performs the calibration procedures for the LVDT's and plots the calibration curve.

ITS16 which controls the G.D.S. activators and logs all the data while an on going plot is displayed on the monitor. Table 5.1 illustrates a flow diagram for programme "ITS16".

PLOT has the facilities to plot the different variables in an x,y format with self scaling facilities and an optional linear regression if needed.

5.3.6.1 Calibration programme "Calib 4"

The programme provides a facility to read 30 readings of one single physical position of the LVDT later to be averaged. The least squares linear regression is plotted along with the gradient (m) and the intercept (c) in the linear equation y=mx+c. After completion of the calibration the ITS16 programme is automatically loaded and run.

5.3.6.2 Control programme "ITS16"

The programme checks if calibration of the LVDT's is required or whether the calibration constants are known. The option of a friction check is available to allow for drag and losses in the hydraulic system, afterwhich the specimen details and loading rate is entered. The specimen is placed in the test apparatus and a surcharge bedding load is applied which includes the friction correction. The specimen is placed in the test apparatus and a surcharge bedding load is applied which includes the friction correction. The specimen is loaded at the desired rate after the initial strain readings are taken. The progression of the specimen stress and strain is plotted on the screen allowing the user a visual check of the state of the test, and whether it is operating properly. The test is terminated after the required number of cycles has been applied or by user intervention. Data may be stored on disk afterwhich the results may be plotted or a new test commenced.
A flow diagram of the control programme is illustrated in Table 5.1.

5.3.6.3 Plotting programme "Plot"

The plotting programme has the facilities to:

(a) Load the data stored on disc.
(b) Tabulate the strains, and also vertical and horizontal stresses.
(c) Plot any of the ten variables against each other and fit a linear regression by least squares of the plot up to failure.

The variables that may be plotted are:

1. Time (sec)
2. % Vertical Strain
3. Axial Stress (kPa)
4. % Horizontal Strain
5. Tensile Stress (kPa)
6. Load (kN)
7. Vertical Strain
8. Horizontal Strain
9. Vertical Displacement (mm)
10. Horizontal Displacement (mm)

The programme calculates the scale to plot all the data of the two listed variables. However, with user intervention different scales may be chosen.

More than one graph may be drawn on the same set of axes either using different line types or pen colours.

The sampling rate is rapid enough so that the curve may be drawn by joining the individual points by straight lines.

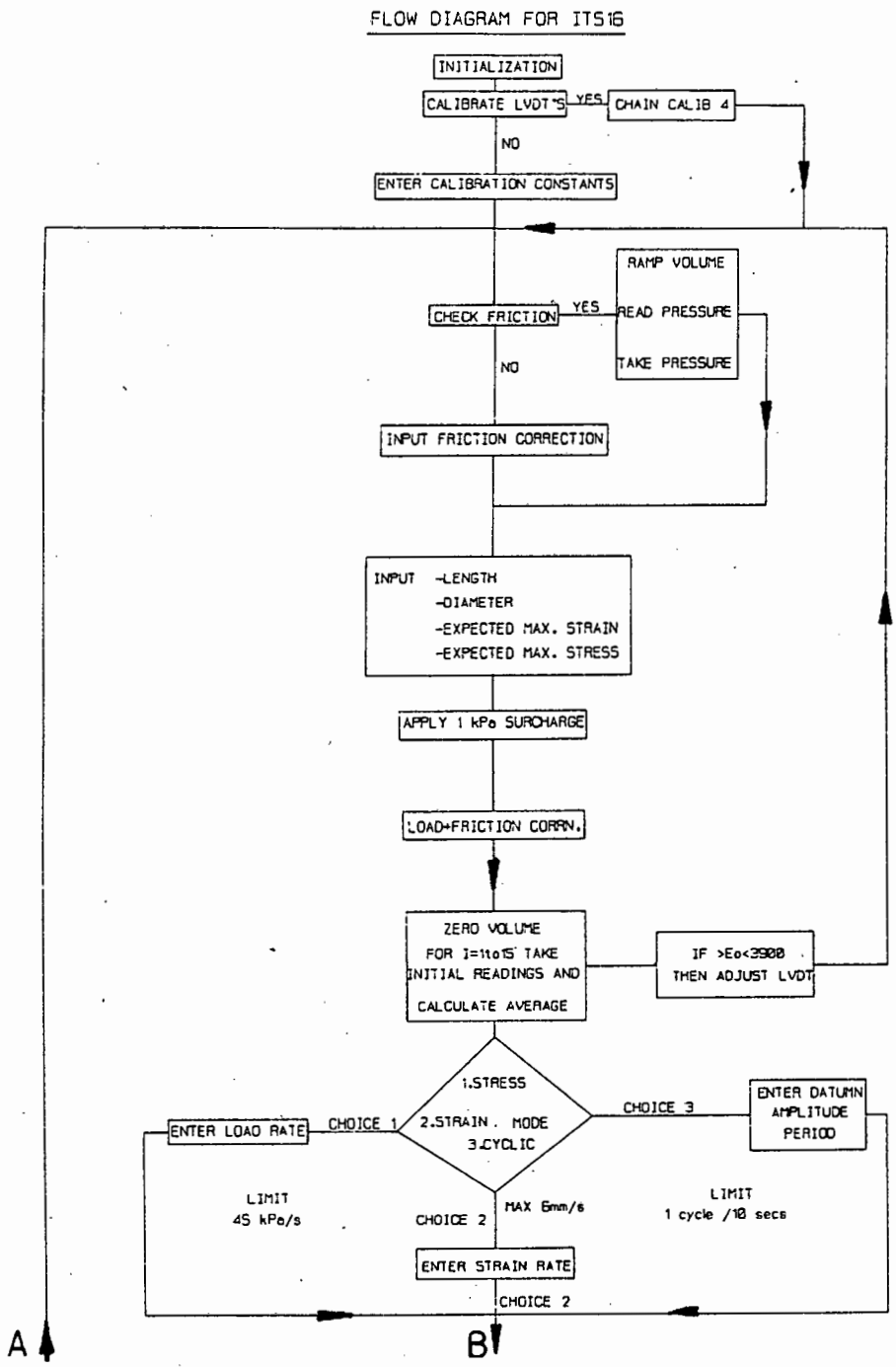

Table 5.1a Flow Diagram for Programme "ITS16"

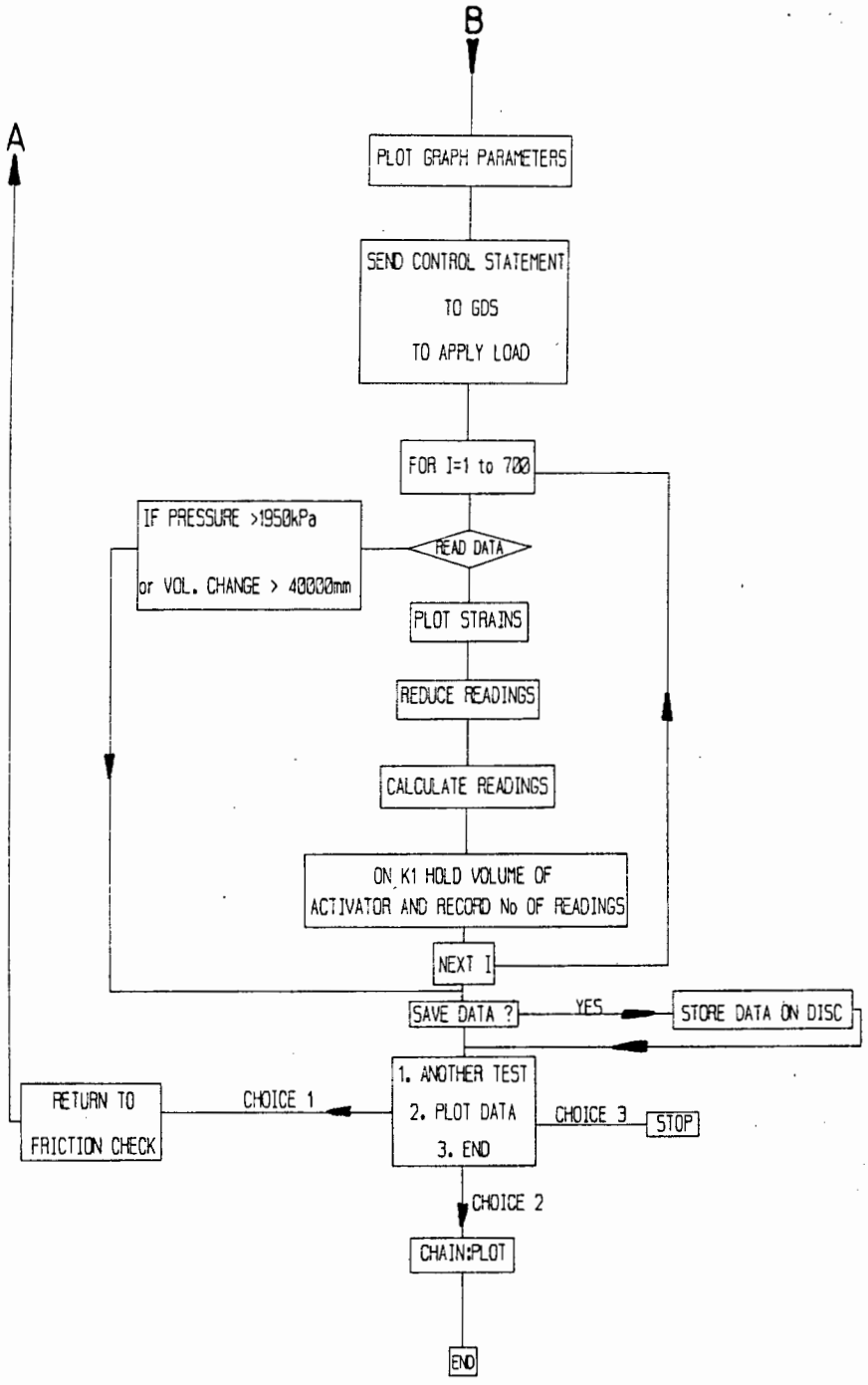

Table 5.1b Flow Diagram for Programme "ITS16"

5.3.7 Analogue to Digital Converter and Calibration of LVDT's

The A-D converter used for this testing/ development work was a MICROLINK produced by Biodata. The microlink is a modular hardware interface, specially designed for connecting laboratory instruments to micro-computers. It is completely compatible with an IEEE-488 standard instrumentation interface.

Calibration of the LVDT's was achieved by using the programme Calib 4 and a test calibration jig which was built to mount the LVDT's and a micrometre on.

The LVDT was mounted and slid along the bed until it was in a position so that the micrometre could be used to measure the operating range and then calibrated using the program to derive the linear equation. This procedure was followed on all three LVDT's.

5.4 Observations during specimen testing

Specimens were moulded by dividing the correct amount of treated soil into 6 layers and compacting each layer into a 115x100mm mould and using a vernier to ensure that each layer is compacted to the correct depth. This was done to ensure that no density gradient would occur.

When specimens were tested a note was made of which end was the top and bottom of the specimen. It is of interest to note that the top of the specimen displays the crack and quite often the bottom has no visible crack when the maximum load is achieved. This observation appears to indicate that a density gradient occurs across the length of the specimen.

Doshi et al(47) indicate that tensile strength increases with density and this was verified with specimen numbers BR18-BR21 compacted at 95% mod. AASHTO density and specimen numbers BR14-BR17 were compacted to 100% mod. AASHTO density. This phenomenom indicates that the compactive effort of the upper preceding layers is transferred down to the lower layers causing them to densify. By ensuring that the plattens remained parallel at all times by clamping the top after a seating surcharge was applied via the ball joint did not prevent the less dense end of the specimen from failing first.

It is disturbing to note that the plane stress analysis assumes that the failure first occurs in the centre of the diameter and length of the specimen, this appears not to happen as cracking occurs at an end of a sample well before failure occurs during testing.

Whether the maximum horizontal displacement should be measured at the end of a sample where failure occurs should be considered, but alternatively if this situation is investigated the stresses would not be easily verified analytically.

During the process of testing some 60 proctor sized specimens, it was found that some deformation ratios were far too large ie., $\varepsilon y/\varepsilon x>14$ resulting in unrealistic Poisson's ratios. This condition is attributed mainly due to the very small horizontal strains experienced while testing lime modified Berea Red soil.

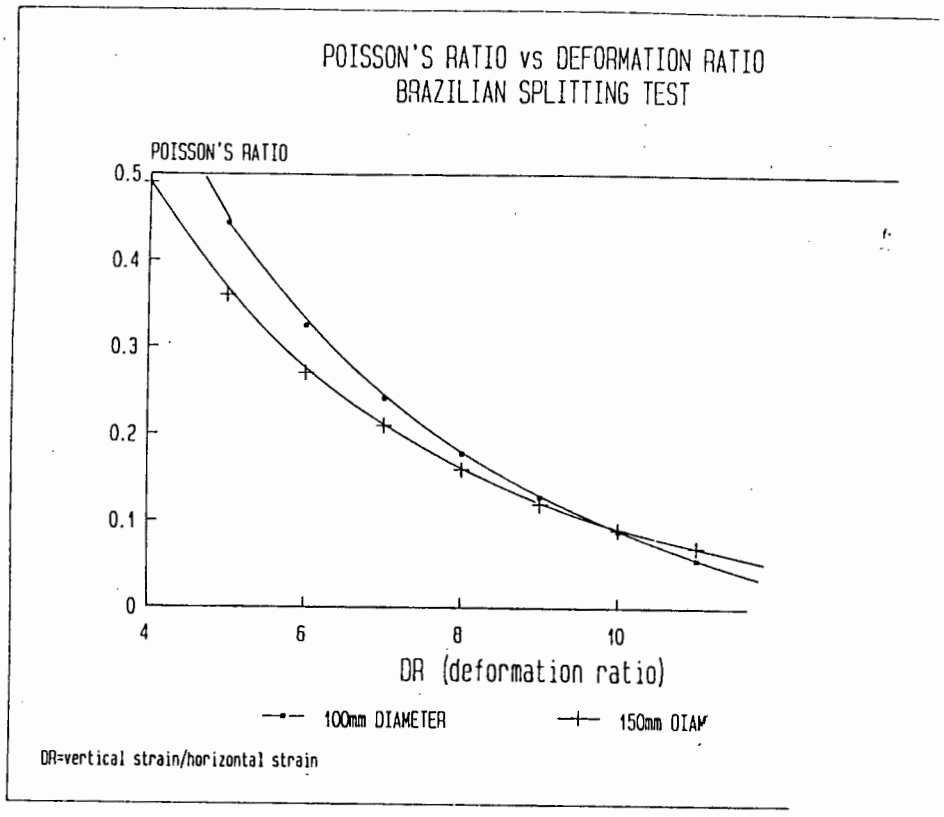

Fig. 5.4 Relationship between Deformation Ratio Poisson's Ratio.

The latter two inherent problems discussed highlight that the ITS is a good indicator of the geotechnical soil properties that can be derived from it, but it appears not always to be the most reliable test since other external properties need consideration.

Berea Red soil compacted to 100% mod. AASHTO density is a highly dilatant material. Hence to obtain an effective tensile stress, it would seem reasonable to load the specimens slowly, allowing negative pore water pressure to disperse and obtain a lower tensile failure stress.

Knowing that the Berea Red soil was to be used as a road material it is normal to compact at or below OMC. Hence the decision to mould and test the specimens at the maximum dry density and OMC appeared to be the correct choice.

To clarify the testing rate dispute, five unstabilized Berea Red specimens were tested at stress rates of 1, 2, 5, 10, 15kPa/s (dry density 1960kg/m^3 at a moisture content of 10,4%) which were the minimum and maximum operating speeds of the equipment built at the time that this investigation was carried out. (The speed has subsequently been increased to 60 kPa/s). It was found that the tensile failure stress was exactly the same. It is thought that the Berea Red soil is a fairly free draining material which allows excess porepressure to be dispersed reasonably fast if unconfined.

It is the author's opinion that a correction for the local straining in the compression zones at the supports could be taken into account, but the question that has to be asked is whether the straining is immediate or proportional to the stress applied as this would clearly affect the deformation ratio D_R. It is interesting to note that Kennedy(22) does not mention this problem, but does loosely say that "the test can be used to evaluate all stabilized materials except cohesionless materials."

5.5 Indirect Tension Testing Results.

ITS tests were performed using a series of additives, based on the percentage dry mass of Berea Red Soil which included 0% to 8% lime in increments of 2% at 7 days and 28 days curing, and 2% to 6% cement at 28 days curing.

5.5.1 Curing of stabilized specimens

Curing was achieved by first extruding the specimen from the proctor mould by means of a jack, which was then weighed. The specimen was labelled and dated and placed in two plastic bags which were individually sealed. Curing was not done in a waterbath as the area they were stored in had a reasonably constant temperature range (15° -21° C).

5.5.2 Loading and testing of ITS specimen

(a) Initialize the programme
(b) Return jack to lower position
(c) Mark target points on specimen ends where load plattens should meet.
(d) Insert specimen line up targets, insert top load platten, and lower vertical reaction rod.
(e) Set horizontal LVDT's and ensure skid plates are clean and square.
(f) Apply a bedding surcharge load.
(g) Run test under computer control.

5.5.3 Calculation of results

The four important properties obtained at failure are summarized below with the derivation of the equations presented in Appendix C.

a) Tensile failure stress: σ_t

$$\sigma_t = 2F(i)/\pi t L_o \times (\sin 2\alpha - t/D_o) \qquad [1]$$

t = width of load platten [mm]
D_o = diameter of specimen [mm]
L_o = height of specimen [mm]
2α = the angle subtended by the load platten and the centre [rad]
$F(i)$ = applied load at reading number (i) [N]

b) Poisson's ratio (for 100 diameter specimens)

$$\gamma = \frac{0,0673D_R - 0,8954}{-0,2494D_R - 0,0156} \quad [2]$$

D_R = deformation ratio (vertical strain/horizontal strain) slope of the best fit line by linear regression from 0 to point of failure.

ç) Elastic modulus (Mpa) (for 100 diameter specimens)

$$E = S_H/H\ [0,9976\ \gamma + 0,2692] \quad [3]$$

S_H = horizontal tangent modulus [applied load (N)/horizontal deformation(mm)] up to the point of failure.

H= height of the specimens [mm].

Total tensile strain

$$\xi_{TF} = X_{TF}(0,1185\gamma+0,03896)/(0,2494\gamma+0,0673) \quad [4]$$

ξ_{TF} = total horizontal deformation at the point of failure [mm].

The latter two are dependant among other factors, on Poisson's ratio which is derived from the deformation ratio ($D_R=\xi y/\xi x$) for their evaluation. It was found, however, that Poisson's ratio was evaluated for the specimen with lower percentages of stabilizer without any difficulty. The specimens with high percentages of stabilizer which were much stiffer, showed a total horizontal displacement at failure of less than 6 microns. This implied an average strain reading of 3 microns on both horizontal LVDT's which is 1 micron above the resolution of the instrument. Therefore test results were not sensitive enough to reliably calculate Poisson's ratio. When unreliable values of Poisson's ratio were obtained especially on stabilized materials, a value of 0,24 was used to derive the other material properties. This was the most representative value achieved during testing of natural Berea Red soil.

5.5.4 The effect of stabilizing additives on ITS of Berea Red soil

The ITS of Berea Red soil increases almost linearly with the increase of additive in the case of both lime and cement as shown in Fig 5.5 and Appendix B.

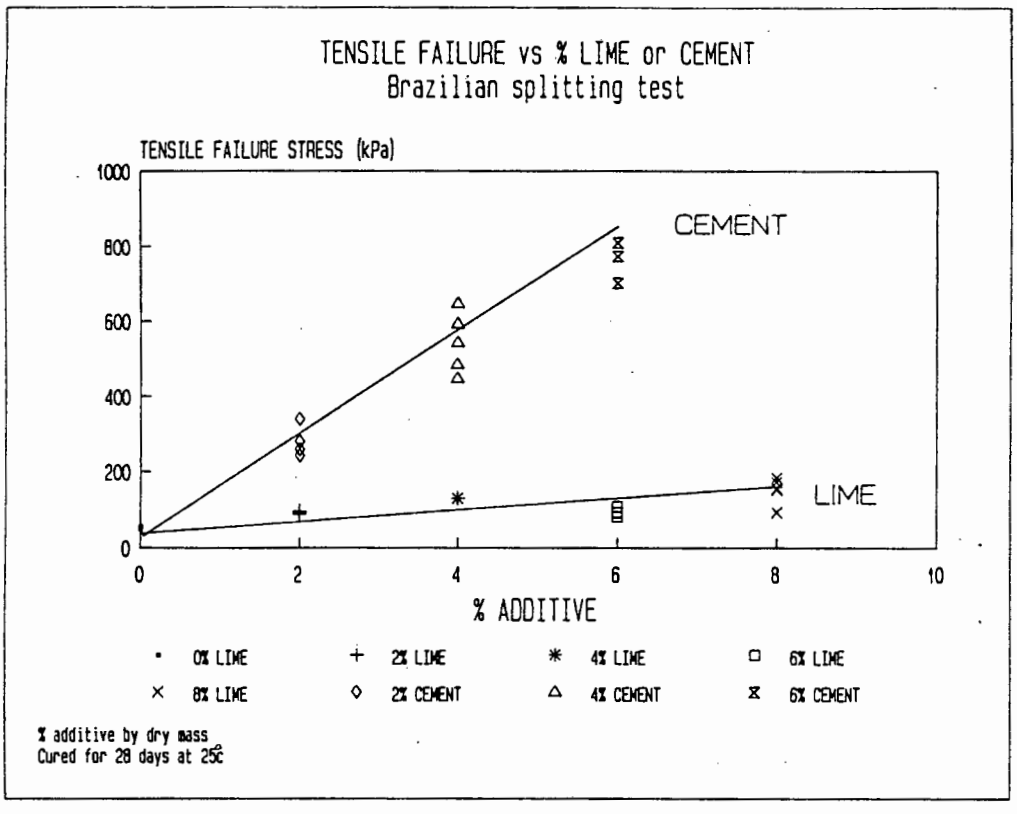

Fig. 5.5 Indirect Tensile failure stress versus % additive added to Berea Red soil

However, the improvement of tensile strength by the addition of cement is eight-fold on the improvement of lime at the same percentage and curing time. It has, however, become apparent from the UCS tests that lime stabilization of Berea Red soil is a slow reaction, which only begins to reach reasonable strengths after 90 days, where, compared to cement in concrete, is known to achieve 95% of its strength after 28 days. Hence, it is not reasonable to compare the two additives at such a young curing age.

5.5.5 The Effect of Young's Modulus derived from the ITS test to the variation of stabilizing additive

Young's modulus was derived from the results obtained from a linear elastic analysis discussed in Section 5.2. The improvement in the strength properties made by the addition of either lime or cement to Berea Red soil are shown in Fig.5.6 and Appendix B. A scatter of results is obtained, but a trend can be observed. The scatter of results is caused by moulded material characteristics and data logging difficulties escpecially with the horizontal strain. Correlation of modulus values obtained from the ITS with triaxial testing will be discussed in Chapter 7.

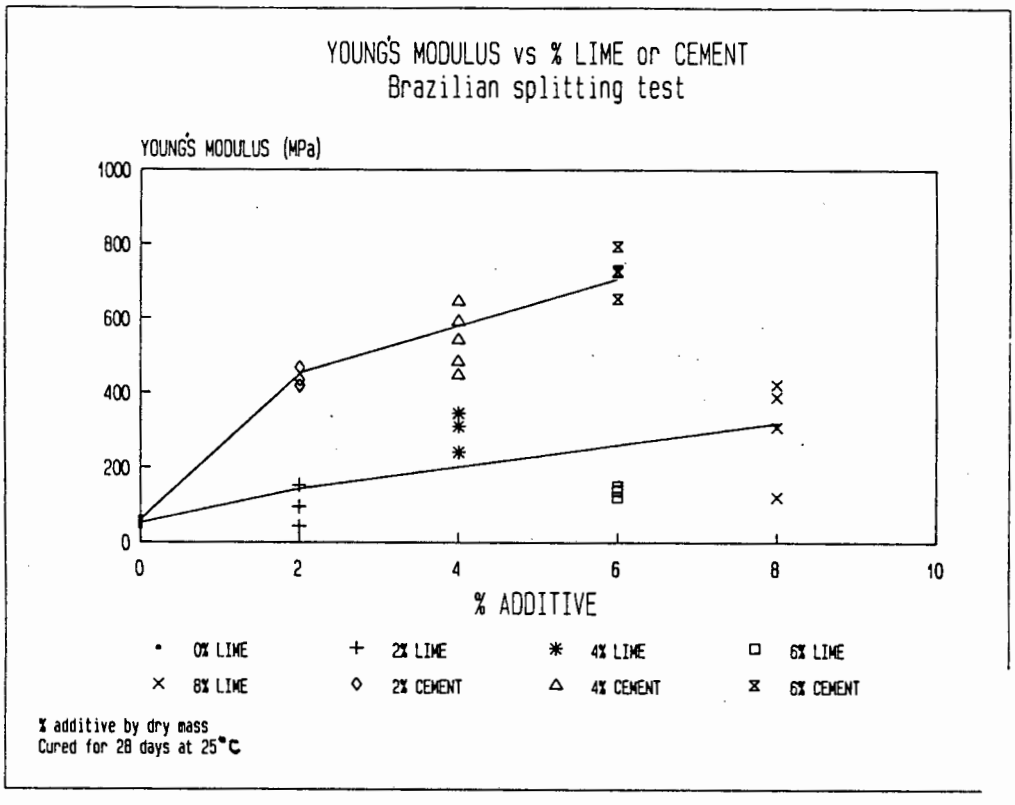

Fig. 5.6 Young's Modulus of stabilized Berea Red soil, derived from ITS tests.

Young's modulus values obtained from triaxial tests reported by Boniface and Olivier(79) (10-52MPa) which correlate favourably to the values obtained from ITS tests performed on natural material as shown in Fig.5.6.

6. ADVANCED TESTING OF NATURAL AND MODIFIED BEREA RED SOIL USING CONVENTIONAL TRIAXIAL TESTING

If a soil was a perfectly linear elastic material it would present no difficulty to determine elastic constants E (Young's Modulus) and ν (Poisson's ratio) from a simple single test. However, soils do not normally posses this property, therefore several special tests were developed to determine the soils engineering properties under controlled conditions. One of these tests was the triaxial test, the implication of which is that three different stresses could be applied along three orthogonal planes of a test specimen. In normal engineering practice standard triaxial tests axisymmetric stress conditions are applied.

The triaxial compression test, as it is used in general geotechnical engineering is a versatile soil test in which triaxial compression is applied where $\sigma_1 > \sigma_2 = \sigma_3$, and the axial principle stress σ_1 acts vertically. Triaxial extension may also be applied where $\sigma_1 < \sigma_2 = \sigma_3$.

The fundamental idea of a triaxial test is to determine the stress-strain and shear properties of the soil under a predetermined stress state.

The stress-strain behaviour of soils is by no means linear and may take on many different forms, ranging from the idealised elastic to an elastic-plastic state which can be compared to the stress-strain behaviour of rubber or mild steel.

The triaxial test procedure known as SHANSEP testing (which is an acronym for Stress History and Normalised Engineering Properties) is a design test procedure to reproduce the stress conditions of the in situ soil. A prediction of the behaviour during, for example, the excavation and construction of a large structure, may be carried out. SHANSEP testing is not easily performed using the standard triaxial cell commonly in use but can be readily applied using a stress path cell. The success of the SHANSEP method depends on close collaboration between the geotechnical design team and the laboratory staff to model the in situ soil conditions to obtain a reliable evaluation of the design parameters.

Bishop & Wesley(85) reported a device in 1975 which they had developed and was capable of reproducing controlled stress and strain paths.

The new triaxial cell was called the Bishop-Wesley hydraulic compression and extension cell. This cell differs from a conventional cell in that axial load as well as cell pressure is applied hydraulically, rather than by a load platten driven at constant speed. Control of the Bishop Wesley cell could be by means of mechano-electrical mercury pressure pots or by means of digital controllers with an integral axial displacement pump which can be controlled by a computer.

A system was developed by Geotechnical Digital Systems (G.D.S.) which, combined with the use of a computer, is capable of controlling most triaxial tests as well as reproducing predetermined stress paths and cycling the deviator stress.

6.1 The G.D.S. Triaxial Testing System

The triaxial testing system as shown in Fig. 6.1 is a schematic diagram which consists of an HP86 micro computer linked to a Bishop-Wesly cell via three microprocessor controlled actuaters called digital controllers. The system has three digital controllers which apply a stress hydraulically in the form of an axial and radial stress and depending on the nature of the test, a back pressure. An additional pore pressure logger may be used for undrained tests. All the controllers have stand alone features which allows the user options to perform pretest checks on the specimen.

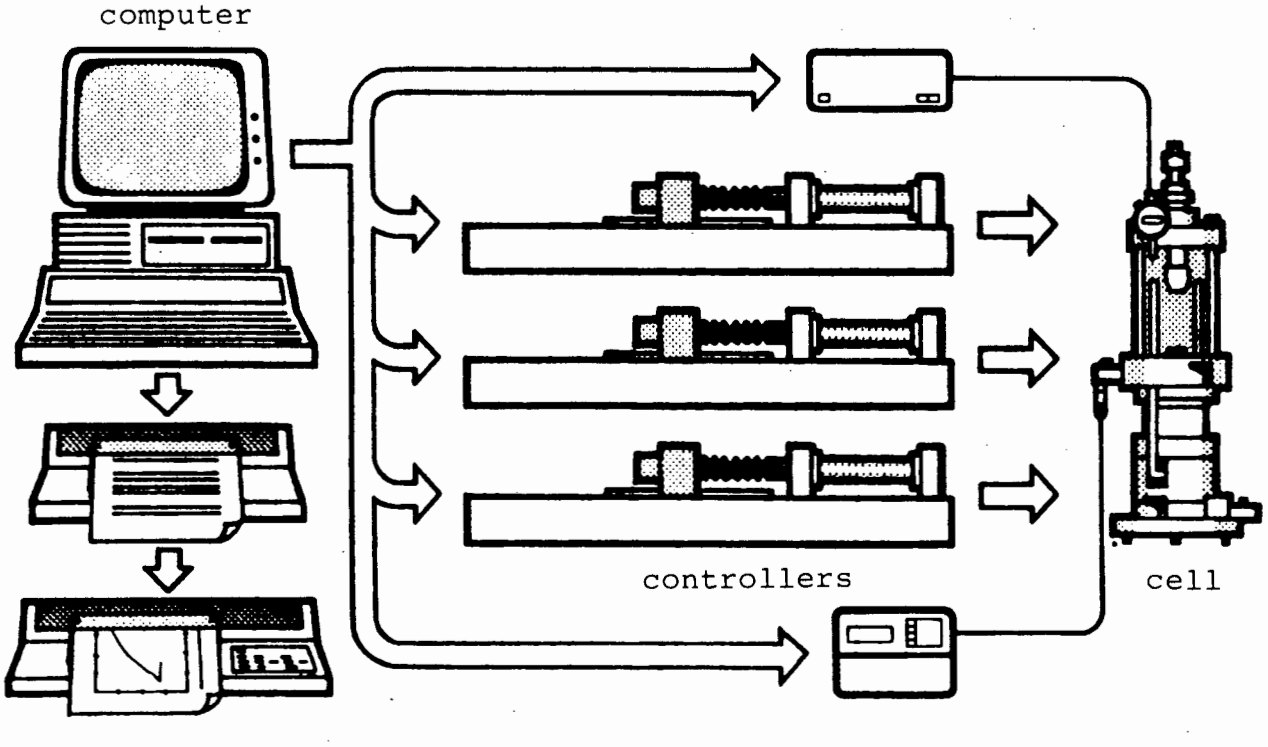

Fig.6.1 Diagrammatic layout of the G.D.S. Triaxial Testing system (Menzies(94)

The Bishop-Wesley cell

The Bishop-Wesley hydraulic stress cell was designed and developed at the Imperial College of Science and Technology, London (see Fig.6.2).

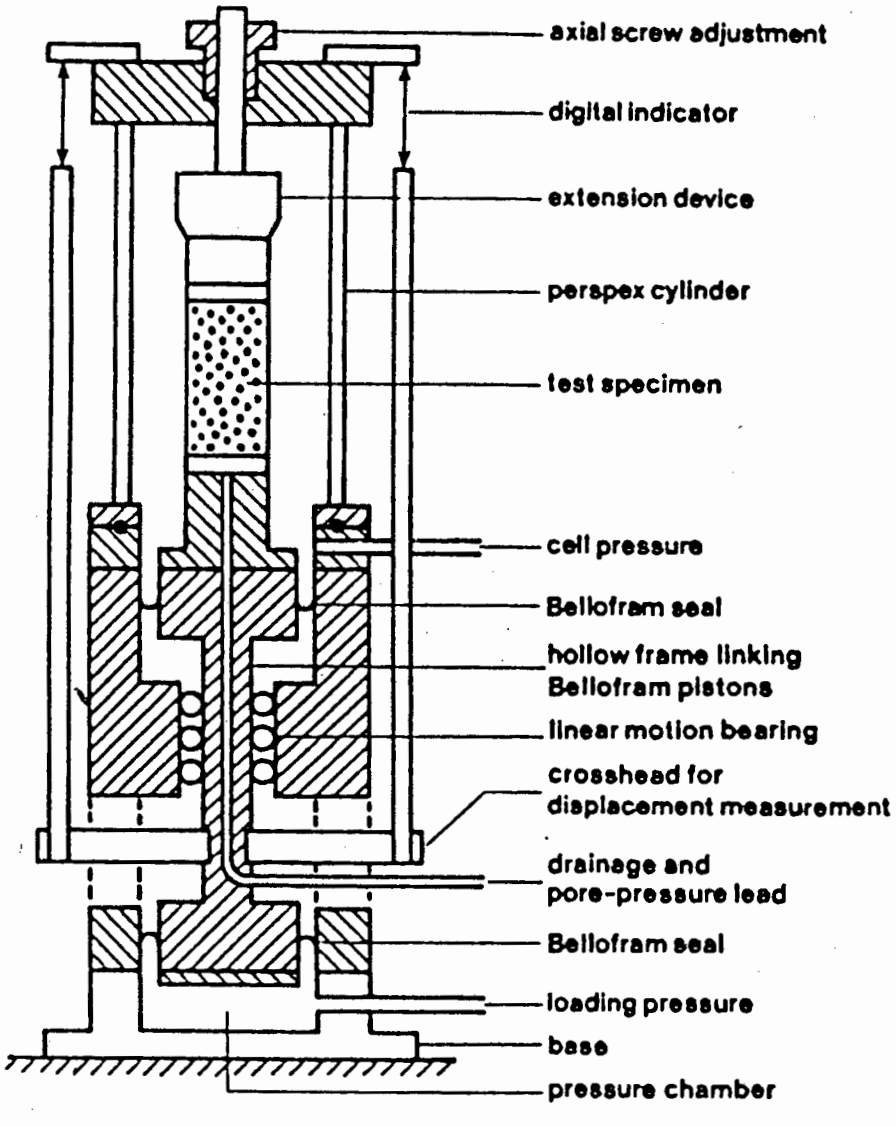

Fig. 6.2 Diagrammatic section through the Bishop-Wesley triaxial cell(Menzies(94))

The cell can accommodate and test 50, 70 and 100 mm diameter specimens.

Successful operation of the cell can only be ensured if deaired water is used in both upper and lower chambers as axial and radial strain is determined by volume change.

Axial deformation rate is controlled and measured by increasing the volume in the lower chamber at a specified rate and removing an equal volume in the cell chamber. Any increase in stress on the specimen is determined by the increase in pressure in the lower chamber.

Axial stress within the sample may be continuously calculated because the strain (lower chamber volume change) may be related to a change in cross-sectional area and the lower chamber pressure may be determined via the ratio of piston and specimen areas. In a computer controlled environment, the stress may be finely monitored and maintained.

Stress paths may be reproduced without causing any discontinuities within the specimen being tested.

Axial tensile stress can be applied but was not done so during this testing program. The digital controller shown in Fig. 6.4 is comprised of three modules, namely the micro processor with pressure transducer, stepper motor, gearbox, and an axial displacement pump.

To increment a volume or pressure, the stepper motor via a gearbox rotates a threaded shaft within a ballscrew which moves the axial displacement pump to achieve the correct volume displacement or pressure. The digital controller has the facility to increase, decrease or maintain a predetermined pressure, or volume. Pressure and volume changes with respect to time can be performed.

The controller communicates with a computer via an IEEE interface. Pressure is measured to 0,2 kPa and controlled to 0,5 kPa. Volume change measurement may be resolved to 1mm^3 which is one thousand times finer than standard volume change gauges used during standard triaxial work.

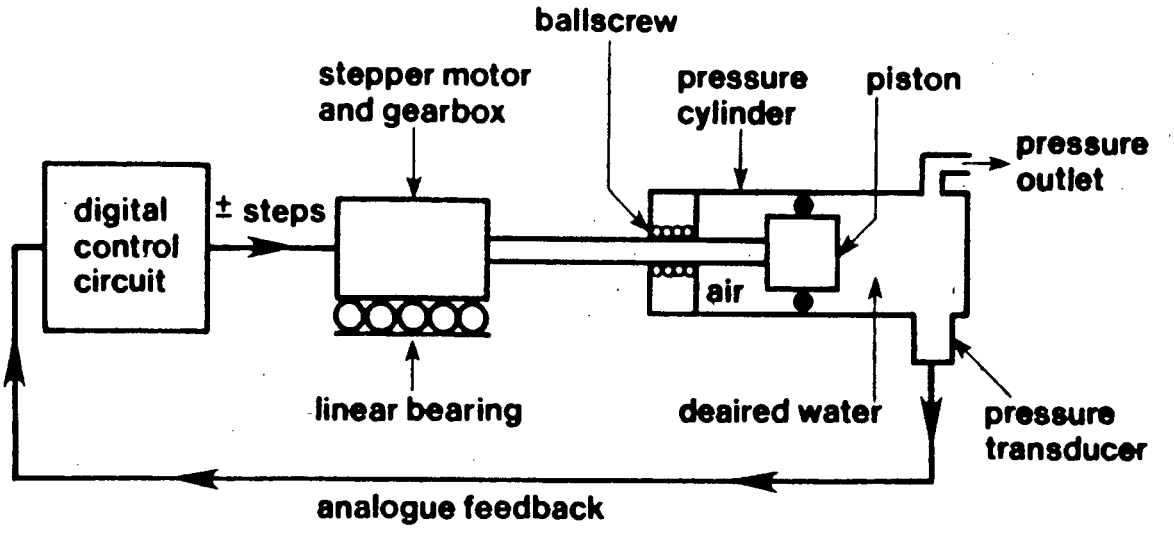

Fig 6.3 Schematic Diagram of the digital controller (Menzies(94))

A pore pressure logger is used to measure undrained pore pressure changes by plumbing a pressure transducer into the pore water block, which is connected to the base of the specimen pore ducts. The pore pressure logger has all the communication capabilities as the digital controller, but cannot change volumes or pressures.

6.1.2 System Operation

The testing system used for this research work was linked to an HP86B computer and the software was supplied by G.D.S.

The software instructs the computer to read volume and pressure changes from the controllers in order to calculate the on-going state of stress, diameter, height, etc. of the specimen. The new parameters are used to update and correct the chosen test path by changing the volume or pressure within the Bishop-Wesley cell chambers.

A wide range of test options are offered by the G.D.S. software as described by Menzies(94). The options which were applied for Berea Red soil testing are listed below:

- ramping of cell pressure and back-pressure to achieve simultaneous saturation

- incremental and ramped evaluation of pore pressure parameter B

- controlled and monitored isotropic consolidation

- consolidated-drained or undrained compression

- cyclic loading by axial stress controlled square, sinusoidal and triangular wave forms; periods down to sea wave period i.e., 1 cycle/minute.

The software is written so that at the end of a test the specimen height, diameter and relevant pressures are carried over to the following test if desired.

Data is stored in the RAM (random access memory) throughout the duration of the test which on termination of a test may be stored on disk. Power failures have caused irretrievable losses of data. A number of simple plot routines are offered to present the test results in appropriate graphs and tables.

6.1.3 Hardware Problems Encountered Prior and During the Testing Program

Prior to the use of the G.D.S. triaxial test apparatus, various problems had to be overcome due to installation and operator difficulties. As the G.D.S. system is the only one of a kind in Africa. All communication and advice with respect to difficulties experienced was sought from the suppliers in the United Kingdom. Many of the problems were overcome by time consuming trial and error. The following problems listed below were experienced and corrective actions are briefly described.

a) Leakdown between cell and back pressure was overcome by using (48 x 3mm) piston o-rings on 50mm specimens to overcome the ingress of cell pressure into the specimen between the membrane and the end caps.

b) Piping and jointing malfunctions were prevented by substituting nylon delivery hoses for P.V.C. as they more suitable for containing the high pressures the system produced. Hose couplers only worked if the pipe face was absolutely square.

c) Loss of manual control due to keyboard lockout was found to be caused by the following factors:

1) Voltage spikes due to heavy industrial plant
2) Voltage drop due to wiring configuration of the laboratory
3) Interference clutter on the IEEE bus due to the plotter being used along with controllers
4) Circulating earth currents via interface cables

d) Erratic oscillations of all activators during a triaxial test was caused by:

1) Long interconnecting piping, causing waterhammer effects
2) Controller reached a maximum or minimum volume or pressure limit causing it to back off, to ensure no damage was caused.

The above problems were overcome by trial and error before testing could commence.

6.2 Preparation and Mounting of Berea Red soil Specimens for Triaxial Testing

Special emphasis has been placed on specimen preparation as many references that were reviewed did not reveal suitable specimen preparation techniques. The standard triaxial testing was performed on specimens moulded at 100% and 95% mod AASHTO compaction, and 0%, 2% and 4% lime by mass. When moulding the lime stabilized specimens the water lime soil matrix had to stand for 4 hours, to ensure that the water was dispersed within the matrix and to simulate typical on site conditions. All the specimens tested in the triaxial apparatus were 100x50ϕmm which was in accordance with the requirements of the A.S.T.M.

6.2.1 Preparation of Natural Berea Red soil specimens

Natural soil specimens were air dried, by placing them on a taupaulin for a day to allow most of the water to evaporate, resulting in a moisture content of about 1%.

The additional water required to increase the moisture content to 10,4% plus an additional 0,5% (i.e. 10,9%) was added to allow for evaporation during handling.

The soil was placed in a plastic bag weighed on a tarred scale. Water was sprayed into the bag in order to achieve an even distribution and minimal moisture loss.

The soil was thoroughly mixed within the sealed plastic bag and was placed in an airtight plastic container. A specimen was taken and tested for the correct moisture content. This was usually found to be 0,3% above required.

The preparation of lime stabilized Berea Red soil was air dried as above to which the required percentage by dry mass of lime was added.

The water was added as described above and allowed to stand for 4 hours, to simulate on site conditions and allow adequate moisture dispersion. A thick walled 2 part split mould with flanged end caps was used for specimen moulding.

A sixth of the total mass of the specimen for each layer was compacted and the height was checked to ensure the correct density. The top of the soil was scored to reduce discontinuities at the interface.

After the final layer had been compacted, the end plug was placed in position and tapped down until the plug flanges were resting on the mould. This guaranteed that the specimen was 100mm high. The specimen was then jacked out, using an extruding plug.

Specimens were weighed and measured immediately after they were extruded. This method worked well and seldom was the mass out by 0,5% assuming the water content was correct, which was checked before and after moulding.

Specimens moulded with lime were placed in old rubber membranes to protect them and then stored in a humid environment.

Before the soil specimens could be mounted, the following preparations and equipment were needed to mount the specimen in the cell. Porous stones were boiled in deaired water for ten minutes to ensure all the air was removed from the stones pores. Four filter papers, two at either end of the specimen were used to prevent bleeding of oxides during saturation.

A standard membrane stretcher was used to place the membrane on the specimen as well as four 48x3mm O-rings. Mounting of the specimen was carried out according to the following procedure. The back pressure controller was set to the target pressure mode at a value of 1kPa. The filter stone and two filter papers were placed on the cell pedestal while water percolated through them. The activator was stopped after 30 seconds.

The specimen (with the membrane on) in the membrane stretcher was placed on to the pedestal while the bottom end of the membrane was gently eased on to the pedestal, followed by the two O-rings ensuring that no creases had been formed. The same was done to the top cap but no O-rings were fitted.

After the membrane stretcher was removed the back pressure activator was set to 1kPa and excess air was kneaded up in front of the uprising water between the membrane and the specimen. When most of the visible air was removed, the top O-rings were placed in position and the top pore-water pressure pipe was installed.

A confining stress of 20kPa was immediately applied by means of vacuum to the specimen to remove excess air. Silicon grease was applied to the top cap seat and reaction rod to prevent slip-stick conditions during testing (Menzies(94)).

Saturation procedure was then followed as described in Appendix C.

6.3 Complications and Procedures Employed to Test Berea Red soil

6.3.1 Negative pore pressures produced during undrained shearing of dilating materials

During the undrained shearing of saturated dense soil, in a triaxial apparatus Head(67), Bishop&Henkel(69) and others found that pore pressure decreases. This condition is bought about by dilation of the lightly packed soil particles. If the initial test conditions are such that the pore pressure becomes negative during shearing, it is possible that cavitation could take place. Cavitation is caused by the reduction of the pore pressure below a certain negative value which causes the water to convert to a gas, and results in an immediate increase in the pore pressure, thus spoiling the test. This condition occurred during the initial stages of testing of Berea Red soil and had to be taken into account. The following section discusses briefly normal procedures to be followed to overcome this condition.

6.3.2. Cavitation of pore water pressure while testing Berea Red soil

During testing of the Berea Red soil it was found that the pore water pressure dropped to a minimum of -40kPa (which is the minimum pressure the G.D.S. activators will tolerate after which they compensate for any additional reduction, nullifying the undrained test).

In soil, it is not possible for the pore water pressure to be less than -100kPa as water changes to gas (i.e., water vapour) at a temperature of approximately 20°C. This is better known as cavitation. The effects cavitation have on the deviator stress are shown in Fig.6.4 after Lambe and Whitman(68). Most dense sands dilate causing the pore water pressure to reduce. In order to allow for this, a minimum pore pressure of 500kPa should be used with naturally a higher cell pressure. Head(67) suggests that the test should be performed on saturated sand in such a manner than the pore water pressure does not drop below 200kPa. Reduction of pore pressure below 150kPa could lead to dissolved air coming out of the solution again in the form of bubbles. In a drained test, the drainage line should be connected to a back pressure system in which a pressure of at least 200kPa is maintained throughout the test.

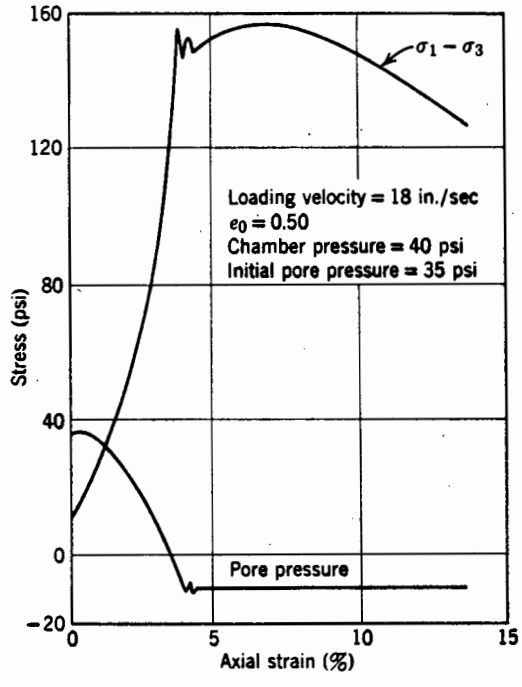

Fig.6.4 Cavitation during undrained triaxial testing of dense sand (Lamb & Whitman(68))

6.4 Investigation into the Effect of Saturation Periods on Lime Stabilized Berea Red soil

Maximum utilization had to be made of the one triaxial cell as many specimens would have to be tested. The result was that the specimens had to be placed in the cell and saturated before the end of the curing period had been reached. The effect of this procedure on the shear strength was investigated on 2% lime stabilized Berea Red soil.

In order to investigate the material behaviour of the Berea Red soil under different moisture conditions, the following tests were performed:

All specimens were moulded on the same day at 2% lime by dry mass and mixed with water to obtain a moisture content of 10,4%.

Each specimen was encased in a rubber membrane and placed in a humid environment.

Specimen 1 was placed into the cell after 7 days of curing and for a period of 21 days was saturated by ramping the cell and back pressures to a maximum of 400kPa. At 28 days after moulding, the specimen was sheared at 2mm/hour in an undrained condition. This was twice as fast as all other testing, but allowed more time to load the other specimen in the cell.

Specimen 2 was cured for 28 days and was immediately loaded into the cell after Specimen 1 was removed, and using the G.D.S. ramp facility, the back pressure/cell pressure was increased quickly and smoothly in steps of 1kPa/25 seconds. This specimen was tested after 9 hours in the same manner.

Specimen 3 was treated as Specimen 2 but sheared after being in the cell for 20 hours.

The main objective of the tests was to be sure that differing saturation times which would include weekends etc., would not significantly effect the test results.

It was found that differences of up to 20 days did not affect the modulus values and stress strain behaviour within the tolerable variation between specimens.

6.5 Evaluation of Stresses in a Pavement during Normal Operational Use.

From the outset of the proposed testing, a decision was made to carry out consolidated undrained triaxial compression tests. The material was to be placed in a pavement as a stabilized subbase or even stabilized basecourse and fill material. Therefore, representative effective confining stresses similar to those expected in situ in the pavement were required, so that the material properties and variations could be examined.

To obtain a representative confining stress, typical highway cross sections were analysed using representative material properties and pavement design depths. The analyses were performed using a programme "ELSYM 5" which analyses 5-layer pavements.

The analysis of flexible pavements includes the analysis of granular material bound with bitumen, cement or lime. Cemented bases or subbases are considered to be in the cracked phase exhibiting granular behaviour as a result of tensile stress caused by shrinkage.

Flexible pavements may be analysed by assuming a pavement to be multi-layered and linear elastic. Programmes used for this type of analysis are usually referred to as mechanistic design procedures.

Linear elastic mechanistic pavement design programmes in use include among others MECD3 (Maree and Freeme), ELSYM 5 (University of California), BISAR (Koninklyke/Shell Laboratium, Amsterdam,) BISTRO and CHEVRON.

The two pavement multilayer linear elastic programmes readily available for this research were ELSYM 5 and BISAR. Both programmes are based on a linear elastic analysis which produce similar stress and strain results for identical load and material conditions. They can be run on an IBM compatible personal computer and uses any standard text editor to generate the data file which is easily loaded and run. The stresss and strain results are automatically tabulated via the printer on completion of the calculations (no graphical representation can be produced). The program Elsym 5 was chosen because of the ease with which the variables could be changed and the programme re-run.

As the objectives of this research did not include for an elaborate numerical pavement study, the readily available computer programme ELSYM 5 was assumed adequate.

6.5.1 Loadings and Engineering properties assigned to the pavement analysis

The legal axle load of 80kN which was applied to the modelled pavement was via a set of dual wheels on either end. Each set of dual wheels were 350 mm apart. The analysis was based on the effect of one set of dual wheels on the pavement. i.e. 2x20kN loads

The program ELSYM5 requires a standard tyre pressure of a heavy vehicle which was assumed to be 520kPa and the load from each tyre was applied over a circular area assumed to be of 110mm radius.

Poisson's ratios of 0,44 were assumed for bituminous materials, and 0,15 for the subbase and 0,35 for all other layers, ie premix, basecoarse and selected subbase (based on work done by Horak(87)).

The range of elastic moduli used was according to the values obtained by the CSIR heavy vehicle simulator and described by Horak(87). The calculated stresses were summarized in graphical format and are shown in Fig.6.5,6.6 and 6.7 for an E4, E3, and E3-stage constructed pavements in a wet region.

The summary shows the effect of loading underneath the tyre of a dual wheel (position 1) and the rapid degradation of stress between the dual wheels (position 2).

Based on the results obtained, a confining stress range from 100kPa to 300kPa was assumed for the standard triaxial compression testing.

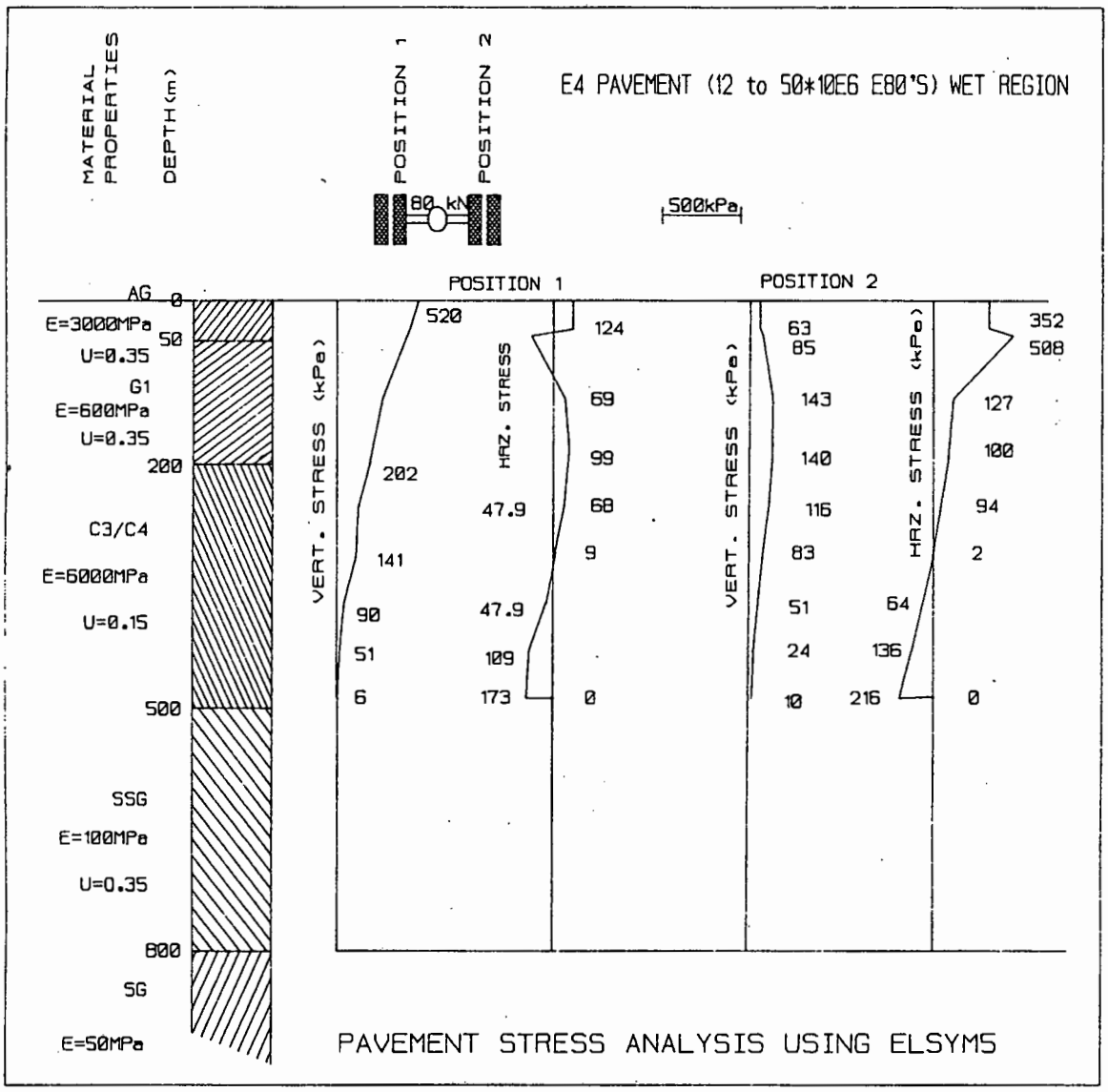

Fig. 6.5 Schematic summary of the estimated stresses for an E4 pavement from the computer program ELSYM5

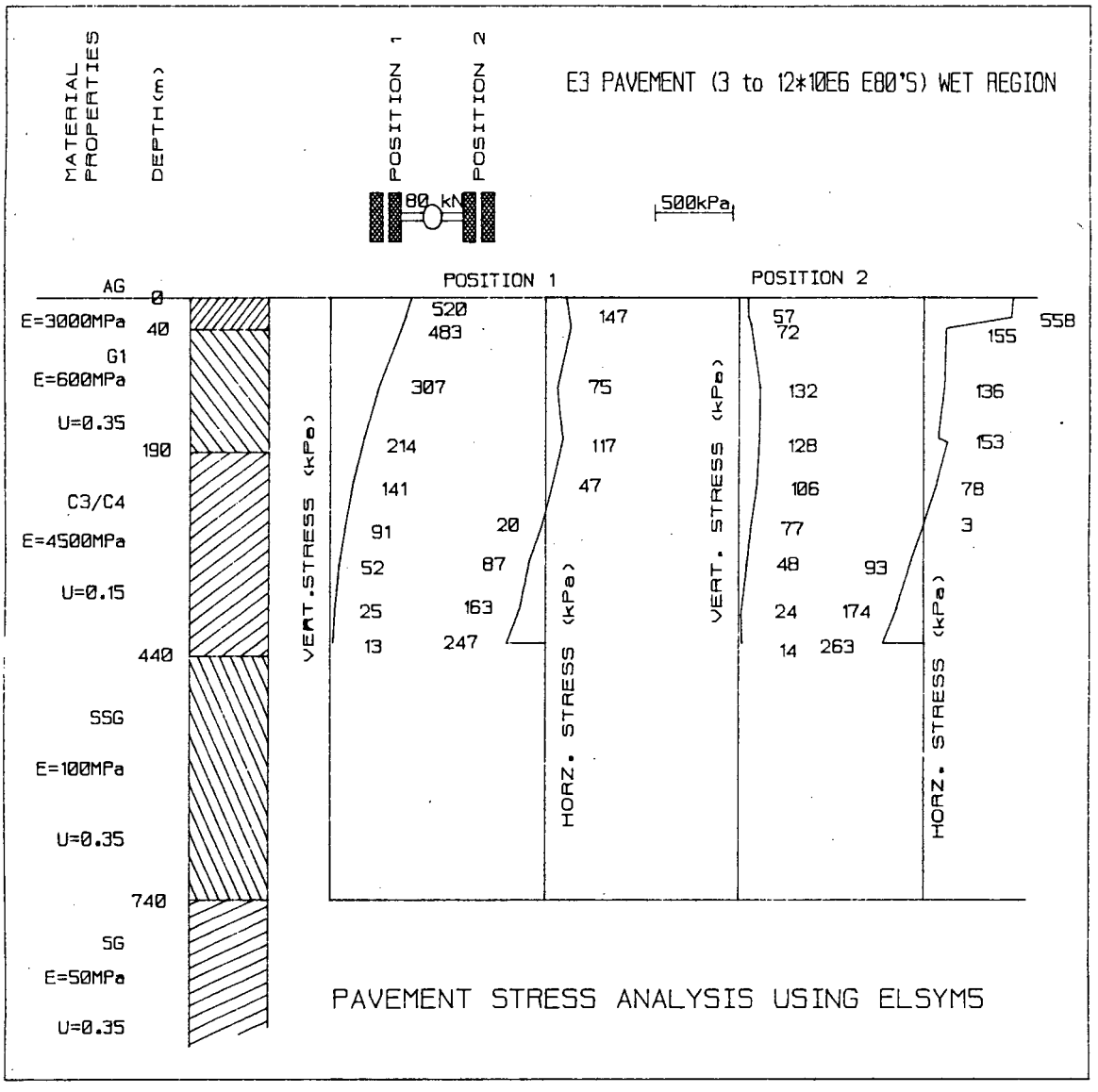

Fig. 6.6 Schematic summary of the estimated stresses for an E3 pavement from the computer program ELSYM5

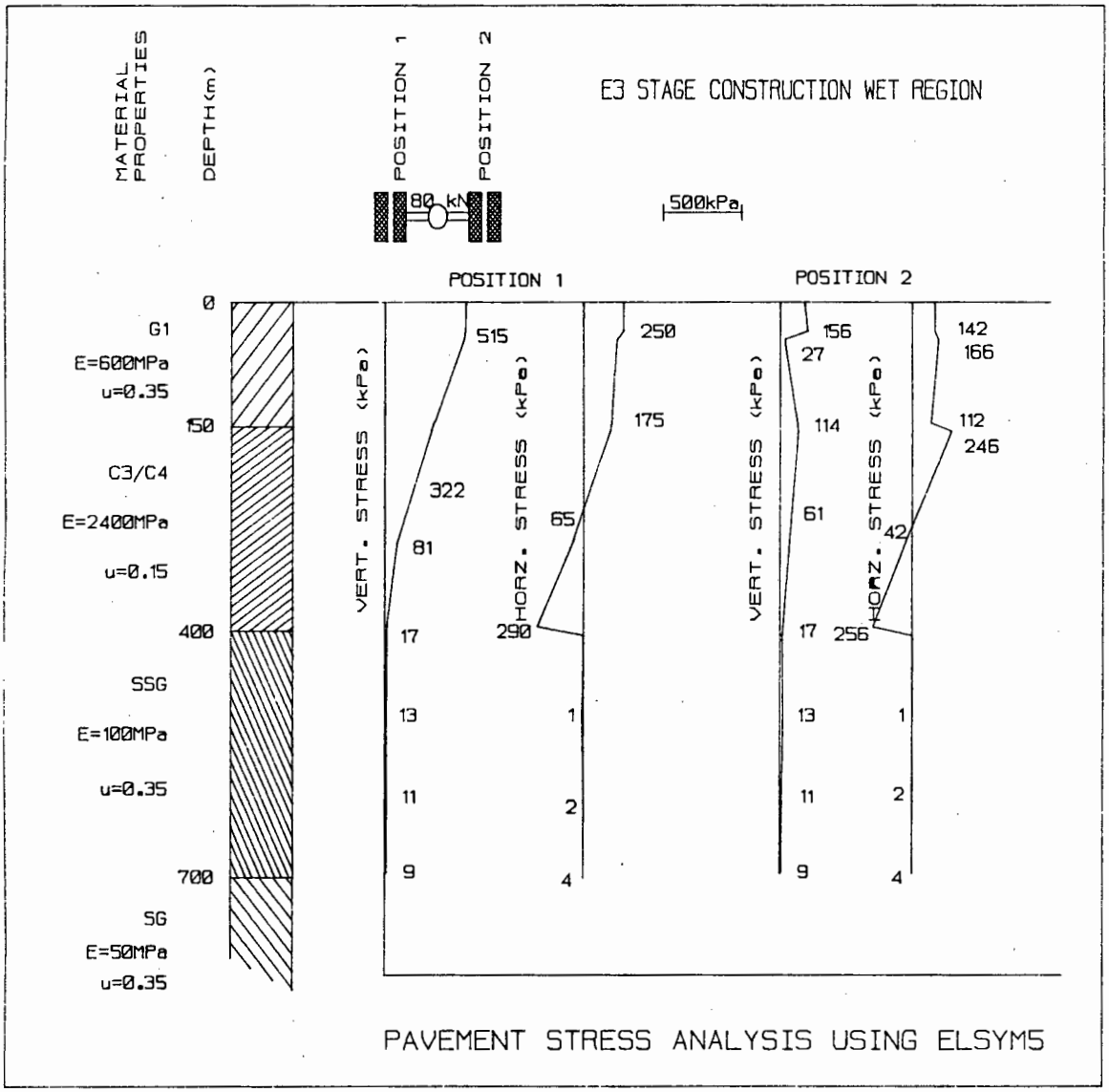

Fig. 6.7 Schematic summary of the estimated stresses for an E3 stage constructed pavement from the computer program ELSYM5

Table 6.1 Summary of horizontal and vertical stresses derived from an elastic pavement analysis

PAVEMENT CLASSIFICATION	HORIZONTAL STRESS (kPa)	VERTICAL STRESS (kPa)
E4	125	480
E3	153	483
E3 STAGE CONSTRUCTED	246	520

6.6 Evaluation of Standard Triaxial Compression Tests Performed on Natural and Modified Berea Red soil

The most important properties for pavement design which can be derived from the stress strain curves and effective stress paths of standard triaxial tests include the elastic modulus, strain at failure, and effective stress paths from which the internal angle of friction and apparent cohesion for a particular material under given test conditions may be determined.

A 100% mod AASHTO density was used as a datum to perform most of the tests. In order to evaluate the effects of a lower compacted density with respect to shear strength parameters, a set of 3 specimens were tested at 95% mod AASHTO density under otherwise similar conditions to the 100% mod specimens.

The initial tangent modulus was derived from the deviator stress versus strain plot. In the case where the choice of the tangent was difficult to determine, particularly for the (95% mod AASHTO density specimens) a secant modulus from zero to half the peak deviator stress was calculated. This would be the equivalent of the maximum vertical stress in a subbase under normal working conditions. The range of moduli values obtained is summarized in Appendix C and Fig.6.8.

There is little increase in the modulus values with increased confinement and lime content over the range tested yet the failure deviator stress is much higher for lime stabilized specimens.

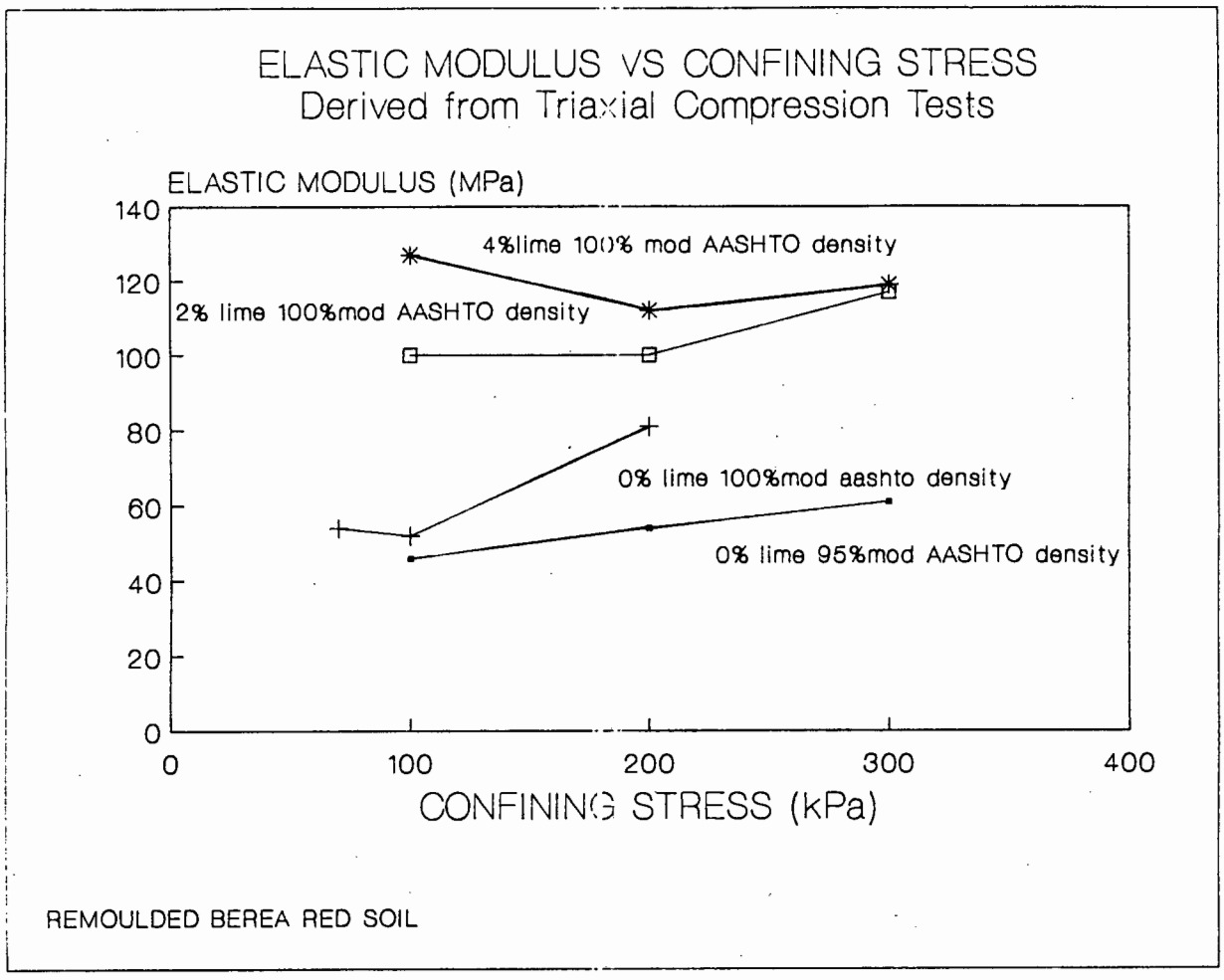

Fig.6.8 Elastic Modulus E of Berea Red soil derived from Triaxial compression Tests

The Young's modulus values obtained from triaxial tests on natural Berea Red soil are comparable to data presented for similar soils presented br Webb(61) and Boniface & Olivier(79), who reported values ranging from 10-52MPa. Poisson's ratio can be derived from volume change measurements taken during the triaxial test. However, as all the testing comprised of consolidated undrained it was not possible to determine Poisson's ratio.

Percentage strain at failure (shown in Table 6.2) is expressed as the strain at which no increase in deviator stress may be applied for an additional application of strain. The lowest failure strains were recorded on natural specimens moulded at 95% mod AASHTO density, and increased for soil which was stabilized with 4% lime and moulded to 100% mod AASHTO density. The averaged failure strains were calculated from 3 tests at varied confining stresses, namely 100,200 and 300kPa as shown in Table 6.1.

Table 6.2 AVERAGE PERCENTAGE FAILURE STRAIN DERIVED FROM TRIAXIAL TESTS OF BEREA RED SOIL

PERCENTAGE LIME (%)	mod AASHTO DENSITY (%)	AVERAGE FAILURE STRAIN ε_f(%)
0	95	2,1
0	100	3,1
2	100	3,24
4	100	3,78

(12 tests)

This behaviour is in contradiction to the results reported by TRB(60). The behaviour of lime treated soil (assuming it is suitable for lime treatment) is reported to produce a considerable increase in elastic modulus and decrease in failure strain. It is thought that the behaviour of Berea Red soil indicates a brittle material due to the sharp initial increase, and rapid drop off of stress at failure during shearing. Berea Red soil does not produce a brittle material, it does, however, appear to produce a larger elastic range with an almost identical elastic modulus with the addition of 2 or 4% lime.

The increased straining over the elastic range can be attributed to the improved cohesion which is discussed below.

The effective stress paths were plotted in order to evaluate the change in shear properties due to different soil treatments and changes in densities. Fig. 6.9-6.11 highlight the changes in shear properties of Berea Red soil moulded with 0%,2% and 4% lime at 100% mod AASHTO density indicates that the effective friction angle ϕ' is reduced with the addition of lime, yet the cohesion is incresed. The results are summarized in Table 6.3. Head(83) observed a similar reduction while shearing lightly cemented soils.

Table 6.3 SUMMARY OF SHEAR PROPERTIES FOR VARIED COMPACTIVE EFFORTS AND PERCENTAGES OF LIME

LIME (%)	mod AASHTO compaction (%)	ϕ' (degrees)	c' (kPa)
0	95	28	70
0	100	42	33
2	100	40	60
4	100	35	80

Head(83) verified this assumption by performing a series of tests on cohesionless sand, which in the one case was in its natural state and the other was cemented. He observed an apparent cementing cohesion in the soil on initial shearing, but on reshearing the same soil no cohesion was apparent.

The first stage of loading mobilizes the cohesive effect of the cementing agent and when the stress level is high enough, breakdown of the cementation occurs. Thereafter the soil behaves as an uncemented natural soil which by that stage has dilated hence, reducing the density.

The high effective friction angle and cohesion of natural Berea Red soil correlates well with the values obtained using the simple shear apparatus discussed in Chapter.3, namely $\phi'=42^{\circ}$ and c'=33kPa.

Barrelling of the samples was the usual failure mode in static compression triaxial tests. However, closer inspection revealed the presence of a typical shear plane in the zone of the barrelling in some of the specimens.

Inspection of the deviator stress strain plots, revealed:

In some tests the stress strain behavior initially displayed a certain amount of stress with no corresponding strain. This condition is caused when the reaction rod in the top of the cell is seated on to the specimen and too much load is applied via the reaction rod before the test is started.

Strain and no corresponding stress is caused by a condition known as "slipstick". If the top cap is not aligned to the axis of the bottom platten then the reaction rod tends to bind to the top cap and with an incremental addition of the deviator stress the rod slips and beds properly. (A silicon grease was used to help eliminate this problem).

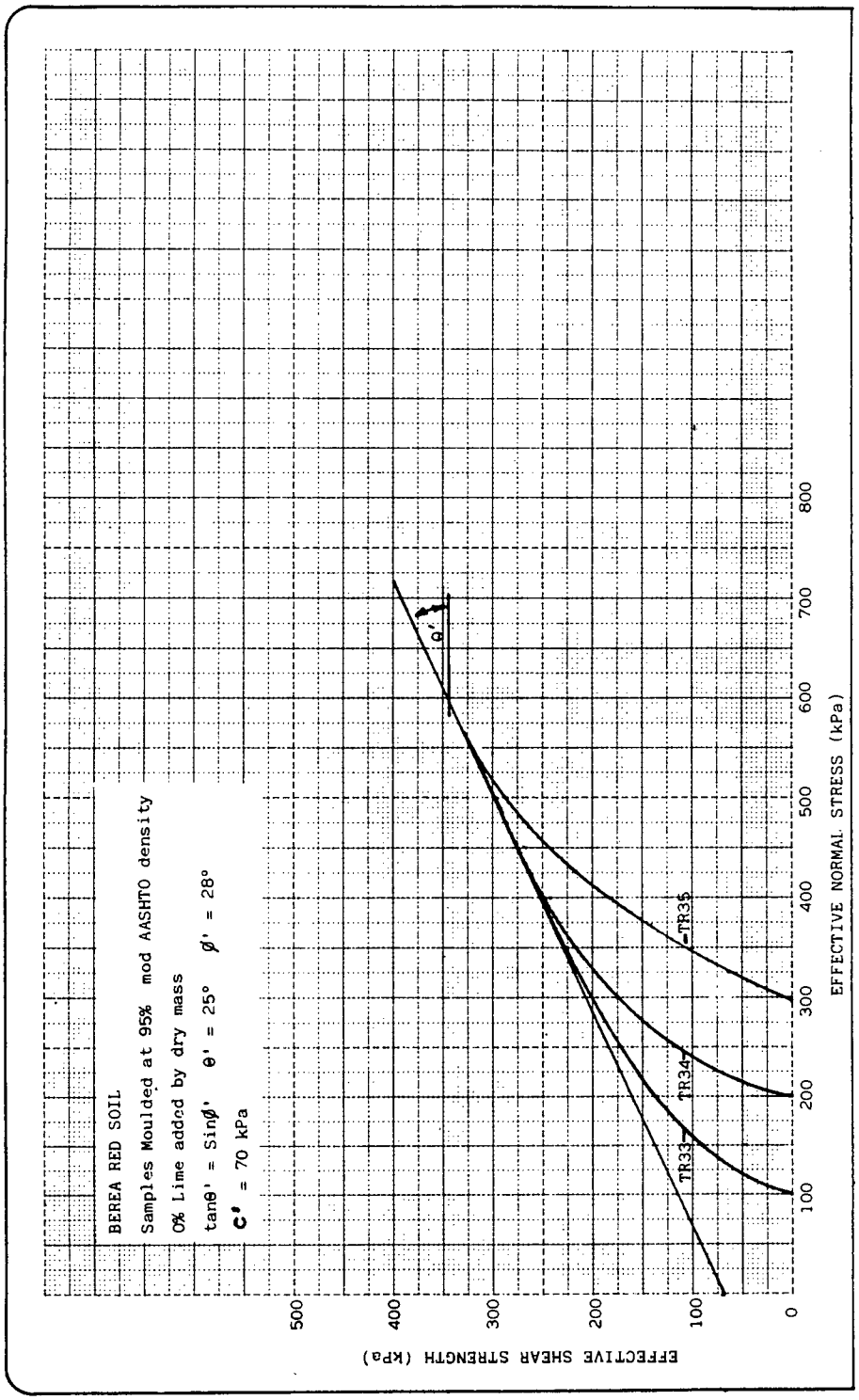

Fig. 6.9 Stress Path Plot of Natural Berea Red soil moulded at 95% mod AASHTO

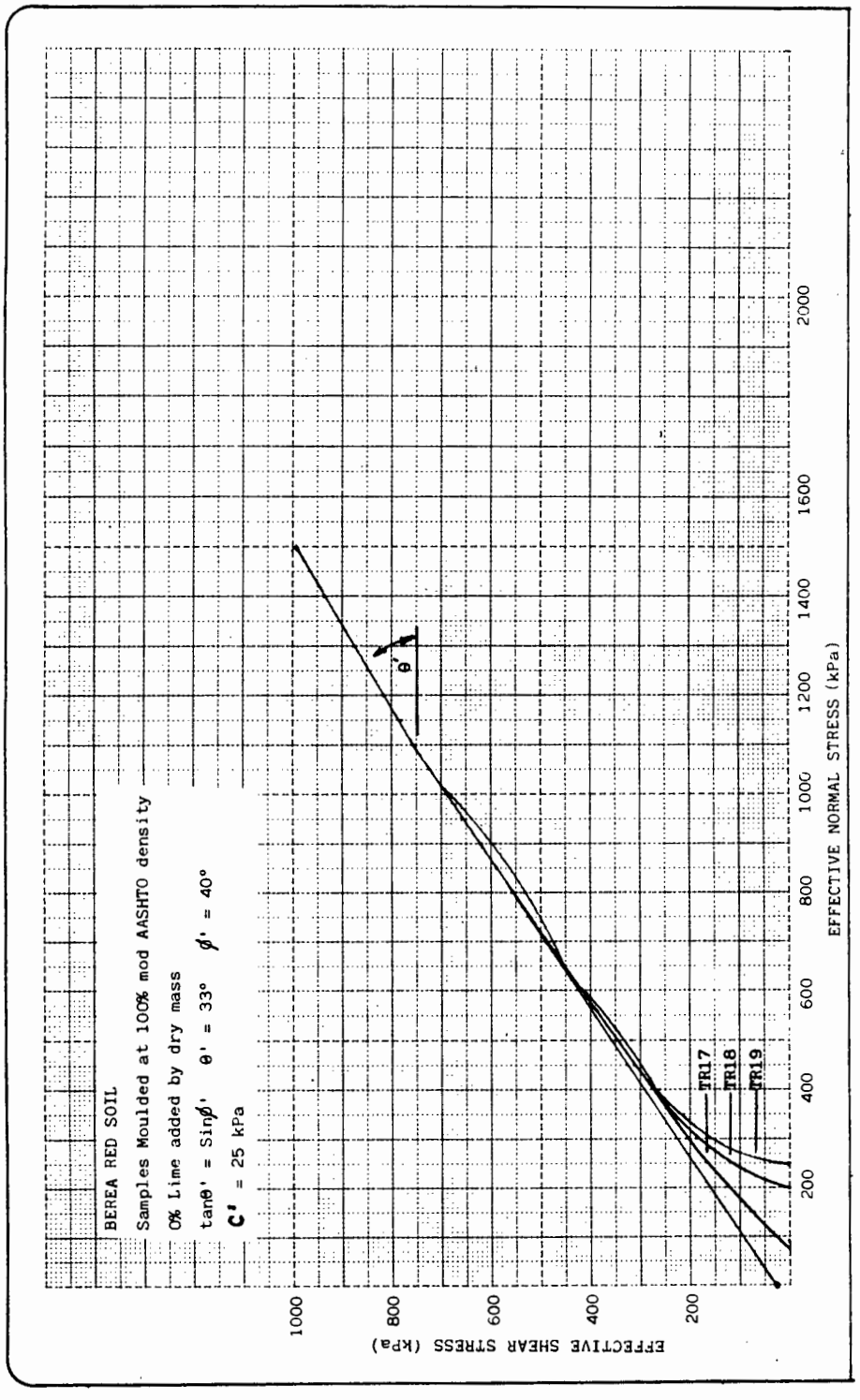

Fig. 6.10 Stress Path Plot of Natural Berea Red soil moulded at 100% mod AASHTO

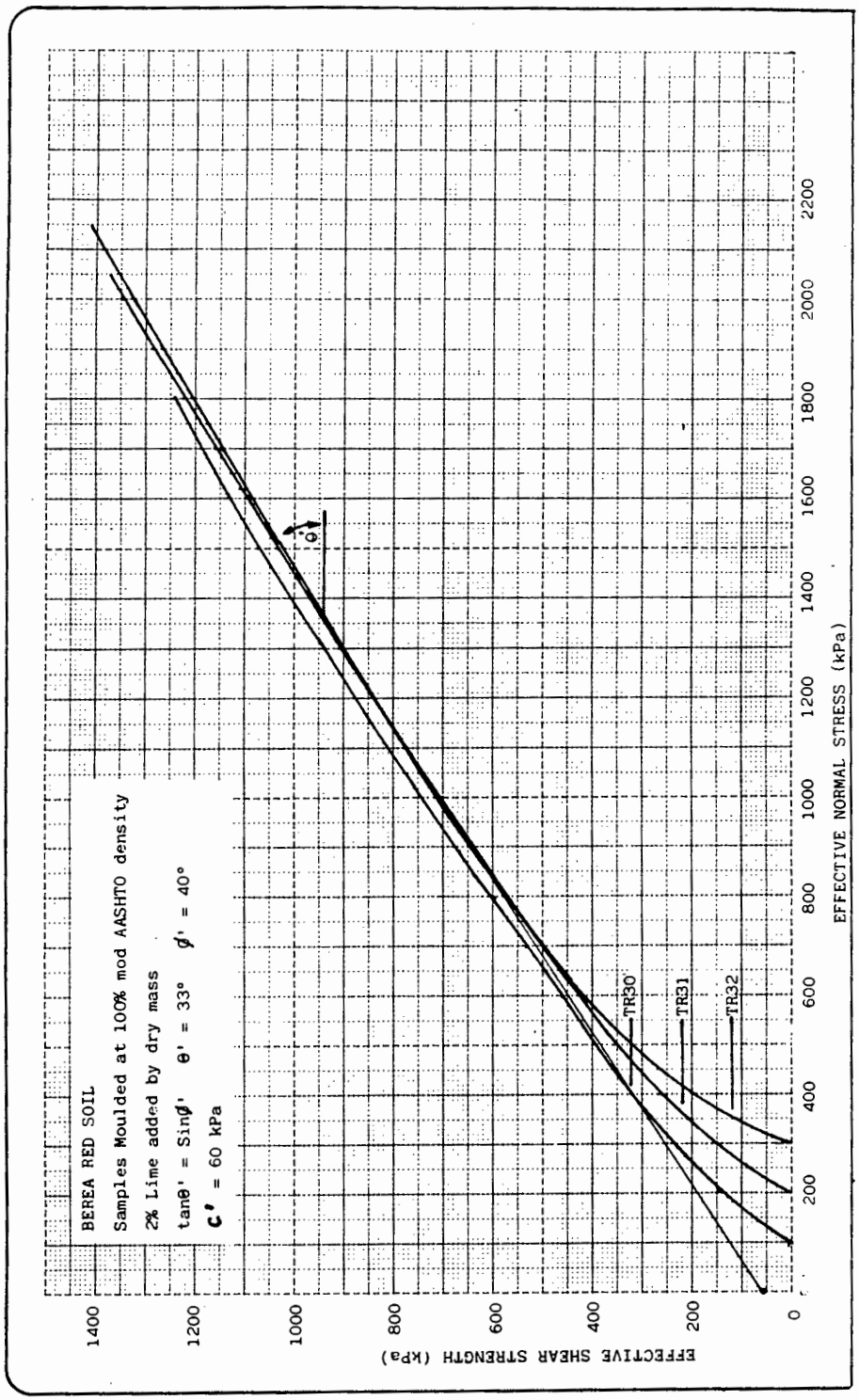

Fig. 6.11 Stress Path Plot of Berea Red soil with 2% lime moulded at 100% mod AASHTO

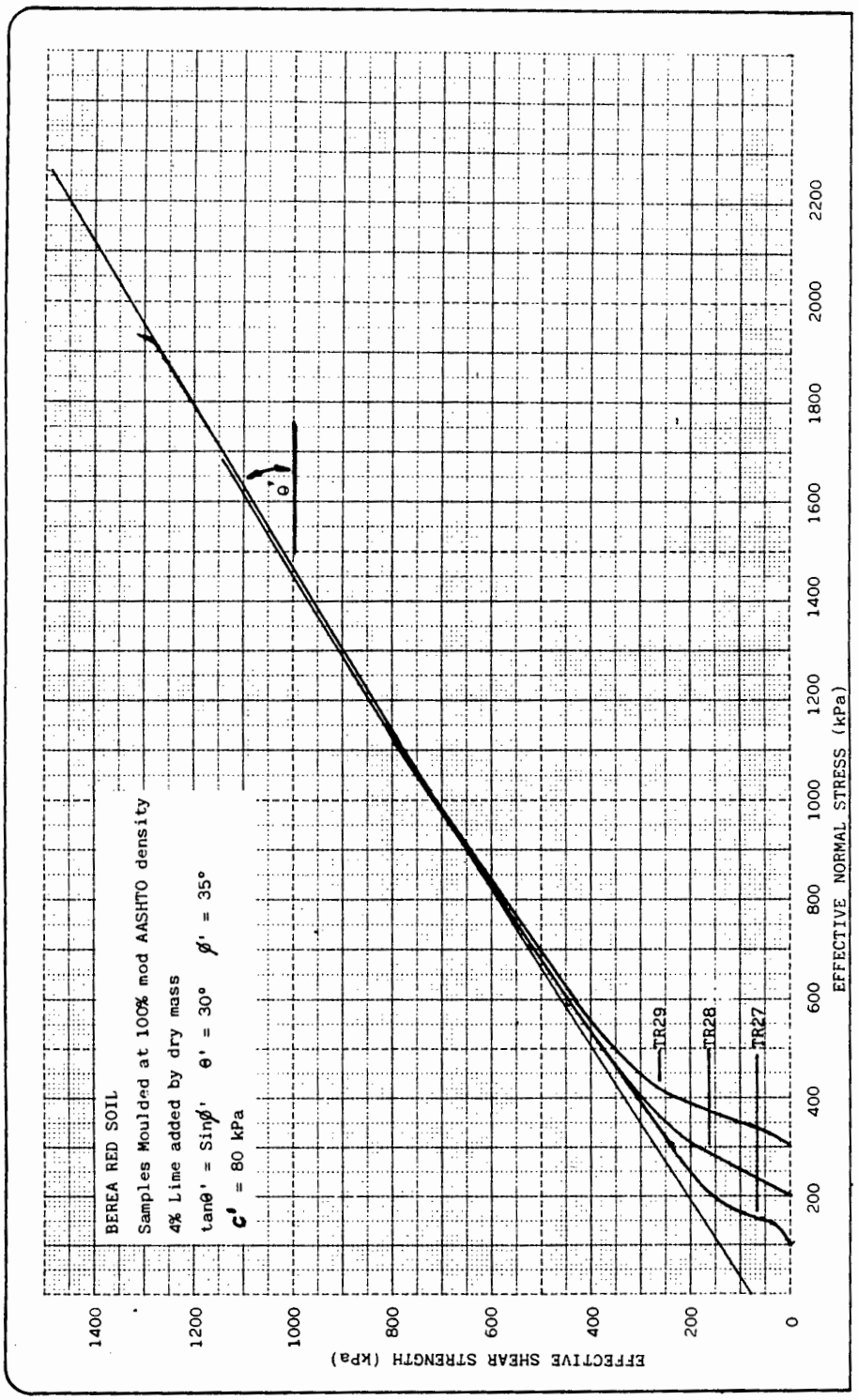

Fig. 6.12 Stress Path Plot of Berea Red soil with 4% lime moulded at 100% mod AASHTO

The shape of the stress strain curves for specimens moulded at 100% mod AASHTO density conforms to an almost idealized perfect elastic plastic stress strain curve.(shown in Fig.6.13 and the individual results presented in Appendix C).

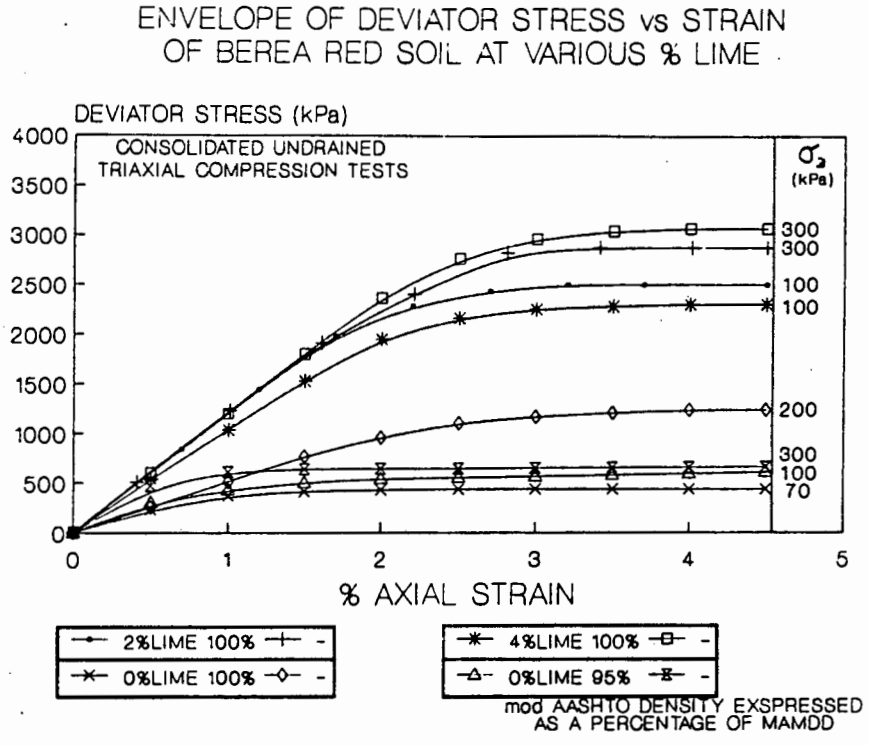

Fig.6.13 Stress strain responses of Berea Red soil subjected to triaxial compression.

If it is assumed that distortion and crushing of the grains does not occur, then deformation is only possible (for a densely packed specimen) if the grains force each other apart resulting in dilatency. It is the dilatency of the specimen that maintains the high shear strength, by increased confining stress due to a pore pressure reduction therefore little reduction of the peak failure deviator stress even after 5% axial strain behaviour could be attributed to a high degree of packing of the grains and dilatency. The result causing the already dense material being forced together.

The specimens moulded to 95% mod AASHTO density display a linear elastic stage as well as a strain hardening range. This change in behaviour as compared to that of specimens moulded at 100% mod AASHTO can be attributed to the lower density, which changes during shearing. Inspection of the pore water response (ie volume change) indicates that the particles are being repacked, resulting in a lower effective stress and denser packing. Further shearing in excess of 0,5% axial strain indicates dilating properties, which is only possible if the particles are forced apart by additional applied stress being applied to the specimen.

7 CYCLIC TRIAXIAL TESTING OF BEREA RED SOIL

7.1 Introduction

The material properties of any engineering material change when subjected to cyclic or repetitive loadings for any length of time. These changes in behaviour can be brought about by a number of factors which may range from among others strain hardening to strain softening.

Pavement materials, in particular, have been reported to exhibit both of the above responses. These responses may be caused by densification, particle reorientation, pore pressure changes and external factors within the pavement materials, when subjected to cyclic loading.

It is the aim in this chapter to investigate verify and predict the behaviour of both natural and stabilised Berea Red soil whilst subjected to cyclic triaxial loading. The behaviour was studied using different testing conditions (i.e., drained, undrained, saturated, and unsaturated).

A series of tests were performed on Berea Red soil at slow cyclic speeds resulting in a limited number of tests being performed due to the long time each test took to perform. The change in material properties due to continued loading and unloading of a soil specimen are summarized in section 7.7.

Rutting is a major concern of pavement engineers and can be described as the summation of all the incremental permanent deformations of the individual structural layers within the pavement whilst subjected to repetitive loading.

If the in situ stresses experienced by the material of interest can be modelled within a cyclic triaxial cell the permanent straining characteristics of a layer can be predicted.

The rutting potential of a material in a pavement may be predicted during its operational life with the aid of numerical models and the data generated during testing procedures.

In order to perform pavement stress analysis it is required that the engineering properties of a material are known. It is well documented that the cyclic stress strain characteristics of a soil are affected by many external factors, such as confining stress, rate as well as duration of loading, and degree of saturation, to name a few.

It is the aim of the following sections to evaluate what effect these factors have during cyclic triaxial tests on soils.

7.2 Permanent Deformation

Whilst a soil is being subjected to repetitive cyclic loading, it undergoes instantaneous and permanent deformations. Instantaneous deformation may be considered as the elastic deflection that occurs when subjected to loading. On removal of the load, an amount of recoverable deformation takes place. This is marginally smaller than the instantaneous deformation. The difference between instantaneous and recoverable deformation is known as the permanent deformation which is non recoverable. Fig.7.1 illustrates schematically the above concept. Yoder et al(91) reports that permanent deformation is caused by two mechanisms:

1) densification of the soil matrix (volume change).

2) repetitive shear deformations known as plastic flow (with no volume change).

In the context of cyclic triaxial testing, the permanent deformation of a specimen can be characterized by three stages with respect to the number of load cycles that are applied.

Initial Strain

When granular materials are subjected to repetitive loads, it is common for the material to undergo considerable initial permanent strain up to approximately 1,000 load cycles after which the permanent strain is quite stable and increases very little. (See Fig.7.1.)

Densification

A soil specimen/pavement material subjected to cyclic loading and unloading will generally show signs of densification. This is more apparent on poorly compacted, uncemented and lightly cemented material as densification is caused by particle reorientation resulting in increased density due to volume decrease. Permanent strain increases very little during the densification stage.

Failure strain

When a specimen has been loaded repeatedly to a stage that densification no longer takes place, failure of the specimen occurs, resulting in large, continuously increasing permanent strain.

Although little evidence of actual failures of cyclic triaxial tests performed on pavement materials have been reported.

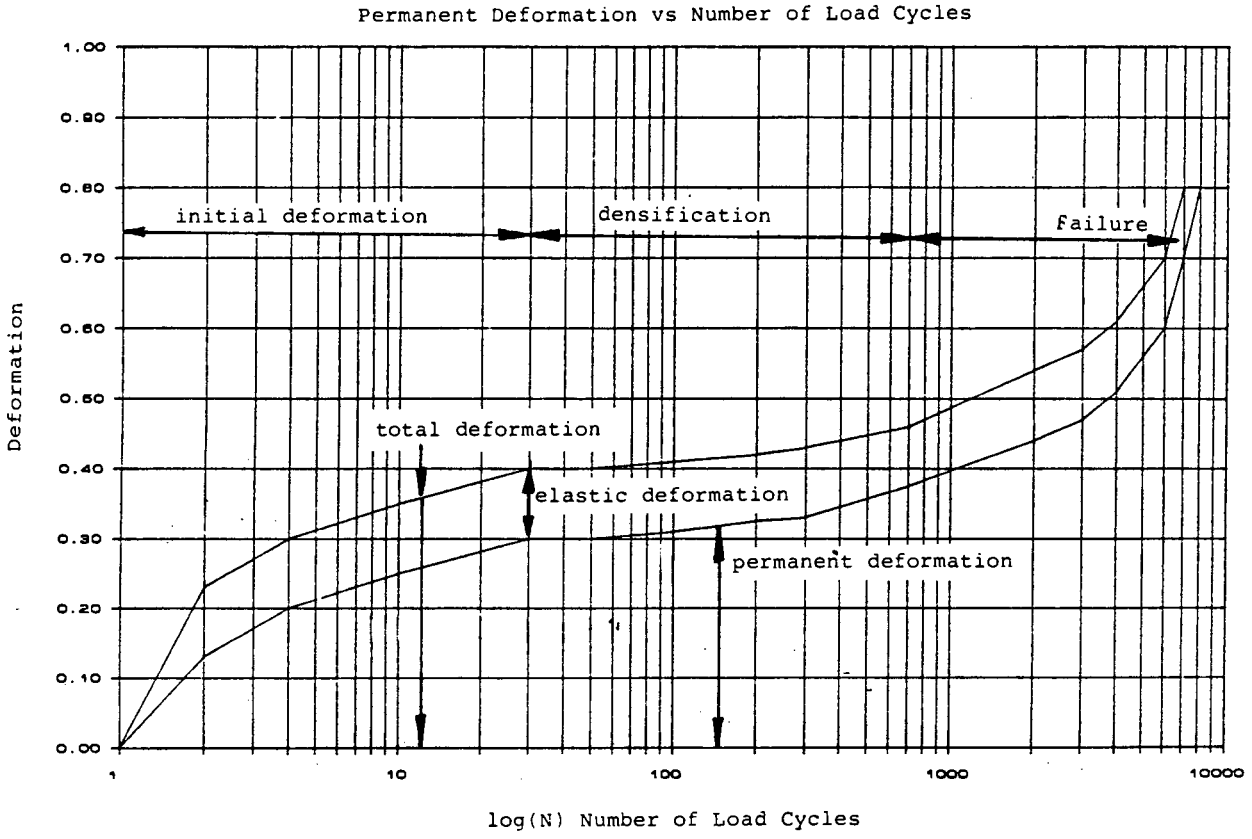

Fig.7.1. Schematic diagram of vertical deformation versus number of load cycles (after Kennedy(18)).

Researchers Lentz et al(88) and Kennedy(18) have found that a relationship exists between the number of loading cycles, N and the permanent strain ε_p. The mathematical relationships have been found to be either linear on a log-log scale or linear on a log linear scale. Hence a simple deformation law for permanent strain can be formulated.

$$\varepsilon_p = aN^b \qquad \text{log-log scale}$$

$$\varepsilon_p = a+b(\log N) \qquad \text{log-linear scale}$$

Where a is the ordinate at N=1 and b is the slope of the straight line approximation

Thus, applying the above deformation law the prediction of permanent strain over the range that a single specimen is tested, remains a relatively simple exercise. However, if a quantitive study is envisaged a relationship between stress and strains is required that will allow the analyst to predict the strain of the material over a representative stress range at a predetermined number of load cycles.

Pavement deformation prediction

Deformation due to plastic flow is the basis upon which two existing types of pavement designs are based, namely an empirical and rational approach.

The empirical approaches are either based on CBR design techniques which rely on a) a comparative index procedure for choosing the material or b) on the limiting subgrade strain criteria, which relies on the strain in the subgrade being limited to deflections in the upper layers. The major disadvantage of the design methods is that the permanent deformation behaviour of the material cannot be predicted with time while being subjected to repetitive loading.

Rational design techniques which are based upon a stress and strain analysis of the individual pavement layers have as yet not been accepted as a means of pavement evaluation in this country. If pavement design procedures are to be improved, it is clear that a means of projecting the pavement behaviour into the future is required in order to evaluate the most suitable material and economic approach. Lentz et al(88), Cuellar et al(29) and others have developed models for predicting pavement deformation from results of permanent strain behaviour determined from cyclic triaxial test data.

7.3 Resilient Modulus

Resilient Modulus (M_R) is defined as the ratio of the cyclic axial deviator stress to the recoverable axial strain in a triaxial compression test and is illustrated graphically in Fig.7.1.

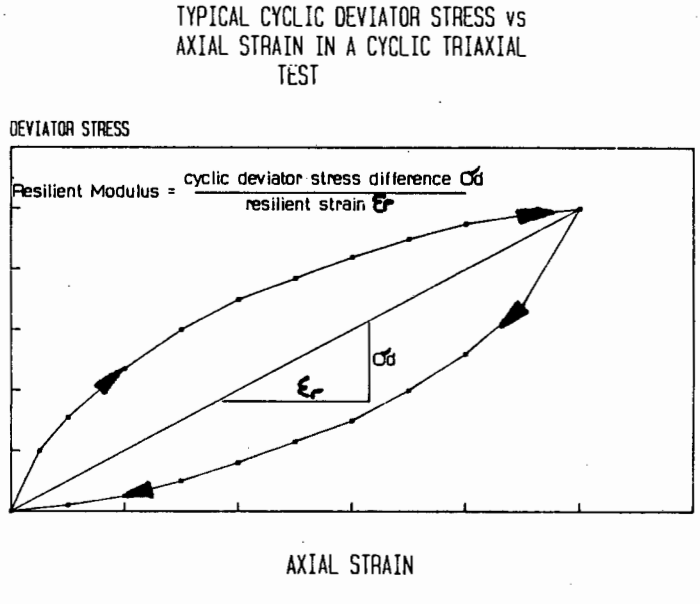

Fig.7.1 Graphical Representation Resilient Modulus

A wide range of tests have been reported by Brown and Hyde (37) and Doshi and Mesdary (47) on all types of pavement materials, ranging from cohesive, non-cohesive, stabilized and non-stabilized materials.

The above tests were conducted on 100mm specimen for large ϕ >10mm particle sizes and 50mm specimens for fine grained soils (ϕ <10mm.). Deformation is monitored using local strain gauges at the middle third of the specimen.

The general trend of M_R response with respect to the number of loading cycles on different soils can be again divided into two categories, namely granular and fine grained materials.

Determination of Resilient Modulus of Granular Materials

Yoder et al(91) reports that cyclic modulus tests performed on granular material show a significantly different behaviour when confinement is varied, but are affected very little by the number of load repetitions.

The usual practice for the determination of resilient modulus in granular materials is to "condition" the specimen with 1000 load repetitions to overcome the initial straining, thereafter the specimen is subject to 200 repetitions at each stress state i.e., over a range of confining stresses σ_3.

The stress dependency of granular materials is modelled using either of the following equations:

$M_R = K1\sigma3\hat{}(K2)$ or $M_R = K_1'\theta^{K2'}$
where K_1 is the y axis intercept and K_2 is the slope of the linear regression fit of the log-log plot.

Resilient Modulus values of granular materials vary according to increased density, saturation and particle shape.

Fig.7.2 shows a typical plot of M_R versus stress state where the sum of the principal stress $\theta = \sigma_1 + 2\sigma_3$.

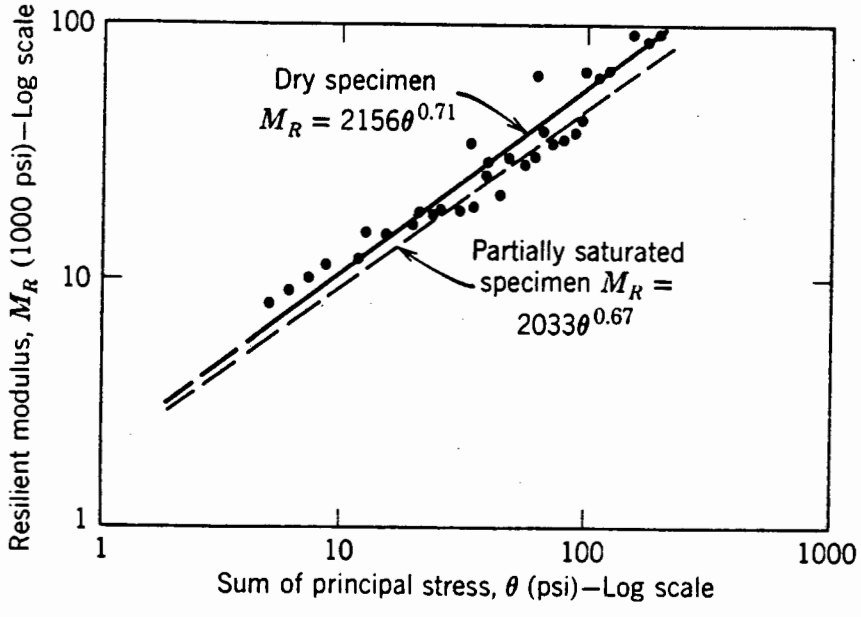

Fig.7.2 M_R response for a typical granular material (Yoder et al (91)).

Determination of Resilient Modulus of Fine Grained Material

The M_R values of fine grained material, unlike granular materials, exhibit stress dependency when subjected to cyclic loads. The trend of fine grained materials is to show a dramatic decrease in resilient modulus with the increase in deviator stress. This tendency comes to a halt at a point, after which the M_R value increases marginally with increased deviator stress as shown in Fig.7.3.

Yoder et al(91) expressed the behaviour of M_R in the two equations for the range of deviator stress shown as

$$M_R = K_1 + K_3[K_2 - (\sigma_1 - \sigma_3)] \text{ for } K_2 > (\sigma_1 - \sigma_3)$$

$$M_R = K_1 + K_4[(\sigma_1 - \sigma_3) - K_2] \text{ for } K_2 < (\sigma_1 - \sigma_3)$$

Where the coefficients K_i (i=1,2,3,4) are defined as illustrated in Fig.7.3

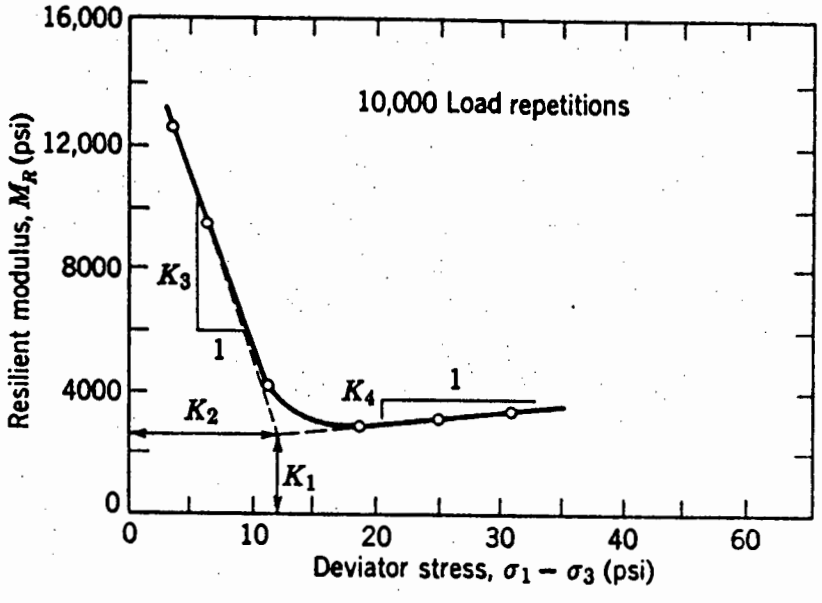

Fig.7.3 Typical Resilient Modulus response of fine grained soil (Yoder et al(91)).

Yoder et al(91) reports that a specimen "conditioning" of 600-1000 repetitions is normally necessary for fine grained soils to overcome the initial strain.

7.4 Factors Affecting Permanent Strain ϵ_p and Resilient Modulus

Water content and degree of compaction

Pumphery et al(24) carried out cyclic triaxial tests on uniform fine Florida quartzitic sand with an AASHTO classification of A3 moulded 3% below optimum moisture content. It was found that permanent strain was 15% less than the same material moulded at optimum. Additionally they found that increased dry density resulted in a reduction of the permanent strain. This behaviour is to be expected since a higher compactive effort appears to decrease the volume of voids in the soil, resulting in more particle interlock.

Peacock and Seed(52) indicated that the development of permanent strain is a function of density and is sensitive to cyclic speed or frequency when varied.

The effect of moisture content on M_R, was found to make no remarkable difference even for material moulded with a moisture content 3% less than optimum. Yoder et al(91) found that fine sand showed a considerable reduction in M_R due to an increase in moisture content. This behaviour is probably due to additional lubrication caused by the increased water content, facilitating more elastic recoverable strain. Fig.7.4 illustrates the effect of both density and moisture content on the M_R values.

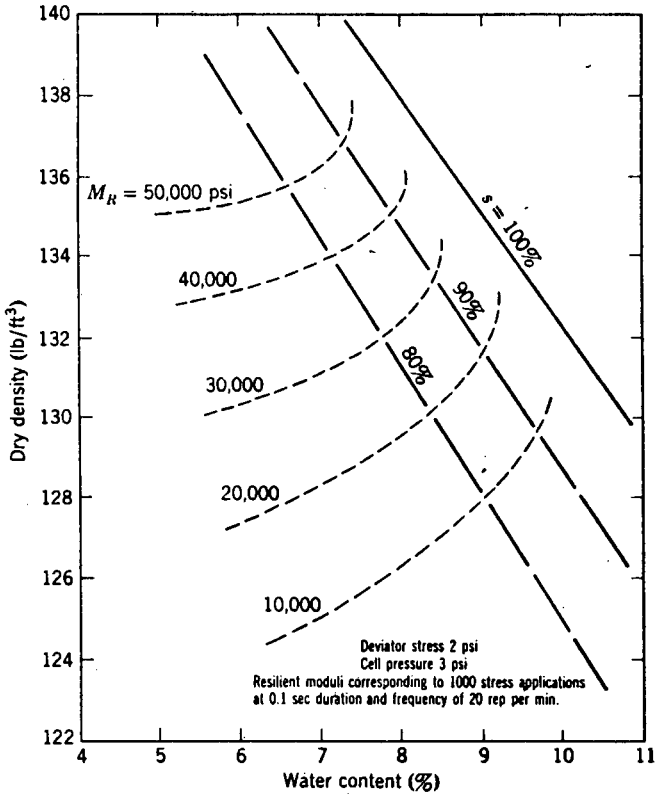

Fig.7.4 Relationship between Resilient Modulus, water content and dry density of fine grained soil (Yoder et al(91)).

Degree of saturation

Rada et al(93) reports that the degree of saturation for a given soil plays a major role in the M_R response. Repeated load triaxial tests indicate that there is a critical degree of saturation, (S_r = 0.80-0.85), above which granular materials become unstable and deteriorate rapidly under repeated loading at normal densities ranging from 93-100% mod AASHTO density. This condition is caused by the loss of inter-particle friction. The behaviour of fine grained soils appears to be less affected by

the degree of saturation on materials moulded at representative pavement densities. This is thought to be caused by the large surface area of the fines resulting in considerably more interparticle contact and increasing the internal friction of the soil matrix.

Cuellar et al(29) states that with dilating sands no significant difference in permanent strain and M_R was observed between the behaviour of dry sand and similar sand specimens tested in a saturated drained condition.

Static confining stress.

A considerable number of researchers namely Pumphery & Lentz(24) Brown & Hyde(37), Park and Silver(36) and Silver and Park(92)) among others agree that a reduction of the permanent strain and an increase of the resilient modulus is apparently due to increased confining pressures on both granular and fine grained materials.

Pumphery & Lentz(24) observed that fine Florida Highway subgrade sand shows no change in the permanent strain at low percentages of the failure stress values, i.e., (20% - 60% static deviator failure strength S_d), however, 75% of S_d results in a three-fold increase of permanent strain for a reduction from 350kPa - 70kPa confining stress.

Cyclic confining stresses

The realistic simulation of in situ behaviour of pavement materials using a triaxial compression testing device to model in situ stresses has been a large concern of many researchers.

Cyclic frequency, shape of load trace and duration

Pavements are subjected to repeated stress applications of varying magnitudes, durations, and frequencies. A satisfactory design procedure requires that the resulting deformations should not exceed a tolerable limit. The influence of stress intensity, frequency, form of stress application, stress history and their practical significance play an important role on pavement material evaluation.

For highway pavements, duration of stress application is not likely to vary appreciably and is usually a fraction of a second for traffic constantly in motion. However, at inter-sections substantially longer periods of stress application (up to several minutes) are developed while in parking areas the duration of stress application may approach several days.

A review was conducted to establish what other researchers had based their cyclic testing frequencies. Wong et al(35) in an attempt to model earthquake loading on 400mm high specimens could apply a maximum cycle speed of 1 cycle/min which was substantially slower than typical earthquake frequencies. However, Wong et al's(35) tests of the effects of loading frequency on granular soils had shown that changes in material behaviour were negligibly small.

Pumphery et al(24) recommended and used an inverted haversine wave form of 0,1 sec duration for all repeated load tests. Their motivation was that the period was equivalent to the time in which a vehicle travelling 50km/h affects a point in the top of the subgrade of a flexible pavement structure.

The load application of 0,1 sec was followed by a 0,9 sec rest period to allow proper damping of the road before the following load was applied. Therefore a frequency of one Hertz (Hz) was applied.

Kennedy(18)'s investigation of resilient modulus for subgrade was based on haversine wave loading applied for 0,1 sec which was then removed for 0,4 sec which is equivalent to a frequency of 2 Hertz. Silver et al(32) recognized the need for a standardized cyclic strength test procedure and with the help of eight participating laboratories performed a series of tests on an identical soil. The findings clearly show that small testing details can significantly alter the test results.
Small deviations in moisture content, density, load trace and confinement from the prescribed test method decreased the cyclic strength of the test sand. Silver et al(32) found that cyclic behaviour is related to:

1) The shape of the cyclic load wave form
2) Small changes in specimen dry unit weight
3) Specimen preparation

It would be natural to expect the latter two factors to have an effect on the behaviour on the soil but the loading wave form was less obvious. Silver et al(32) investigated the effect of wave shape at a frequency of 1Hz on cyclic strengths by using three different wave shapes (as defined in Fig.7.6);

1) Sine wave
2) Square wave with a degraded rise time where the wave shape did not have an instantaneous change in speed in either the loading or unloading portion of the cycle
3) Square wave with a very fast rise time

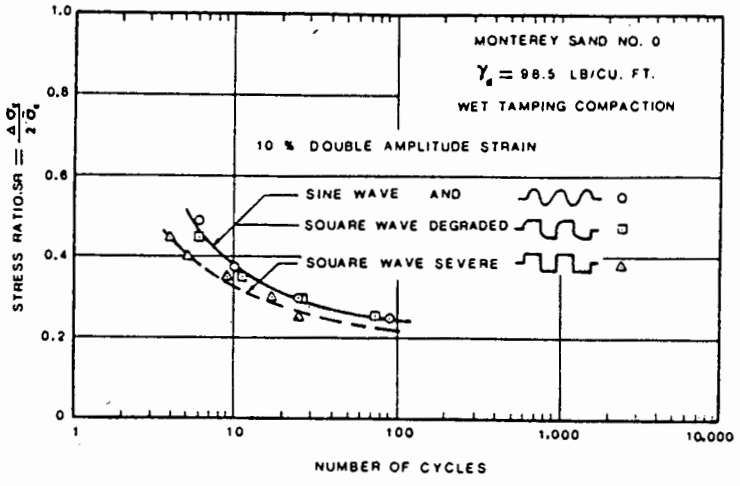

Fig.7.6 Effect of Wave Shape on Cyclic Triaxial Strength of Monterey test Sand (Silver et al(32)).

The results of these tests shown in Fig.7.6 indicate that the wave form has an influence on the stress ratio (S_r). It can be clearly seen that specimens tested using a fast rise time square wave form, show strength values about 15% less than those using a sine wave or degraded square wave pattern.

Detailed investigation by Silver et al(32) of the fast rise square wave indicated that a stress wave was set up at the time of the instantaneous velocity change during the loading, causing the stress wave to be propagated through the specimen. The effect showed up as spikes in the pore pressure response. Pore pressure in this loading type increased more rapidly, resulting in lower strength values. The results implied that fast rise time square wave load application should not be used in cyclic strength testing, and that it is more meaningful to use either a degraded square wave with a rise time of 10% of the loading period or a sine wave load pattern to prevent the damaging effect of shock wave propagation through the specimen.

Timmerman et al(25) performed a series of strain controlled tests in which the frequency of loading varied from 2,5Hz to 25Hz. They concluded by noting that the frequency affects the rate of strain but not the final strain. Hence, the resilient modulus values are a function of frequency.

Stewart(54) performed cyclic triaxial tests on well graded railroad ballast to investigate the effects of repeated loading. Since railway loadings consist of a mix of different wheel loadings, rather than constant repetition of the same magnitude, various load combinations were applied to the specimen. All the tests were performed at 1Hz and no information on the loading shape was provided.

The results of the random loadings indicated that increasing the applied deviator stress beyond a past maximum level, increased the permanent strain. Decreasing the deviator stress below a past maximum value resulted in negligible additional strain accumulation. The final cumulative strains that developed in the variable amplitude tests were independent of the order of the applied stresses. It was suggested that a superposition method could be used for mixed load conditions.

Diyaljee et al(55) presented a simplified procedure for determining permanent strain of free draining cohesionless soils for the use in transport support systems. In addressing the frequency application of repeated deviator stress, they stated that the frequency was varied to allow complete specimen drainage for each cycle. Frequencies of 4,6 and 11 cycles/min were used in up to 10,000 repetitions. Diyaljee concluded, that with slow rates of cycling, no effects on permanent strain due to a change in frequency were apparent.

To investigate the effect of duration of stress application on soil deformation under repeated loading, Seed et al(53) undertook an in depth experimental study on silty sand. The results of tests performed on specimens of silty sand subjected to stress repetitions of constant intensity but with different intervals between applications and different durations of stress application are presented in Fig.7.7 and 7.8.

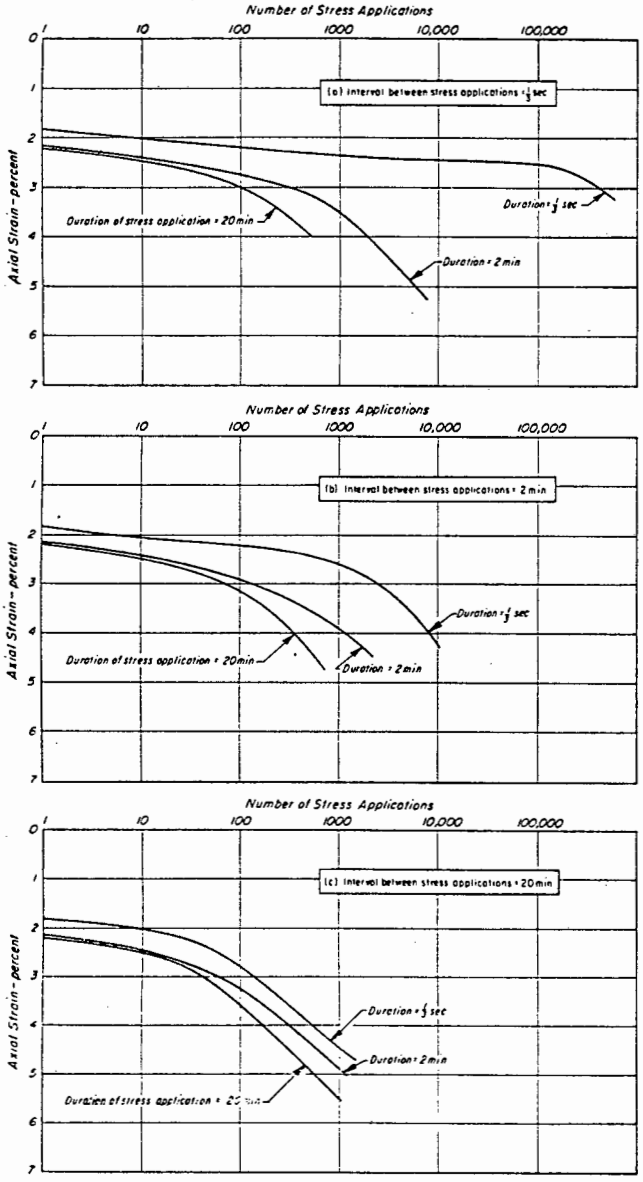

Fig.7.7 Effect of Duration of Stress Application on Permanent Deformation of Silty Sand.

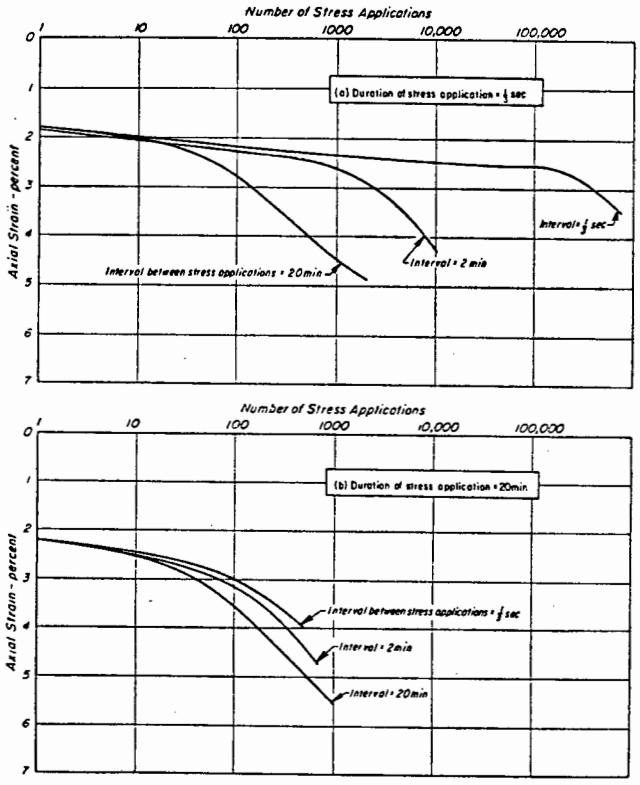

Fig.7.8 Effect of Interval between Applications on Permanent Deformation of Silty Sand (Seed et al(53)).

Throughout the study, the maximum applied stress was 70% percent of the static failure strength.

As expected, the results show that an increase in the duration of the stress application on the deformation of the specimens varies considerably depending on the interval between applications. When the interval between load applications was only 0,33 sec an increase in the duration of the stress application from 0,33 sec to 120 sec had an enormous affect on the resulting deformations. However, the effect of the same variation in duration of stress applications was increased from 2 to 20 minutes and became very small.

In view of the fact that the strength and deformation characteristics of sands are the result of physical changes to the particle orientation, it is surprising that the interval between load applications, when the sand is apparently unstressed, would have an appreciable influence on the results. However, a comparison of the data (Fig.7.9) shows that some phenomenon occurs during the unload period which is apparently largely responsible for the differences in results obtained.

A comparison of the test data for specimens subjected to stress applications of the same duration, but with different intervals between applications was presented in Fig.7.9.

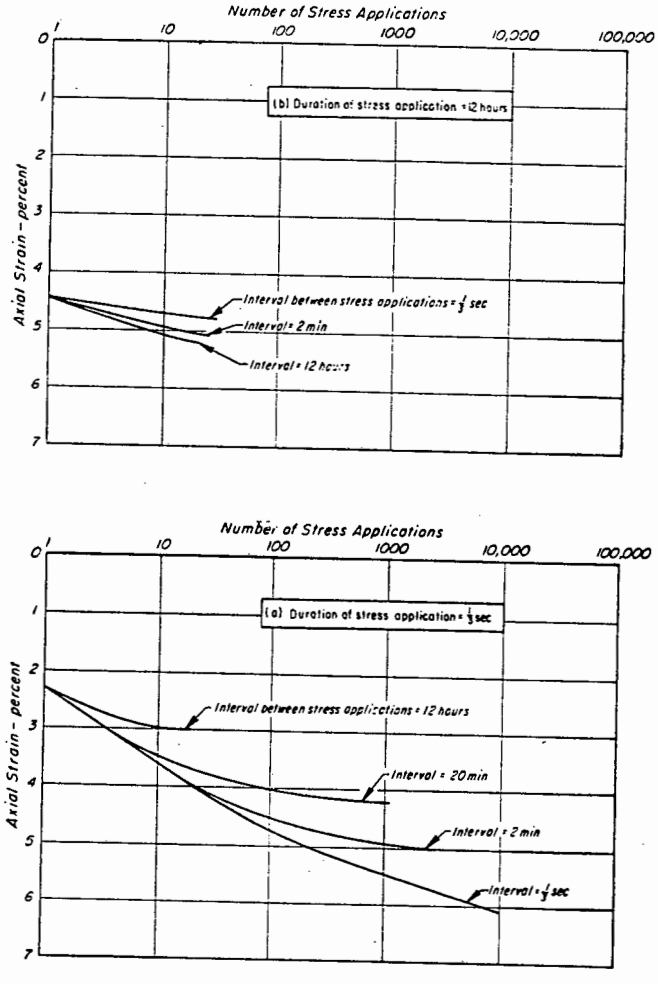

Fig.7.9 Effect of interval between stress applications on deformation of silty clay (Seed et al (53)).

Seed et al(53) noted that when the stress applications were short, an increase in the interval between applications lead to very large increases in deformation of the specimens. For stress applications of longer periods, the same type of effect but of much smaller magnitude were observed. Since the stress intensity and period of application is identical in these cases, the differences must necessarily result from changes occurring in the intervals between stress applications.

Seed et al(53) concluded that absorbed water layers on the surface of sand particles may influence the deformation characteristics of these soils as they do for clays. Thus, application of a deviator stress may result in high stress intensities at points of contact between particles, causing absorbed water films to be displaced and resulting in essentially true contact between particles. Such contact would produce high frictional resistance to relative particle displacement.

When the stress is removed, the displaced water film may require time to regain its original condition, so that if a second stress application is applied after a very short interval, high frictional resistance would develop. On the other hand, a long interval between stress applications would permit more complete re-establishment of the water film and a somewhat reduced frictional resistance leading to relatively larger deformations such as those observed in the tests.

Intervals between stress applications exceeding the time to complete redevelopment of the moisture film would influence the results very little, suggesting that the effect of interval between applications would decrease with increasing magnitude of the intervals. Seed et al(53) believed the results provide evidence of the probability of a stress history effect in sand which must be considered when dealing with short term periods of stress application.

Permanent strain and resilient modulus are affected by many external factors. However, although some external influences on sand have been described it is thought that each material has a different responce when subjected to cyclic loads in a triaxial cell. With special reference to Berea Red soil a summary of salient points are highlighted.

- Increased density reduces the permanent strain and increases the resilient modulus. Yoder & Witzac(91) and Silver et al(32).

- Increased confinement reduces permanent strain and increases resilient modulus. The effect of cyclic confining stress is negligible and a mean value is sufficient for testing purposes. Brown & Hyde(37).

- Saturation exceeding 80% in granular materials, renders them unstable. Fine grained materials are less susceptible to instability at high degrees of saturation. Yoder & Witzac(91).

- The duration of deviator stress application if increased, increases the permanent strain. Wong et al(35), Seed et al(53).

- Rapid rise time loading patterns such as a square wave trace would result in a higher resilient modulus response. Silver et al(32), Seed et al(53).

- Frequency of load application affects the rate of strain but not the total strain. Increased frequency results in a higher modulus response. Peacock & Seed(52), Seed et al(53).

In conclusion, the in situ loading conditions should be closely modelled in the triaxial cell to the conditions expected in the pavement, in order to achieve a reliable prediction of the pavement's behaviour when in use.

7.5 Choice of Representative Testing Procedures for Cyclic Triaxial Testing of Berea Red Soil

A typical element of in situ soil in a pavement, when subjected to cyclic loading, would generally exist under a non-hydrostatic state of stress prior to the application of the cyclic load. If the soil element is considered to have been consolidated under the anisotropic conditions, then the principal directions of the superimposed cyclic stresses will generally not be the same as those of the static state. During cyclic loading of a pavement, rotation of the principal stress directions will occur. The cyclic triaxial test is frequently used to obtain information on the behaviour of the soil element under cyclic conditions, but the limitation exists that cyclic shear stresses cannot be applied to the principal planes along with the fact that the test is simplified by maintaining the confining pressure at a constant value while only axial deviator stress is cycled.

The most commonly used cyclic triaxial tests can be sub-divided into two main categories, one in which the deviator stress is symmetrically varied about a non-hydrostatic stress state.

The latter has two categories, one in which the cyclic deviator stress is greater than the static confining stress and the other which is less. The latter case would not cause shear stress reversal to occur on any plane.

In the test programme cyclic triaxial tests were performed by consolidating under a hydrostatic stress to achieve an initial effective stress state. A cyclic deviator stress was applied which alternated from 25kPa to a required maximum positive cyclic deviator stress. (A minimum deviator stress of 25kPa eliminated slipstick conditions during loading and unloading) as explained in section 6.1.

Tensile deviator stress was not applied as additional visco elastic membranes (as described in section 6.2) were not available to allow the deviator stress to be reduced below the hydrostatic state of the specimen.

Choice and description of cyclic stresses applied to triaxial specimens

The choice of cyclic axial stress and confining stress was based upon the elastic stress strain analysis summarized in Figs.6.5-6.7. The highest axial stress calculated in a layer was found to be in the E3 pavement just underneath the bituminous layer. An axial stress of 470kPa was chosen and increased by 20% to allow for an overload factor. An average confining stress in the same layer was found to be 100kPa and was not increased by a load factor. In summary an axial stress was cycled between 565 and 125kPa. A schematic of the stresses applied to triaxial specimens is presented in Fig.7.10. The deviator stress is expressed as $\sigma_1-\sigma_3$ and ranged from 25 to 465kPa.

The maximum period which could be applied in this research was 1 minute. The effective confining stress is the difference between the cell pressure (550kPa) and the applied back pressure (450kPa). The effective confinement chosen was 100kPa and facilitated ease of comparison of test results as reported in Seed et al(53), Diyaljee et al(55), Peacock et al(52), and Timmerman et al(25).

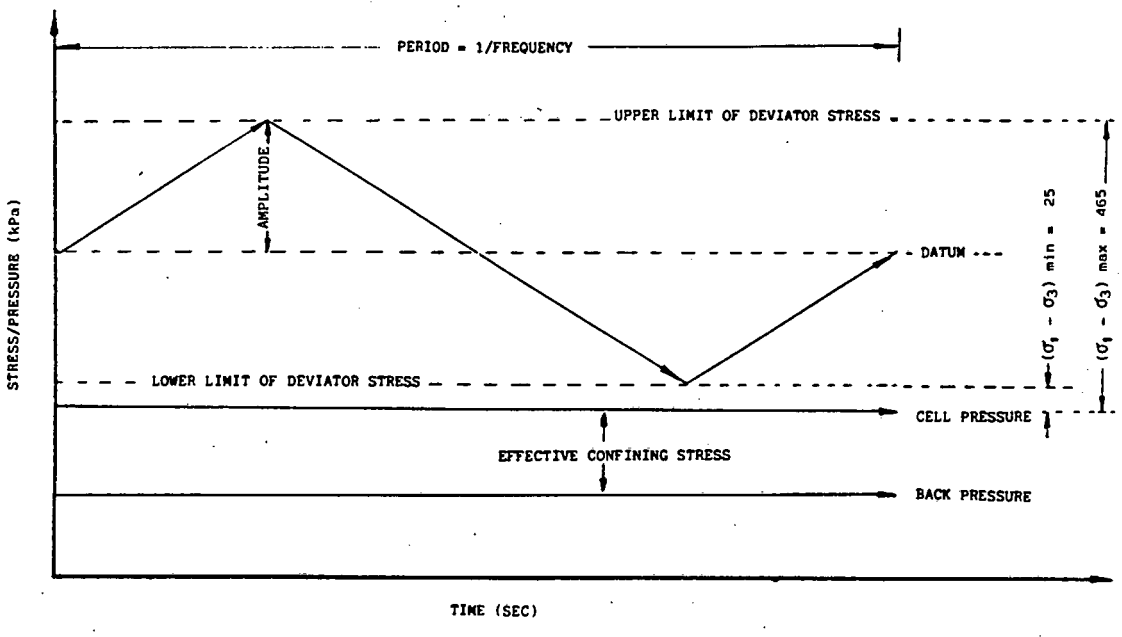

Fig.7.10 Schematic diagram of the stresses applied to a triaxial specimen undergoing cyclic loading

Frequency of load applications and limitations of the test device

The standard G.D.S package (as it is presently marketed) is capable of applying three loading wave forms, namely square, triangular and sinusoidal.

The maximum possible load application rate, which could be applied at the time of testing natural Berea Red soils at

All specimens were moulded at 100% mod AASHTO density and optimum moisture content. On addressing the topic of in situ subgrade or subbase moisture contents, Emery(50), found that Natal subgrades in the coastal area were, in the worst cases, of the order of 1,05 OMC. However, most specimen testing for this investigation was performed in a saturated state, which is equivalent to 1,5 OMC.

The question whether the test specimens should be saturated, unsaturated (wet or dry) and whether they should be drained or undrained is addressed in the testing programme that follows.

7.6.1 Investigation into the Effect of the Wave Form of the Cyclic Deviator Stress on Berea Red Soil

A series of cyclic triaxial tests were performed on a 2% lime stabilized specimen, which had been cured for 150 days at 100% mod AASHTO density.

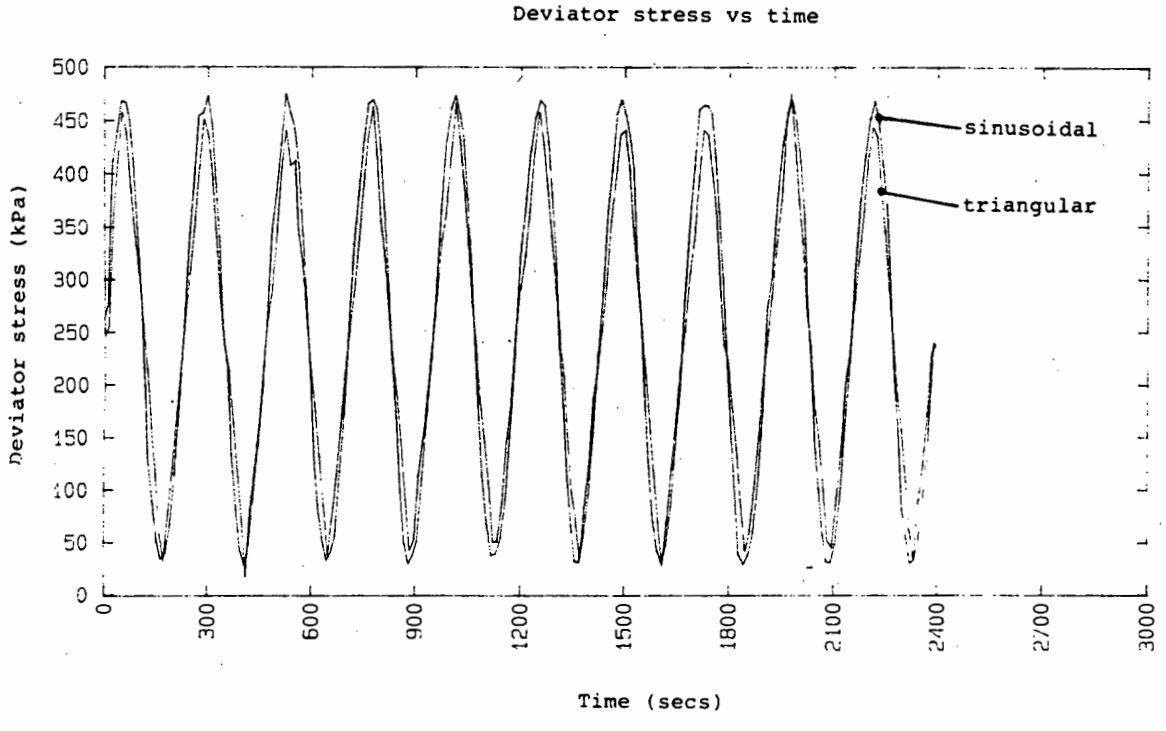

Fig.7.11 The response of Berea Red soil subjected to a sinusoidal or triangular deviator stress (25-465kPa) versus time with a confining stress of 100kPa

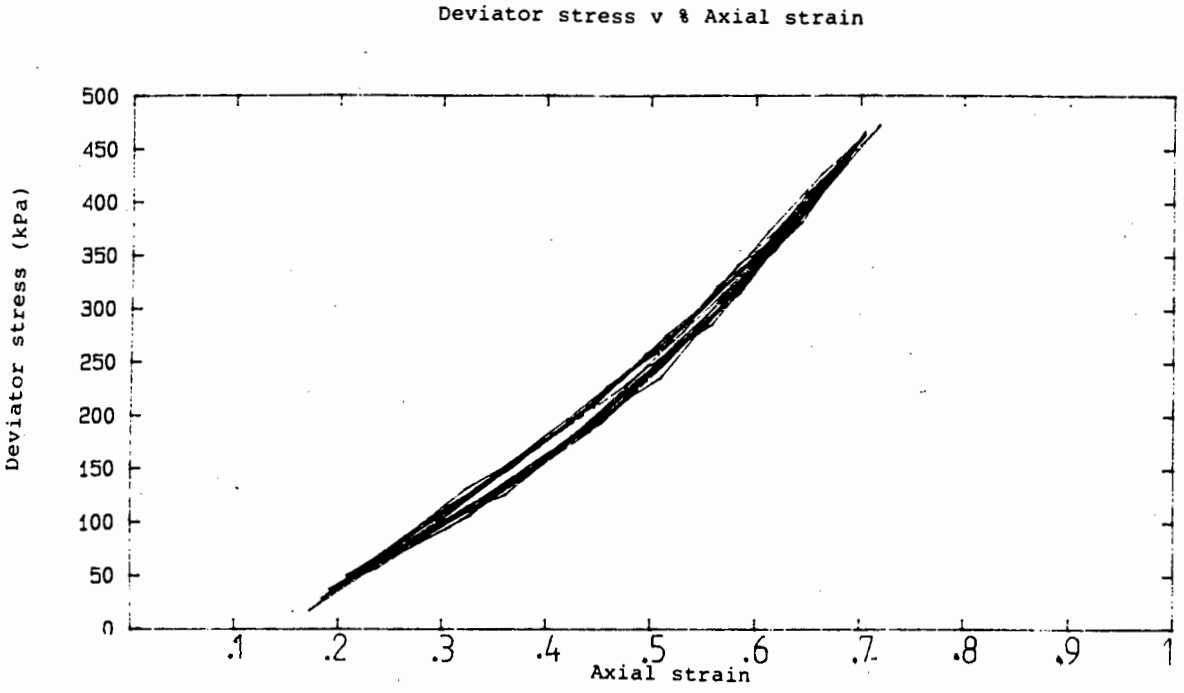

Fig.7.12 The response of Berea Red soil subjected to a sinusoidal and triangular deviator stress (25-465kPa) versus axial strain with a confining stress of 100kPa

The objective of the test was to establish whether the Resilient Modulus would occur when a soil was subjected to various deviator stress loading patterns and period. The specimen used had been moulded to 100% mod AASHTO density and subjected to 30,000 cycles at 1 cycle/min prior to the commencement of the above investigation. Inspection of the prior strain behaviour revealed that all shake-down and some densification had taken place within the specimen.

It was envisaged to subject the specimen to two deviator wave forms, namely sinusoidal and triangular. The wave forms were to be applied over a range of frequencies from 1 cycle/min to 1 cycle/10 mins in increments of 1 minute. i.e., 20 tests. A series of deviator stress versus time cycles were plotted (see Fig.7.11). At the peak of the deviator stress versus time a discontinuity can be seen.

This condition sometimes occurs when the digital controller cannot keep pace with the stress/pressure gradient it should be applying. If the targeted stress is not reached and a new instruction is given by the programme the previous instruction is abandoned.

The area of sinusoidal versus time deviator stress trace is larger than the equivalent triangular deviator stress trace. This seems to imply that the Berea Red soil cyclic response is time and stress dependant which is in support of Silver et al(32), Seed et al(53) and Peacock et al's(52) findings.

The response of resilient modulus to the varied load traces and periods are summarized in Fig.7.13, where it can be seen that a sinusoidal wave trace produces a substantially lower resilient modulus at the frequencies investigated.

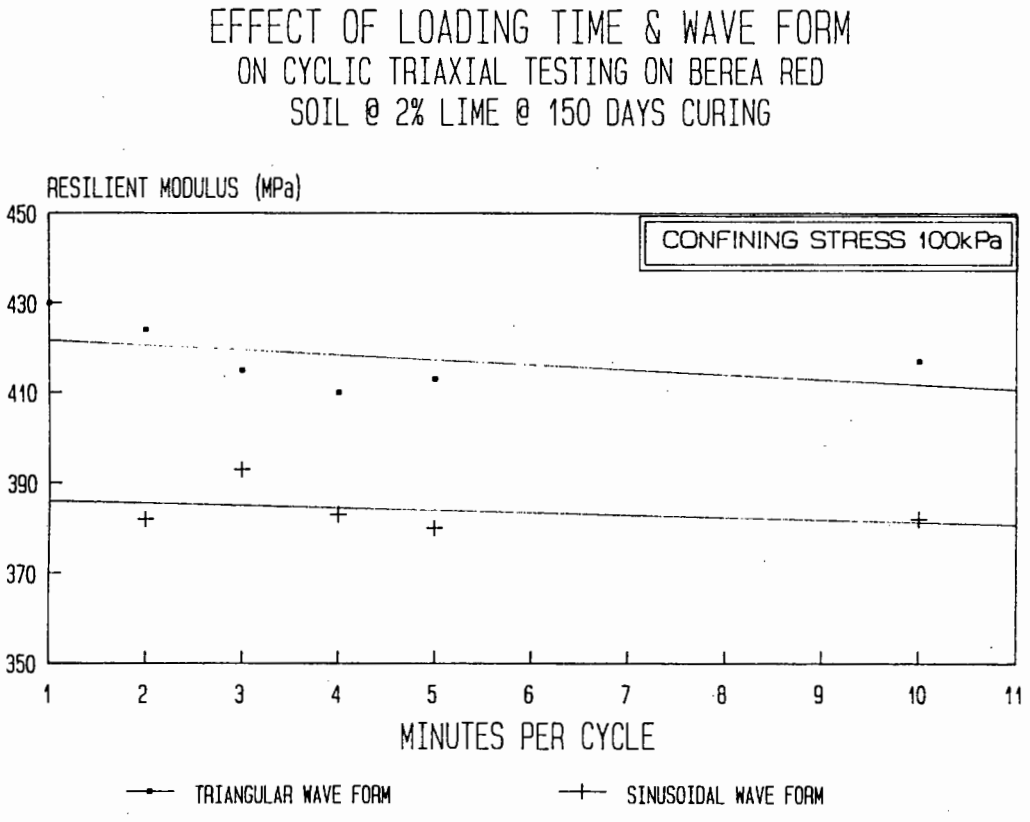

Fig.7.13 Effect of deviator stress frequency during loading

7.7 Evaluation of Lime Stabilized Berea Red Soil

7.7.1 Response of Berea Red soil to the degree of saturation during cyclic triaxial loading

The permanent strain characteristics of Berea Red soil modified or unmodified with lime at 28 days are dependant on the degree of saturation.

Permanent strain

In order to evaluate the effects of saturation, specimens of varying lime contents were compacted to 100% mod AASHTO density and treated in two ways:

1) Sufficient back pressure (450kPa) was applied in order that the B value of 0,95 was obtained, which indicated about 100% saturation (hereafter called saturated).
2) The same effective confining stress (100kPa) was applied as in (1), but a low back pressure of 100kPa was applied to flush out excess air in the test apparatus tubing. Berea Red soil compacted to 100% mod AASHTO density produced a degree of saturation from 77% to 83% (hereafter called partially saturated).

A saturated drained test on natural Berea Red soil was performed in order that the effects of free drainage could be evaluated and compared to the performance of undrained saturated and partially saturated soils. It can be seen in Fig.7.14 that the permanent strain decreases with increased percentage lime content.

This is due to the cementation brought about by the lime, which increases with increased lime content. This behaviour is apparent in both saturated and partially saturated soils.

The permanent strain characteristics of unsaturated soils are twice that of saturated soils. This is contrary to normal belief that generally saturated soils possess higher permanent straining potential than the identical unsaturated soils.

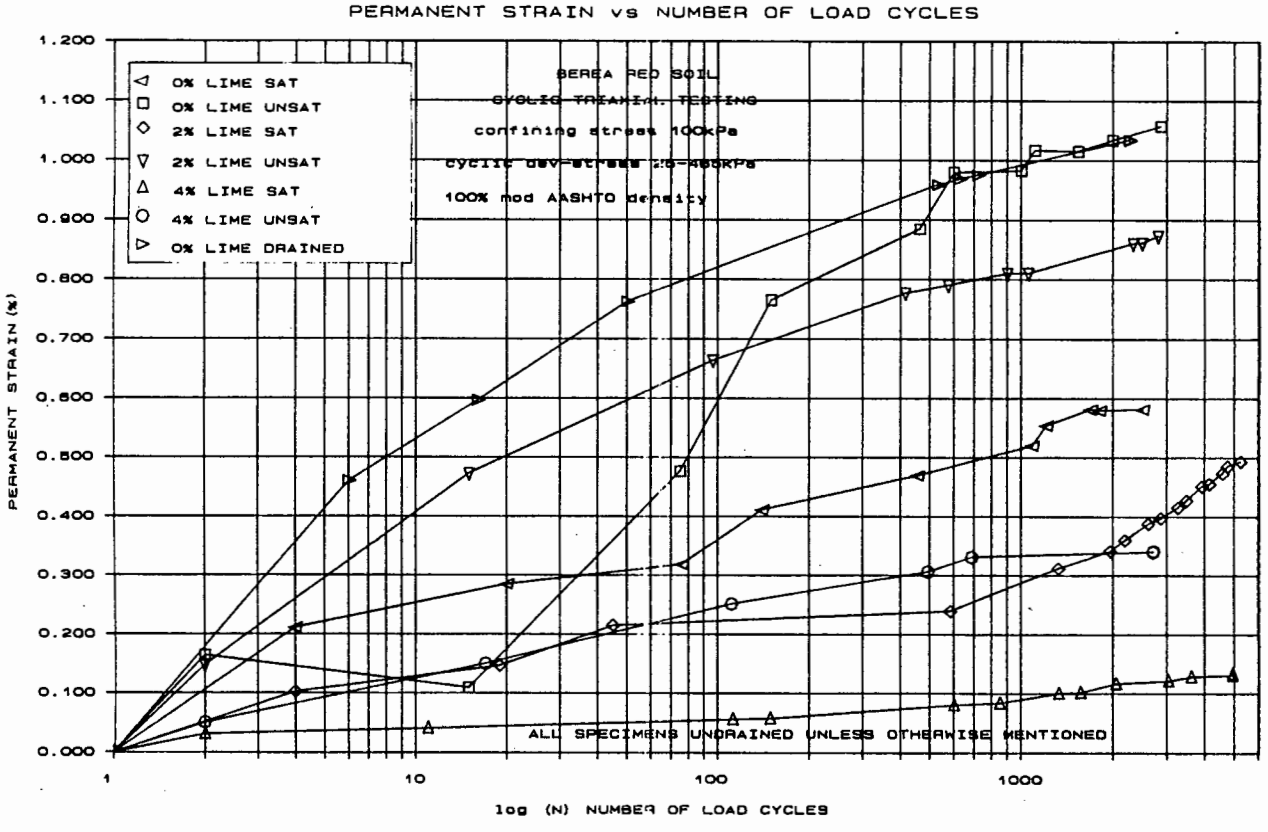

Fig.7.14 Permanent strain characteristics of lime stabilized Berea Red soil

The permanent straining characteristics of undrained saturated specimens when subjected to cyclic loading are less than the identical undrained unsaturated specimen for apparently the following reasons.

i) In an undrained test the soil specimen is cyclically loaded during which distortion but no volume change is allowed.

ii) Loading of undrained saturated soil specimens is shared by the pore water (which is assumed incompressible) and the soil skeleton (which possesses limited compressibility). Hence, large axial strains are prevented by the pore "incompressible" water.

iii) In the case of the unsaturated undrained specimen, the load would be carried by the incompressible pore fluid, consisting of a mixture of water and an undissolved air, is transferred to the soil skeleton. Upon loading the pore air would compress or steadily dissolve into the pore water, thus allowing volume changes and deformation to take place.

The above assumptions are verified by cyclically loading a drained saturated natural Berea Red soil specimen moulded at 100% mod AASHTO density and which is then allowed to undergo volume change. It is illustrated in Fig.7.14 how the partially saturated undrained and saturated drained tests converge after an initial shake down period of 600 cycles.

From the results it is not obvious whether saturated or partially saturated conditions under undrained or drained test methods should be used to investigate a subbase pavement material's stress strain relationships.

From this it can be concluded that the drainage conditions within a pavement as well as the resilient modulus response to varied drainage conditions within a triaxial cell should be established.

A series of tests on specimens were performed to determine the effect that the degree of saturation had on the stress strain relationship.

Resilient modulus

The resilient modulus characteristics of Berea Red soil modified and unmodified with lime at 28 days, appear to be influenced by the varying degrees of saturation in an undrained cyclic triaxial test.

As pavement material evaluation is based on cyclic stress controlled triaxial tests to simulate the applied wheel loads, the main variable which would influence resilient modulus would be the recoverable strain of a soil. Resilient strain appears to be affected by the degree of saturation in exactly the same manner that permanent strain is affected. Hence, the higher modulus shown in Fig.7.15 are found to be for saturated undrained specimens as no volume change is allowed.

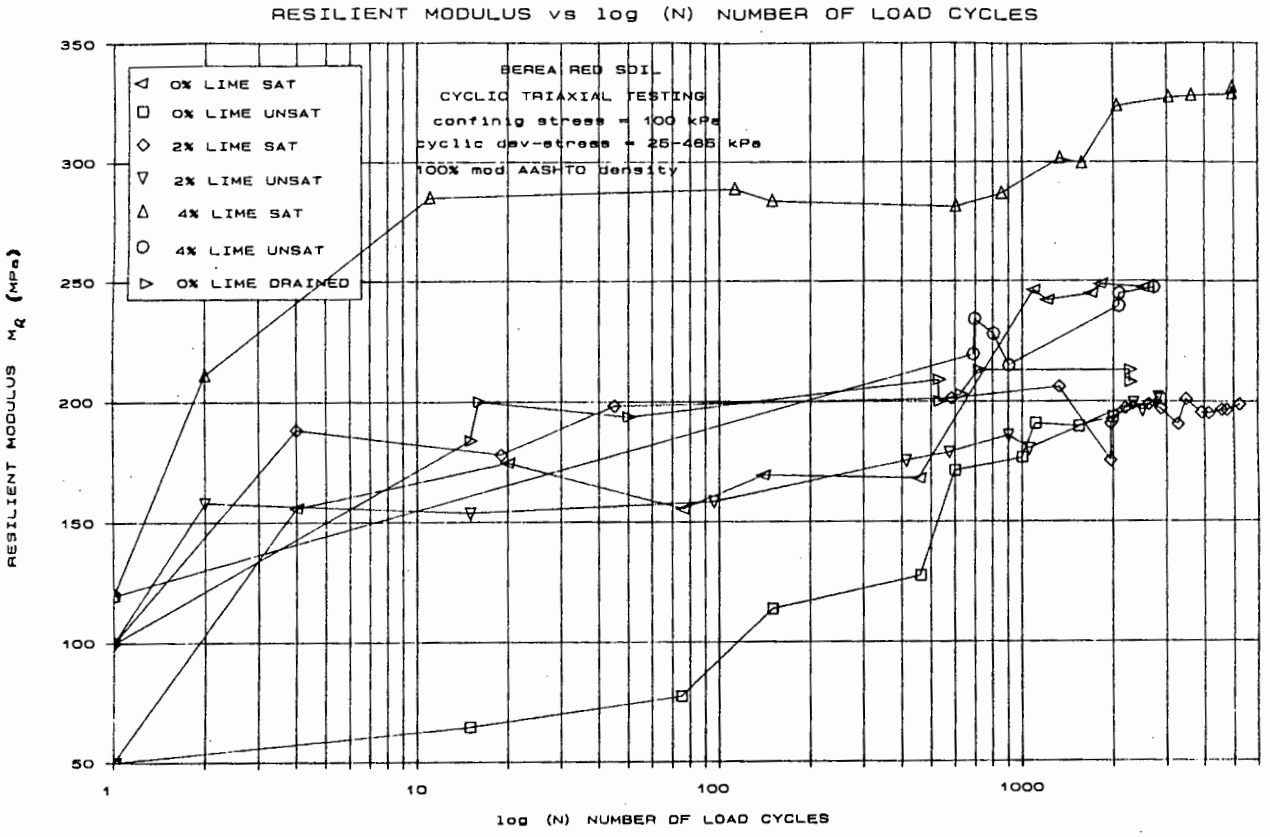

Fig.7.15 Resilient modulus characteristics of lime stabilized Berea Red soil

The increase of resilient modulus with the number of applied load repetitions is caused by the gradual densification of the soil skeleton. The sharp increase in modulus of unstabilized Berea Red soil specimens moulded at 100% mod AASHTO density illustrates that densification of the soil occurs with greater ease due to the absence of cementation.

It appears that improved modulus runs parallel to increasing permanent strain. Hence, under traffic the resilient modulus of a natural Berea Red soil subbase should improve. The degree to which the improvement would occur could not be predicted because of the limited test data.

The causes of the minimal improvement of the resilient modulus when modified with lime could be attributed to the lack of cementation at 28 days curing. A series of UCS tests to verify the above idea were presented in Chapter 4 and are assumed to apply to triaxial specimens. The results of the tested material from the cyclic triaxial test data showed a 25% improvement in the resilient modulus while the standard triaxial compression test showed a 100% improvement in the Young's modulus with the addition of lime. This is illustrated in Fig.7.15. (load No.1 is illustrated as the Young's modulus response). A larger improvement in resilient modulus was expected with the addition of lime and the poor performance was thought to be caused by insufficient curing time or the use of the incorrect stabilizing additive. Therefore, a further investigation was conducted to evaluate the effect of accelerated curing techniques.

7.7.2 Response to cyclic loading of Berea Red soil modified with lime, using accelerated curing

The resilient modulus of Berea Red soil, modified with lime, showed little improvement over the natural material tested. In order to determine whether the curing period was responsible for the lack of performance, it was decided to compare the response of the soil using a rapid curing technique to the material cured in humid conditions for 28 days at 22°C. Rapid curing was chosen because unconfined

compression tests had indicated a substantial failure strength increase from 1MPa to 4.4MPa for rapid cured specimens (see Fig.4.7). The rapid cure technique was performed according to the procedure outlined in section 4.7 on unconfined compression testing. i.e., at 60 C for 45 hours.

Two specimens were moulded and rapid cured with 2% and 4% lime at 100% mod AASHTO density, respectively. In both cases cyclic triaxial testing was performed in a saturated undrained condition and the performance is compared to modified soil humid cured for 28 days and natural Berea Red soil.

Permanent strain

The material response to permanent strain was found to be less for soils which were rapid cured as opposed to specimens that were humid cured for 28 days. This behaviour indicates that more cementation has probably occured when compared to the 28 day curing period for lime stabilized Berea Red soil. It could be assumed that the 28 day curing period does not appear to produce representative specimens that give a clear indication of the long term behaviour of the soil.

The results shown in Fig.7.16 indicate that the addition of 4% lime reduces the permanent strain of the same material moulded with 2% lime. Unstabilized soil deforms permanently more than five times that of Berea Red soil stabilized with 4% lime and rapid cured.

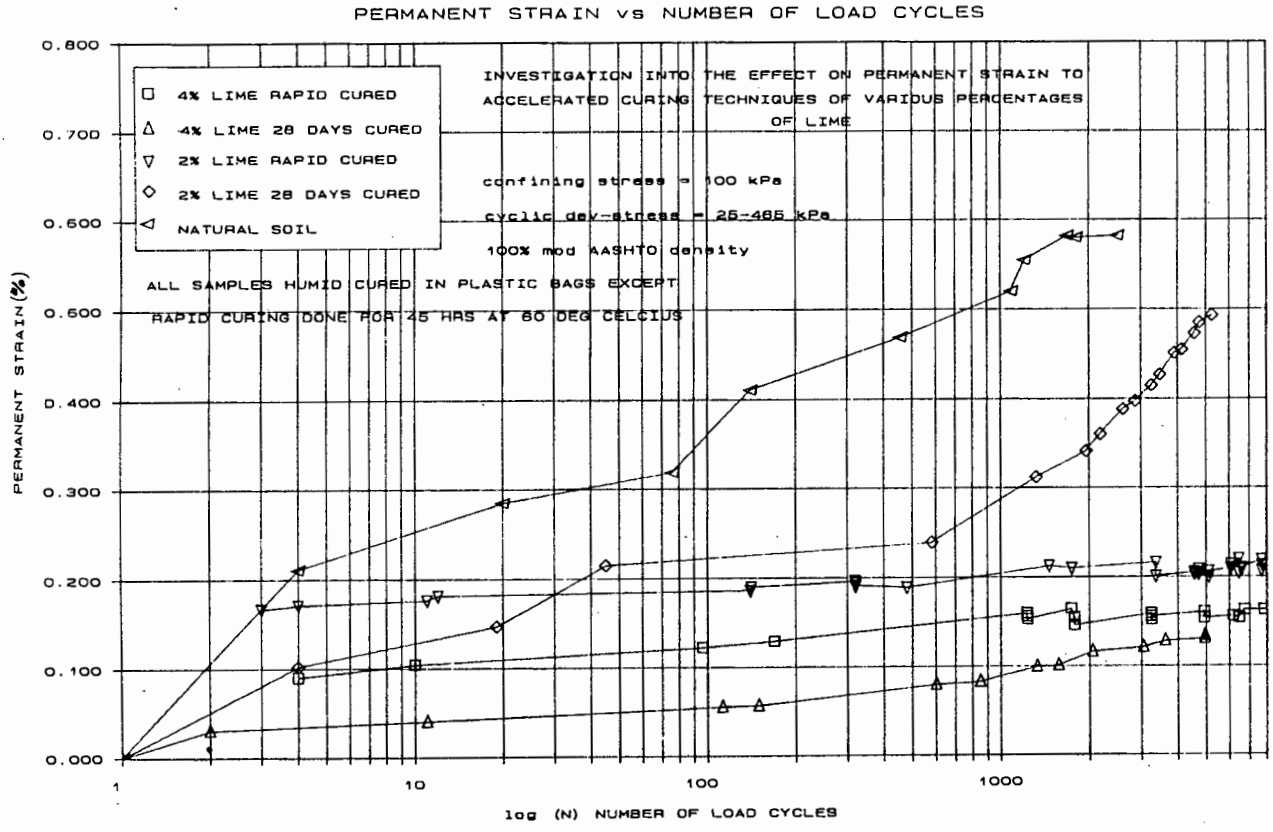

Fig.7.16 Permanent strain of rapid cured lime stabilized Berea Red soil

Resilient modulus

Test results showed that the response of the resilient modulus of Berea Red soil when rapid cured with lime is improved by fifty percent when compared to the identical humid cured specimen response. Indications are that if representative long term modulus values are to be applied for the design of a road pavement, the rapid curing technique should be used. Fig.7.17 indicates the behaviour of resilient modulus to the number of cycles applied. It is interesting to note that after the first one hundred cycles the modulus response of the rapid cured 2% and 4% lime stabilized specimens converge and remain the same throughout the tests. This behaviour could imply that the addition of more than 2% lime produces no additional gain in the resilient modulus.

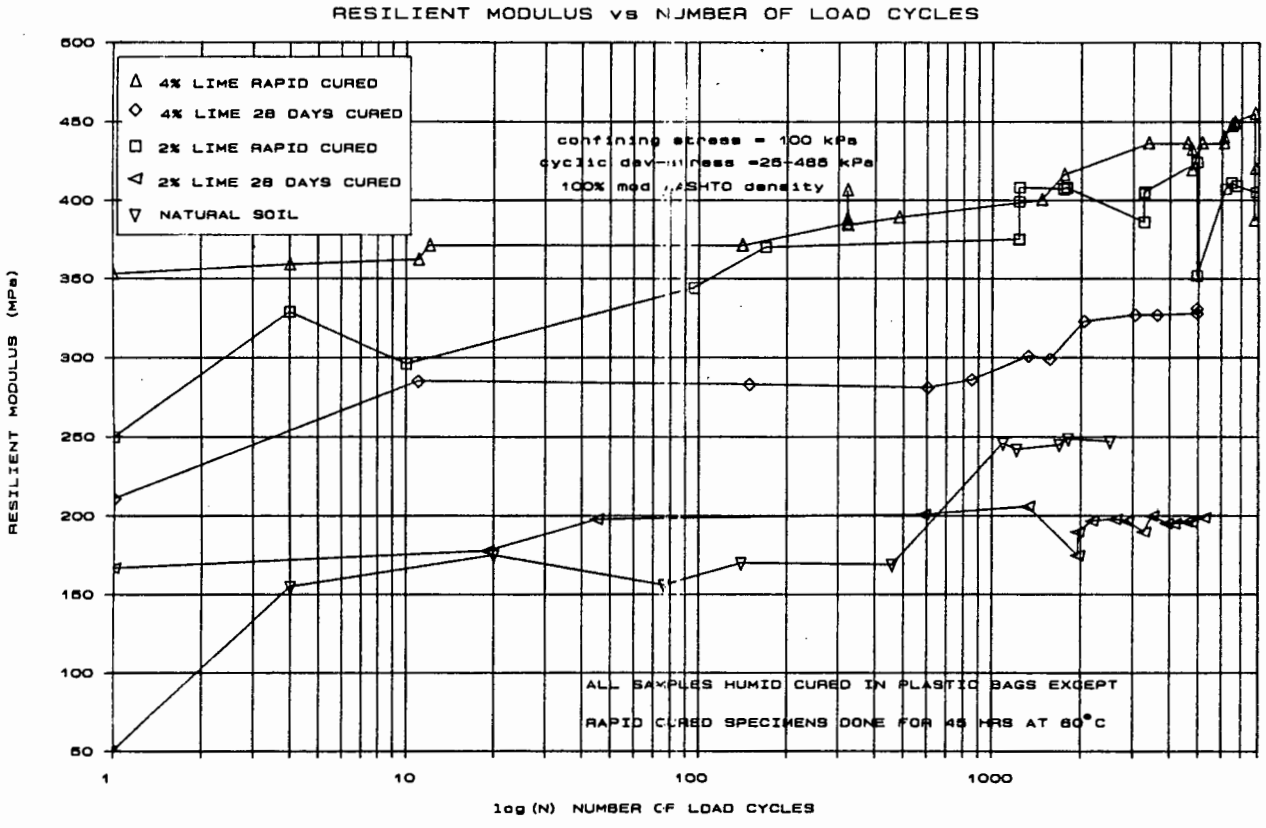

Fig.7.17 Resilient modulus of rapid cured lime stabilized Berea Red soil

Comparison of the behaviour of the permanent strain and modulus response in Fig.7.16 and Fig.7.17 shows that the two rapid cured tests tend to converge. Due to the time taken to perform one test, it was not viable to continue cycling for more than 6,000 cycles, unfortunately leaving the long term behaviour of the various treatments unanswered. As rapid curing accelerates the normal humid curing period, a possible improvement of the modulus response could be expected if long humid curing periods were allowed to take place. Therefore a specimen humid cured for four months and repetatively loaded for 40,000 cycles was likely to clarify the behaviour of the material when subjected to long term curing and a large number of load cycles.

7.7.3 Response of lime stabilised Berea Red soil cyclically loaded after 120 days humid curing

Short term cyclic triaxial tests on lime stabilized Berea Red soil (>6000 cycles) indicated that no additional improvement was achieved with the increase of 2% to 4% lime and that permanent strain characteristics tend to converge after 8,000 cycles (see Fig.7.16). On the basis of the above observations a 2% lime stabilized specimen, moulded at a 100% mod AASHTO density and humid cured for 120 days was used to perform a cyclic triaxial test which exceeded 40,000 cycles. The specimen was saturated and tested undrained for the first 25,000 cycles, and thereafter the test was continued in a drained condition. It should be stated that due to the slow rate at which the testing equipment operated the duration of the test exceeded one month. The test results of the first 15,000 cycles were lost due to an interruption of the power supply to the test apparatus.

Pore water response

The pore pressure of saturated and unsaturated Berea Red soil subjected to cyclic loading remains unchanged during the first 6,000 load cycles applied to undrained specimens. However, during the long term test the pore pressure decreased due to the positive increase in the volume due to dilation. The results of which, caused pore pressure to dissipate from 450kPa to 320kPa within the first 25,000 cycles (see Fig.7.18).

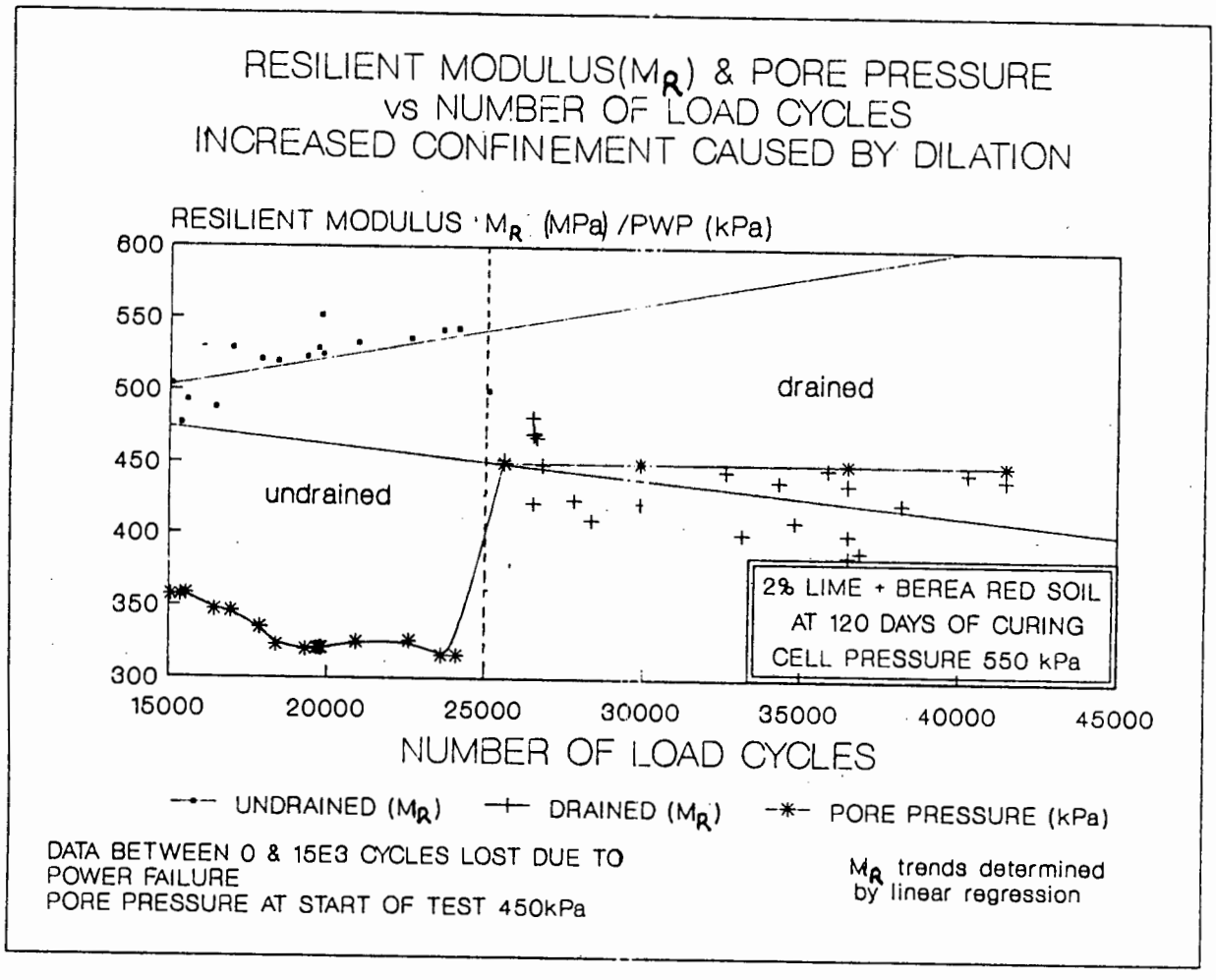

Fig.7.18 Resilient modulus and pore pressure response of a 2% lime stabilized Berea Red soil specimen humid cured for 120 days

As the effective confinement had increased from 100-200kPa, the test was stopped and the original effective confinement was applied.

Resilient modulus

Resilient modulus versus number of cycles is presented in Fig.7.18. Best fit straight lines determined by the least squares method were used to project the resilient modulus. The increase in resilient modulus with higher confinement due to the pore pressure reduction is apparent. If the lines of M_R and pore pressure of the undrained test are projected back to cycle number one, the M_R value is found to be approximately 430MPa. The projected M_R values shown in Fig.7.18 correlate well with those obtained from the rapid cured soil specimens. The M_R values of the drained test are found to be 450MPa at the start of the drained test and the negative slope, which indicates a reduction in M_R could indicate failure.

As resilient modulus of more than 450MPa at a confining pressure of 100kPa could not be achieved using 2% or 4% lime by either rapid or long term curing under various testing conditions, it was decided to investigate cement as a possible stabilizer as the unconfined strength of Berea Red soil had indicated that a considerable increase in failure strength could be achieved.

7.7.4 Response of cement stabilized Berea Red soil

Berea Red soil was mixed with 2% and 4% ordinary Portland Cement and humid cured for 28 days to investigate the response to cyclic loading.

Permanent strain

The effect of permanent strain with increased number of load cycles is illustrated in Fig.7.19 when moulded with cement and it would appear that after 200 - 800 cycles a densification process is occurring, probably caused by the failure of the cement bonds, resulting in a denser material which has partially cracked.

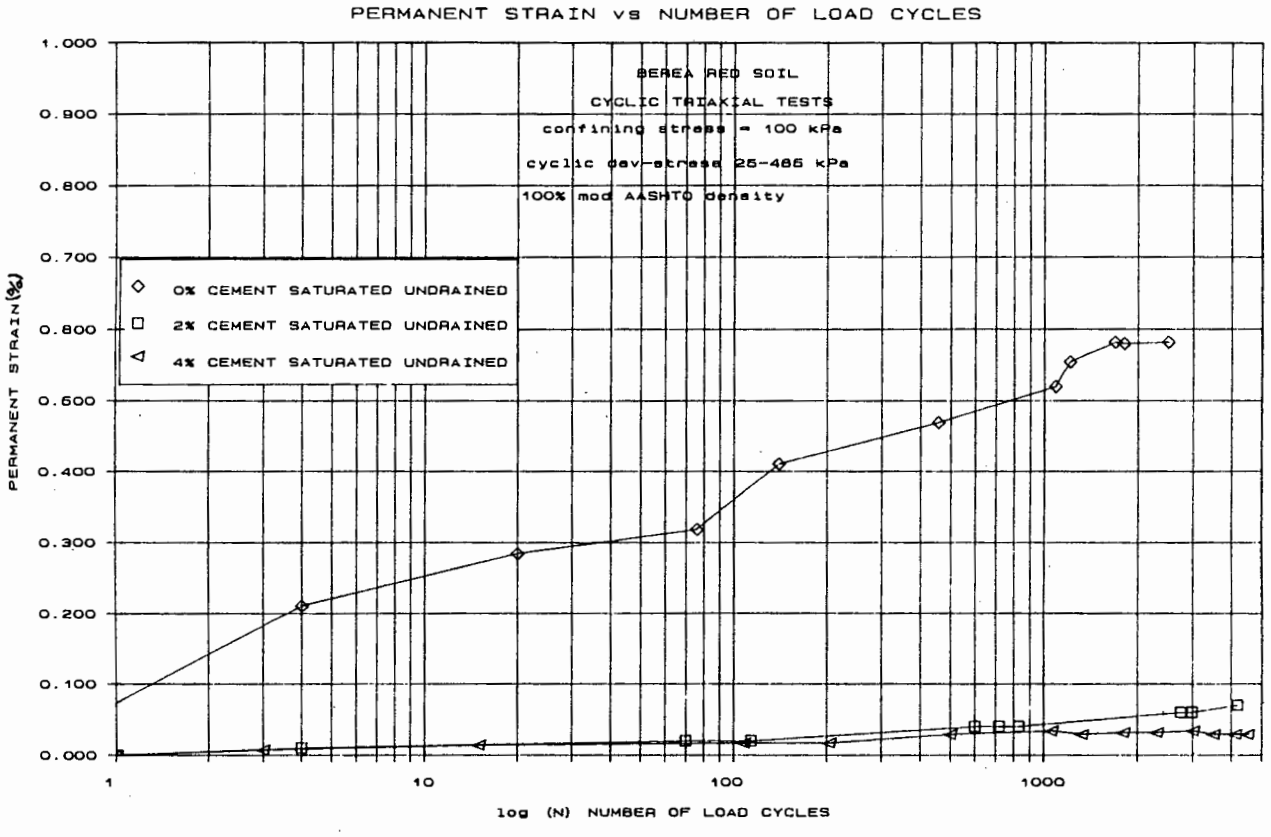

Fig.7.19 Permanent strain response of cement stabilized Berea Red soil to cyclic loading

However, it should be noted that when the permanent strain characteristics of cement stabilized soil shown schematically in Fig.7.19 are compared to those of lime stabilized soil shown in Fig.7.16, they are found to be nearly tenfold smaller. Cyclic tests in excess of 100 000 cycles would be the only means of evaluating the straining and cracking behaviour of cement soil.

Resilient modulus.

It can be seen in Fig.7.20 that the resilient modulus of cement stabilized Berea Red soil changes very little with increased number of loadings. This behaviour is probably due to the high degree of cementation of particles which prevents any initial shakedown behaviour of the soil. However, the increase in resilient modulus in the 200-800 cycles area is likely due to the slight change in particle packing as discussed in the previous section.

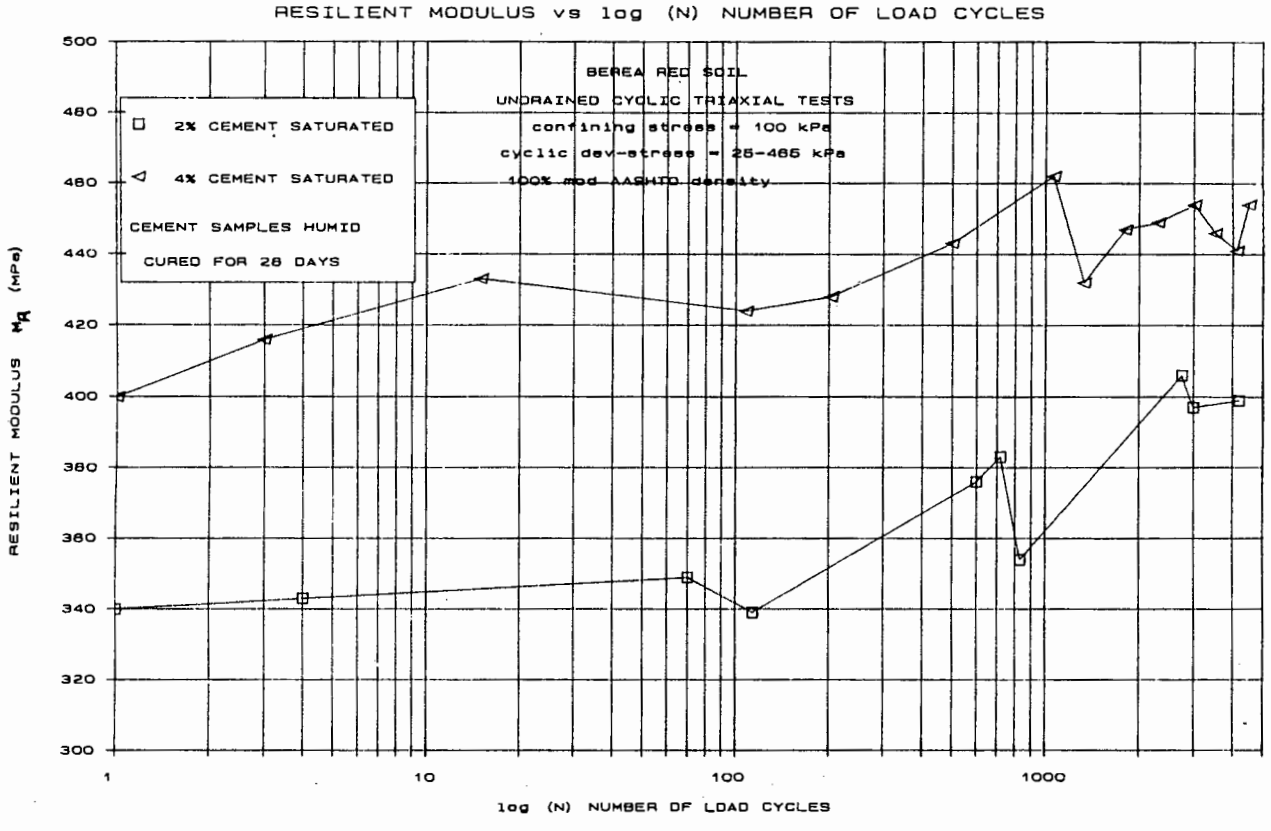

Fig.7.20 Resilient modulus response of cement stabilized Berea Red soil to cyclic loading

7.8 Comparison of the Modulus of Berea Red soil after various triaxial treatments.

A summary of the triaxial testing carried out on stabilized and unstabilized soil, is presented in Table 7.1. The variation in modulus values during static, cyclic loading and unloading, and static loading to failure after cyclic loading had been applied.

TABLE NO. 7.1 Comparison of the effect of the variation in moduli due to various triaxial test procedures

ADDITIVE	%	TEST DESCRIPTION	MODULUS (MPa) OF ELASTICITY		
			E^s	M_R	E^f
Lime	0	Drained Saturated	54	220	250
	0	Undrained Saturated	54	200	319
	0	Undrained Unsaturated	-	185	294
	2	Undrained Saturated (H28)	127	210	204
	2	Undrained Unsaturated (H28)	-	200	321
	2	Drained Saturated (Rc)	-	400	360
	2	Undrained Saturated (H120)	-	470	390
	4	Undrained Saturated (H28)	100	330	380
	4	Undrained Unsaturated (H28)	-	250	281
	4	Drained Saturated (Rc)	-	420	460
Cement	2	Undrained Saturated (H28)	-	400	428
	4	Undrained Saturated (H28)	-	450	328

* (H28) H Humid Curing
28 Number of curing days

(Rc) Rapid Curing
60°C for 45 Hours

* E^s Elastic Tangential Modulus from static triaxial tests

* M_R Resilient Modulus

* E^f Elastic Modulus after specimen has been cyclically loaded.

* Average of resilient moduli determined from values obtained after 3000 cycles had been applied.

The results in Table 7.1 are derived from triaxial tests with an effective confinement of 100kPa. The results illustrate that the modulus increases, probably due to the particle re-orientation. Even the static moduli E^F in most cases are increased after repetitive loading. This phenomenen is more marked in the case of natural materials and becomes less obvious when increased stabilisation is added.

Summary to cyclic triaxial testing

In order that a pavement soil may be evaluated correctly in a cyclic triaxial test apparatus, the ideal test procedure needs to be determined. The aim of the preceeding Chapter was to establish which test technique would highlight the representative properties of a soil when tested within the stress range to be applied to the envisaged pavement layer.

The following observations were noted when various testing procedures were applied.

Permanent strain observations based on these tests:

1) The cyclic triaxial tests indicate that if the severest permanent strain characteristics are to be determined, a specimen should be tested in a saturated drained condition.

2) Undrained saturated cyclic testing underestimates the strain by more than 50%.

3) Permanent strain is reduced in proportion to the percentage lime added to Berea Red soil of either humid or rapid cured specimen.

4) The addition of cement to Berea Red soil reduces the permanent strain by tenfold compared to that of lime stabilised material.

8. CONCLUSIONS

The research was undertaken to establish whether Berea Red soil could be employed in its natural state to perform as a selected subgrade or subbase in a road pavement. Three stabilizers worthy of consideration were used to modify the natural soil, namely lime, cement and a blend of lime and slagment. Lime was preferred because of its ease of application and longer working and mixing time allowed before compaction.

A literature review was undertaken to establish whether any geotechnical testing had been carried out on Berea Red soil. The results of the review revealed that reported soil mechanical testing could be subdivided into two catagories; pavement design and stability analyses. The pavement design tests included indicators and CBR's whilst the stability analysis tests consisted of oedometers and triaxial compression tests.

Research commenced with the undertaking of standard soil mechanical tests which included indicator, CBR and oedometer tests.

The grading curves of natural Berea Red soil indicates that 78% of the material is sand and the remaining 22% consists of 9% silt and 13% clay. Modification was apparent in the grading by inspecting the curves of Berea Red soil after lime was added. This behaviour is reported by many researchers to be brought about by flocculation of the clay particles.

Natural Berea Red soil had a plasticity index of 7 on material passing the 0,425mm sieves but an apparent plasticity index increased to 23 on material passing the 0,075mm sieve. This indicated that the behaviour of the clay fraction is masked by the high percentage of sand. An activity was determined to be 0,5 which indicated that the clay fraction consisted of a mixture of illite and kaolinite.

An average maximum mod AASHTO dry density of 2000kg/m^3 was determined for natural and lime stabilized soil, a low void ratio of 0,36 and a high degree of initial saturation of 0,77. The high density is attributed to the grading which facilitates most of the voids to be filled with smaller particles. When Berea Red soil is moulded to 95% of the maximum dry density, a low compressibility and low collapse potential was observed (1%) on soaking. The material properties indicate that Berea Red soil in its natural or untreated state would be suitable for a subgrade or subbase layer provided good compaction was achieved.

The CBR of natural material was found to be 65 at a 100% mod AASHTO density which appears high for a subgrade material, yet it can be improved by the addition of 2% lime and according to conventional design recommendations suggests that the material is suitable as a subbase, untreated or treated but as mentioned earlier does not allow any prediction with respect to straining behaviour under repetitive loading.

Unconfined compression tests on Berea Red soil moulded with 2 or 4% lime, lime slagment or 2% cement when humid cured for up to 28 days show little improvement over 1 MPa. This value appears to be the limiting compression strength of the material. It is however higher than the minimum of 0.750 MPa allowed for on a low grade cemented pavement layer.

A literature review on the effects the addition of lime has on fine grained soils was undertaken and revealed that the behaviour is comprised of a two stage reaction. The lime reaction consists of (i) an immediaate modification known as flocculation and agglomeration due to cation exchange and (ii) a pozzolanic cementing reaction. The high iron oxide content coating on the clay minerals was found to retard the pozzolanic activity for sometime.

Rapid curing of lime and lime slagment soil mixtures is recognised as a means of accelerating the cementation processes and reducing the curing time. The UCS failure strengths of rapid cured specimens was found to have increased by a margin of 300%. To take account of the chemical reaction in a stabilized material which increases the strength of the specimen significantly with time, it is recommended to apply the rapid curing technique.

The development of a computer controlled static indirect tensile strength test apparatus provided the facility to investigate the tensile behaviour of the pavement material and at the same time obtain some preliminary information on the material quality of the specimen. This allowed a distinction between high and low strength properties of the test materials and this provided a general guide for the selection of superior materials for additional cyclic testing. The results of the ITS test program indicated that the indirect tensile strength of Berea Red soil increases linearly with the percentage increase of additive by dry mass. ITS improved by a factor of 8 if a lime additive was replaced by cement as a stabilizer. The ITS test was fouond to be a convenient and easily applicable test procedure and should be considered in routine testing of pavement materials.

The results of the saturated consolidated undrained triaxial tests revealed that the internal angle of friction decreased with the addition of lime, whilst the cohesion increased. The behaviour can be attributed to the lubricating effect the lime has on the friction between the fines.

The failure stress of the treated material was considerably higher than the natural material, but no significant improvement in the stress strain relationship at the expected stress level in the pavement was apparent. This allows the conclusion that improved load carrying capabilities of the lime treated material could not be expected.

An extended literature review on cyclic triaxial testing revealed that many parameters influenced the material behaviour when subjected to cyclic loading.

These included among others: density, confining stress, degree of saturation, deviation stress level, loading trace shape, frequency and duration of deviator stress application.

Results of the cyclic triaxial testing program show that the highest resilient modulus was obtained when the specimens were moulded and rapid cured with lime or cement and tested in a saturated undrained state. Additional curing time resulted in an improved resilient modulus. An increase in effective confining stress resulted in an increase of the resilient modulus. This was observed for both natural and stabilized material.

The shape of the deviator stress load trace was found to influence the resilient modulus whilst all other variables remained constant. In the case of a triangular loading shape, the resilient modulus was higher than the identical test with a sinusoidal loading shape. This behaviour applied to periods from 1min to 10mins.

The elastic strain for a long period (10mins) was about twice the strain experienced in short periods (1min). It is therefore of the utmost importance to select an appropriate load application period when simulating traffic loading.

In cyclic triaxial testing equal attention should be applied to the representative test type, ie the degree of saturation and drainage conditions. Higher permanent strain, (in general about 25%) was observed in partially saturated undrained or saturated drained tests when compared to the identical saturated undrained test. The degree of saturation was found to effect the permanent strain of natural or stabilized material.

Although these observations do not reflect directly onto pavement design procedures, it does highlight the importance of testing in a partially saturated drained condition for the determination of resilient modulus for road pavement layers.

The investigation of the permanent strain characteristics of Berea Red soil revealed that long periods (here 10mins) of loading caused the severest permanent strain.

As with the elastic strain behaviour this observation is only valid for the number of cycles applied (<10000) in this work.

Permanent strain characteristics of natural Berea Red soil can be reduced by stabilizing the material with either lime or cement by a factor of three in the case of lime and a factor of eight in the case of cement.

In order to simulate a pavement layer in a cyclic triaxial apparatus, the material should be tested in a partially saturated, drained state so that the adequate confining stress may be maintained constant at all times and the porewater may be expelled or drawn in as the material compresses or dilates.

With this overview of research findings which is to be seen in the context of a much wider investigation on Berea Red soil as a pavement material, it can be concluded that the soil mechanical results will meet the requirements with respect to strength parameters of low volume roads.

The advanced soil mechanical testing of Berea Red soil does not yet allow a definite conclusion with regard to the application of the material in selected pavement layers of a high volume road. The important parameters have been identified and valuable test data accumulated. The derived trends compare favourably with other research work. Nevertheless to substantiate these findings, additional indirect tensile and cyclic triaxial testing is needed, some of which is of a fundamental nature.

9. RECOMMENDATIONS

The following topics for investigation are suggested by problems encountered during the course of the research. These topics are directed toward clarifying areas of uncertainty in this study that arose and were not investigated during the research.

The laboratory results obtained during this research should be compared to those from on site conditions, to establish whether the material behaviour in the triaxial cell resembles that in the field under the assumed conditions.

An ITS apparatus was built that was capable of performing repetative stress or strain controlled tests. A series of tests should be undertaken to investigate the resilient modulus and straining characteristics of Berea Red soil when subjected to repetative load.

A suggested method of improving the cyclic triaxial load application rate using the existing GDS controllers, is presented in Appendix E. However a feasability study should be made to determine a method of increasing the cyclic speed to internationally accepted standards of 2Hz and comparison of the results obtained from the slow cyclic speeds to the rapid cyclic speeds should be made.

10. REFERENCES

1. Hondros G. The evaluation of Poisson's ratio and the modulus of materials of a low tensile resistance by the Brazilian test. AUSTRALIAN JOURNAL OF APPLIED SCIENCE Vol.10, 1959.

2. Timoshenko S. and Goodier J.N. THEORY OF ELASTICITY McGraw-Hill, New York, 3rd Edition, 1970.

3. Wright P.J.F. Contents of an indirect tensile test on concrete cylinders. MAGAZINE OF CONCRETE RESEARCH Vol. 7-8, 1955-56.

4. Sokolnikoff I.S. MATHEMATICAL THEORY OF ELASTICITY McGraw-Hill, 2nd Edition, 1946.

5. Muskhelishvili N.I. SOME BASIC PROBLEMS OF THE MATHEMATICAL THEORY OF ELASTICITY 4th Edition 1963, P Noordhoff, Groningen.

6. T.R.B. Special Report 162, TEST PROCEDURES FOR CHARACTERISING DYNAMIC STRESS-STRAIN PROPERTIES OF PAVEMENT MATERIALS Washington, 1975.

7. Krishnayya V.G., Eisenstein Z.M. and Morgenstern N.R. BEHAVIOUR OF COMPACTED SOILS IN TENSION Journal of the Geotechnical Engineering Division, A.S.C.E. Sept, 1974.

8. Uriel S. and Mier F. DISCUSSION OF BEHAVIOUR OF COMPACTED SOIL IN TENSION Journal of Geotechnical Engineering Division, A.S.C.E. June, 1975.

9. Jumikis A.R. ROCK MECHANICS 2nd Edition, Trans Tech Publications, 1983.

10. Young R.N., Towsend,F.C. LABORATORY SHEAR STRENGTH OF MATERIALS A.S.T.M., S.T.P 740, 1981.

11. Ajaz A. and Parry R.H.G. AN UNCONFINED DIRECT TENSION TEST FOR COMPACTED CLAYS Journal of testing and evaluation, May, 1974.

12. Hawkes I. Mellor M. and Gariepy S. DEFORMATION OF ROCKS UNDER UNIAXIAL TENSION International Journal of Rock Mechanics, Mining Science and Geomechanical Engineering, Vol.10, 1973.

13. Fainhurst C. ON THE VALIDITY OF THE "BRAZILIAN" TEST FOR BRITTLE MATERIALS International Journal of Rock Mechanics, Mining Science and Geomechanical Engineering, Vol.1, 1964.

14. Davies J.D. and Stagg K.G. SPLITTING TESTS ON ROCK SPECIMENS Proceedings of 2nd Congress of Rock Mechanics, Beograd, 1970.

15. Wijk G. SOME THEORETICAL ASPECTS OF INDIRECT MEASUREMENTS OF THE TENSILE STRENGTH OF ROCKS International Journal of Rock Mechanics, Mining Science, and Geomechanical Engineering, Vol.15, pp 149-160, 1976.

16. Sundaram S.and Corroles F. BRAZILIAN STRENGTH OF ROCKS WITH DIFFERENT ELASTIC PROPERTIES IN TENSION AND COMPRESSION International Journal of Rock Mechanics, Mining Science and Geomechanical Engineering, Vol.17, 1980.

17. Fang H.Y. and Deutch W.L. BEHAVIOUR OF COMPACTED SOIL IN TENSION Journal of the Geotechnical Engineering Division, A.S.C.E., Sept, 1974.

18. Kennedy T.W. CHARACTERISATION OF PAVEMENT MATERIALS FOR FUNDAMENTAL STRUCTURAL ANALYSIS Lecture Notes.

19. Department of the Army. ENGINEERING AND DESIGN LABORATORY SOILS TESTING Washington, May, 1980.

20. Hadley W.O., Hudson W.R. and Kennedy T.W. AN
21. EVALUATION OF FACTORS AFFECTING THE TENSILE
22. PROPERTIES OF ASPHALT TREATED MATERIALS
Research Report 98-2 & 98-9 & 98/10, - Centre of Highway Research.

23. Ismael N.F., Alkhalidi O. and Mollah M.A. SATURATION EFFECTS ON CALCEROUS DESERT SANDS TRR 1089.

24. Pumphery N.D. and Lentz R.W. DEFORMATION ANALYSIS OF FLORIDA HIGHWAY SUBGRADE SAND SUBJECTED TO REPEATED LOAD TRIAXIAL TESTS TRR 1089.

25. Timmerman D.H.and Wu T.H. BEHAVIOUR OF DRY SANDS UNDER CYCLIC LOADING Journal of Soil Mechanics and Foundations Division, A.S.C.E., July, 1969.

26. Seed H.B. and Lee K.L. LIQUIFACTION OF SATURATED SANDS DURING CYCLIC LOADING Journal of Soil Mechanics and Foundations Division, A.S.C.E., Nov, 1966.

27. Khosla V.K. and Wu T.H. STRESS STRAIN BEHAVIOUR OF SAND Journal of Soil Mechanics and Foundations Division, A.S.C.E., April, 1976.

28. Schwab H.H. SETTLEMENT AND PORE PRESSURE DUE TO CYCLIC LOADING International Conference of Soil Mechanics and Foundation Engineering, Vol.3, 1981.

29. Cuellar V., Bazant Z.P., Krizek R.J. and Silver M.L. DENSIFICATION AND HYSTERESIS OF SAND UNDER CYCLIC SHEAR Journal of Soil Mechanics and Foundations Division, A.S.C.E., May, 1977.

30. Mitchell R.J. and King R.D. CYCLIC LOADING OF AN OTTAWA AREA CHAMPLAIN SEA CLAY Canadian Geotechnical Journal, Vol.14, 1977.

31. Khosla V.K. and Singh R.D. INFLUENCE OF A NUMBER OF CYCLES ON STRAIN Canadian Geotechnical Journal, Vol.15, 1978.

32. Silver M.L., Chan C.K., Cadd R.S., Lee K.L., Tiedemann D.A., Townsend F.C., Valva J.E. and Wilson J.H. CYCLIC TRIAXIAL STRENGTH OF STANDARD TEST SAND Journal of the Geotechnical Engineering Division, A.S.C.E., May, 1976.

33. Castro G. and Christian J.T. SHEAR STRENGTH OF SOILS AND CYCLIC LOADING Journal of the Geotechnical Engineering Division, A.S.C.E., Sept, 1976.

34. Youd T.L. and Craven T.N. LATERAL STRESSES IN SANDS DURING CYCLIC LOADING Journal of the Geotechnical Engineering Division, A.S.C.E., Feb, 1975.

35. Wong R.T., Seed H.B. and Chan C.K. CYCLIC LOADING LIQUIFACTION OF GRAVELLY SOILS Journal of the Geotechnical Engineering Division, A.S.C.E., June, 1975.

36. Park T.K. and Silver M.L. DYNAMIC TRIAXIAL AND SIMPLE SHEAR BEHAVIOUR OF SAND Journal of the Geotechnical Engineering Division, A.S.C.E., June, 1975.

37. Brown S.F. and Hyde A.F.L. SIGNIFICANCE OF CYCLIC CONFINING STRESS IN REPEATED LOAD TRIAXIAL TESTING OF GRANULAR MATERIAL TRR 537, 1975.

38. Annaki M. and Lee K.L. EQUIVALENT UNIFORM CYCLE CONCEPT FOR SOIL DYNAMICS Journal of the Geotechnical Engineering Division, A.S.C.E., June, 1977.

39. Silver M.L. and Seed H.B. DEFORMATION CHARACTERISTICS OF SANDS UNDER CYCLIC LOADING Journal of the Soil Mechanics and Foundations Division, A.S.C.E., August, 1971.

40. Prater E.G. CYCLIC SHEAR RESISTANCE ON NON COHESIVE SOILS Journal of the Geotechnical Engineering Division, A.S.C.E., Jan, 1980.

41. Hardin B.O. and Drnevich V.P. SHEAR MODULUS AND DAMPING IN SOILS:DESIGN EQUATIONS AND CURVES Journal of the Soil Mechanics and Foundations Division, A.S.C.E., July, 1972.

42. Dupas J.M. and Pecker A. STATIC AND DYNAMIC PROPERTIES OF SAND CEMENT Journal of the Geotechnical Engineering Division, A.S.C.E., March, 1979.

43. Selig E.T. and Chang C.S. SOIL FAILURE MODES IN UNDRAINED CYCLIC LOADING Journal of Geotechnical Engineering Division, A.S.C.E., May, 1981.

44. Richard R.M. and Abbot B.J. VERSATILE ELASTIC PLASTIC STRESS-STRAIN FORMULA Journal of Engineering Mechanics Division, A.S.C.E., August, 1975.

45. Donald A.W.T., Harvey R.C. and Burley E. STRESS STRAIN CHARACTERISTICS OF SAND Journal of Geotechnical Engineering Division, A.S.C.E., May, 1975.

46. Desai C.S. and Wu T.H. A GENERAL FUNCTION OF STRESS STRAIN CURVES Proceedings of the 2nd International Conference on Numerical Methods, Blacksberg, Virgina, 1976.

47. Doshi S.N. and Mesdary M.S. ESTIMATIONS OF DYNAMIC MODULUS OF SOIL CEMENT Journal of Australian Road Research Board, Vol.15 No.2, June, 1985.

48. Bush III A.J. and Alexander D.R. PAVEMENT EVALUATION USING DEFLECTION BASIN MEASUREMENTS AND LAYERED THEORY TRR 1022, 1985.

49. Kinder D.F. TRIAXIAL TESTING OF ROAD MAKING MATERIALS Australian Road Research, March, 1987.

50. Emery S.J. PREDICTION OF PAVEMENT MOISTURE CONTENT IN SOUTH AFRICA Proceedings of the 8th Regional Conference of Africa on Soil Mechanics and Foundation Engineering, Harare, 1984.

51. Brink A.B.A. ENGINEERING GEOLOGY OF SOUTHERN AFRICA Vol.4, Building Publishers Pretoria, November, 1984.

52. Peacock W.H. and Seed H.B. SAND LIQUIFACTION UNDER CYCLIC LOADING Journal of Geotechnical Division, A.S.C.E., May, 1968.

53. Seed H.B. and Chan C.K. EFFECT OF DURATION OF STRESS APPLICATION ON SOIL DEFORMATION UNDER REPEATED LOADING Proceedings of the 5th International Conference of Soil Mechanics, Paris, 1961.

54. Stewart H.E. PERMANENT STRAINS FROM CYCLIC VARIABLE AMPLITUDE LOADINGS Journal of Geotechnical Engineering Division, A.S.C.E., June, 1986.

55. Diyaljee V.A. and Raymond P. REPETITIVE LOAD DEFORMATION OF COHESIONLESS SOIL Journal of Geotechnical Engineering Division, A.S.C.E., October, 1982.

56. TMH1 STANDARD METHODS OF TESTING ROAD CONSTRUCTION MATERIALS National Institution for Transport and Road Research, Second Edition, 1986.

65. Nwakanma C.A. and Cabrera J.G. FACTORS INFLUENCING THE POZZOLANI ACTIVITY OF RED TROPICAL SOILS Seventh Regional Conference for Africa on Soil Mechanics and Foundation Engineering, Accra, 1980.

66. Shen C.K. and LI S.K. LIME STABILIZATION OF CLAY-SAND MIXTURES Highway Research Board 315, 1970.

67. Head K.H. MANUAL OF SOIL LABORATORY TESTING Vol.3, effective stress testing, Penteh Press, 1986.

68. Lambe T.W. and Whitman R.V. SOIL MECHANICS Wiley and Sons, 1969.

69. Bishop and Henkel. MEASUREMENT OF SOIL PROPERTIES IN THE TRIAXIAL TEST 2nd Edition, William Clowes and Son, 1964.

70. Black D.K. and Lee k.l. SATURATING SOIL SAMPLES BY BACK PRESSURE Journal of Soil Mechanics and Foundations Division, A.S.C.E., 1973.

71. Rad N.S. and Clough G.W. NEW PROCEDURE FOR SATURATING SAND SPECIMENS Journal of the Geotechnical Engineering Division, A.S.C.E., Vol.110 No.9, September, 1984.

72. Carvalho de C., Domaschuk L. and Mieussens C. DISCUSSION ON THE NEW PROCEDURE FOR SATURATING SAND SPECIMENS Journal of the Geotechnical Engineering Division, A.S.C.E., Vol.110 No.9, September, 1984.

73. Errera L.A. STRESS PATHS AND COLLAPSING SOILS MSc. Thesis, Department of Civil Engineering University of Cape Town, 1977.

74. Jennings J.E. and Knight K. A GUIDE TO CONSTRUCTION ON OR WITH MATERIALS ESTABLISHING ADDITIONAL SETTLEMENT DUE TO COLLAPSE OF THE GAIN STRUCTURE Proceedings of the 6th Regional Conference for Africa, 1975.

75. Knight K. and Dehlen G.L. THE FAILURE OF A ROAD CONSTRUCTED ON A COLLAPSING SOIL Proceedings of the 3rd Regional Conference of Africa, 1963.

76. Weston D.J. COMPACTION FOR COLLAPSING SAND ROAD BEDS Proceedings of the 7th Regional Conference for Africa, 1980.

77. Schwartz K. COLLAPSIBLE SOILS, PROBLEM SOILS IN SOUTHERN AFRICA The Civil Engineer in South Africa, 1985.

78. Jones D.L. and van Alphen G.H. COLLAPSING SANDS, A CASE HISTORY Proceedings of the 6th Regional Conference for Africa, 1980.

79. Boniface A. and Olivier H.J. SOME CHARACTERISTICS OF BEREA RED FORMATION IN THE GLENWOOD TUNNEL, DURBAN Symposium on the Engineering Geology of Cities in South Africa, September, 1981.

80. Brink A.B.A. ENGINEERING GEOLOGY OF SOUTHERN AFRICA Vol.3, Building Publishers, Pretoria, November, 1985.

81. Schwartz K. COLLAPSIBLE SOILS State of the Art Report, Civil Engineer in South Africa, July, 1985.

82. Lowe J. and Johnson T.C. USE OF BACKPRESSURE TO INCREASE THE DEGREE OF SATURATION OF TRIAXIAL TEST SPECIMENS A.S.C.E., Research Conference of Shear Strength of Cohesive Soils, 1960.

83. Head K.H. SOIL LABORATORY TESTING Vol.2, Pentech Press, 1981.

84. Lambe T.W. and Whitman R.V. SOIL MECHANICS Wiley and Sons, 1969.

85. Bishop A.W. and Wesley L.D. AN HYDRAULIC TRIAXIAL APPARATUS FOR CONTROLLED STRESS PATH TESTING Geotechnique 25 No.4, 1975.

86. Skempton A.W. THE PORE PRESSURE CO-EFFICIENTS A AND B Geotechnique, 1954.

87. Horok E. ASPECTS OF A DEFLECTION BASED MECHANISTIC OVERLAY DESIGN APPROACH FOR FLEXIBLE PAVEMENTS C.S.I.R. report RP/20, May, 1986.

88. Lentz R.W. and Baladi G.T. CONSTITUTIVE EQUATION FOR PERMANENT STRAIN OF SAND SUBJECTED TO CYCLIC LOADING TRR 810, 1981.

89. Uzan J. CHARACTERIZATION OF GRANULAR MATERIAL TRR 1022, 1985.

90. Potter D.W. and Donald G.S. REVISION OF NAASRA INTERIM GUIDE TO PAVEMENT THICKNESS DESIGN Journal of Australian Road Research Board, June, 1985.

91. Yoder E.J. and Witszac M.W. PRINCIPALS OF PAVEMENT DESIGN 2nd Edition J.Wiley and Son Inc. 1975, 1st Edition, 1959.

92. Silver M.L. and Park T.K. TESTING PROCEDURE EFFECTS ON DYNAMIC SOIL BEHAVIOUR Journal of Geotechnical Engineering Division, A.S.C.E., October, 1975.

93. Rada G. and Witczak M.W. COMPREHENSIVE EVALUATION OF LABORATORY RESILIENT MODULI RESULTS FOR GRANULAR MATERIAL TRR 810, 1981.

94. Menzies B. A COMPUTER CONTROLLED TRIAXIAL SYSTEM ASTM, Symposium of Advanced Triaxial Testing of Soil and Rock, June, 1986.

APPENDIX A

a) Compaction tests

Moisture density relationship of natural Berea Red soil

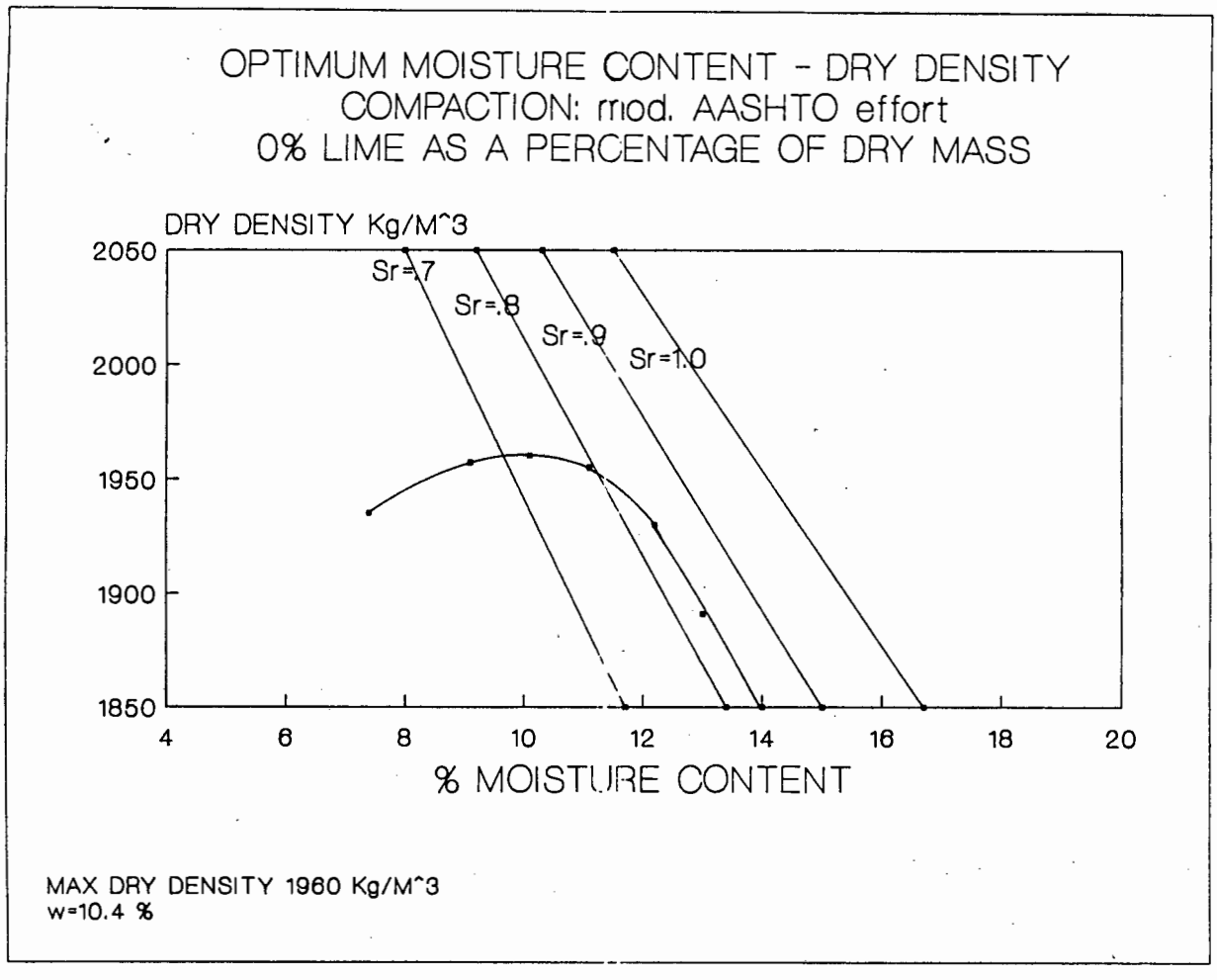

Moisture density relationship of Berea Red soil modified with 2% lime

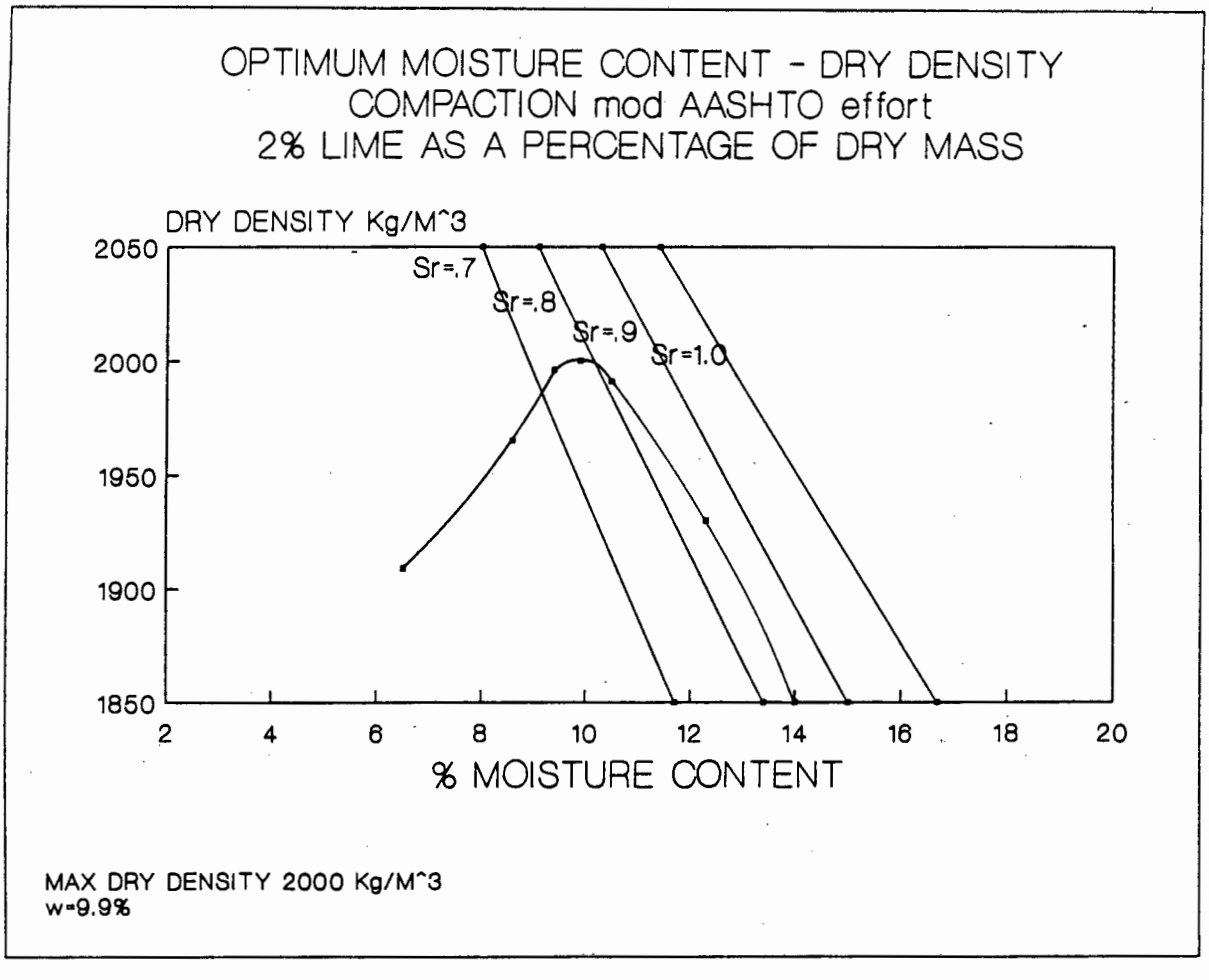

Moisture density relationship of Berea Red soil modified with 4% lime

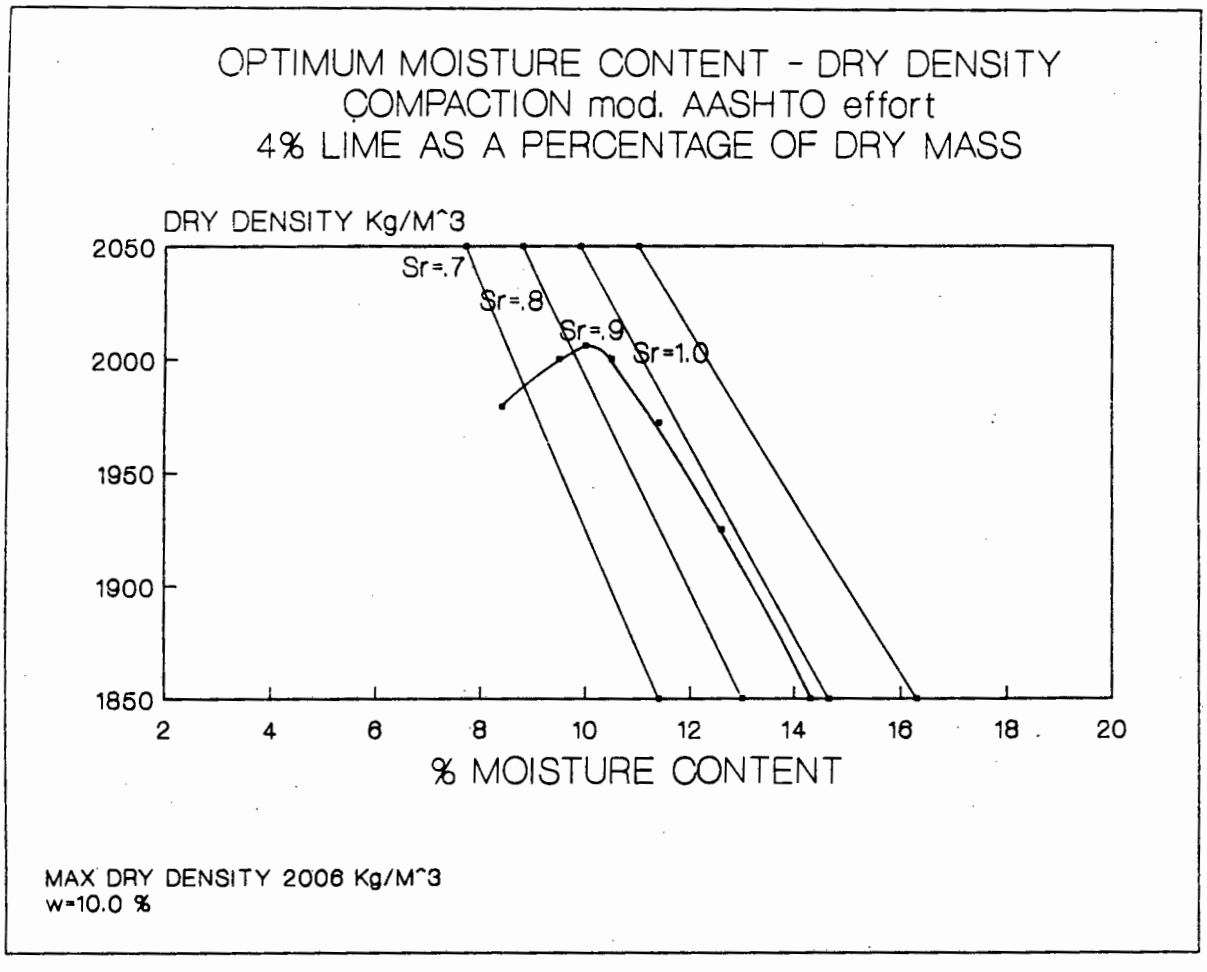

b) Indicator tests

Grading curve and Atterberg limits of natural Berea Red soil

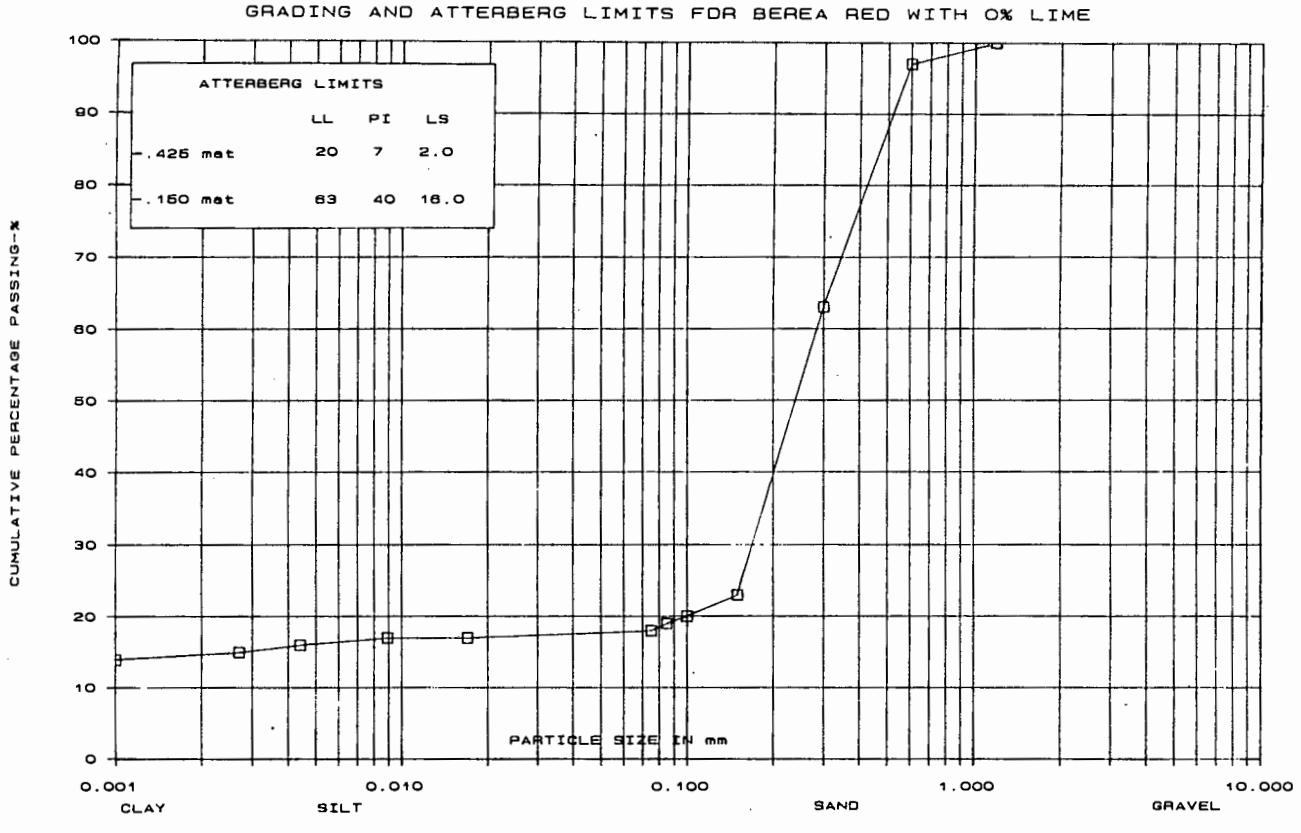

Grading curve and Atterberg limits of Berea Red soil modified with 2% lime

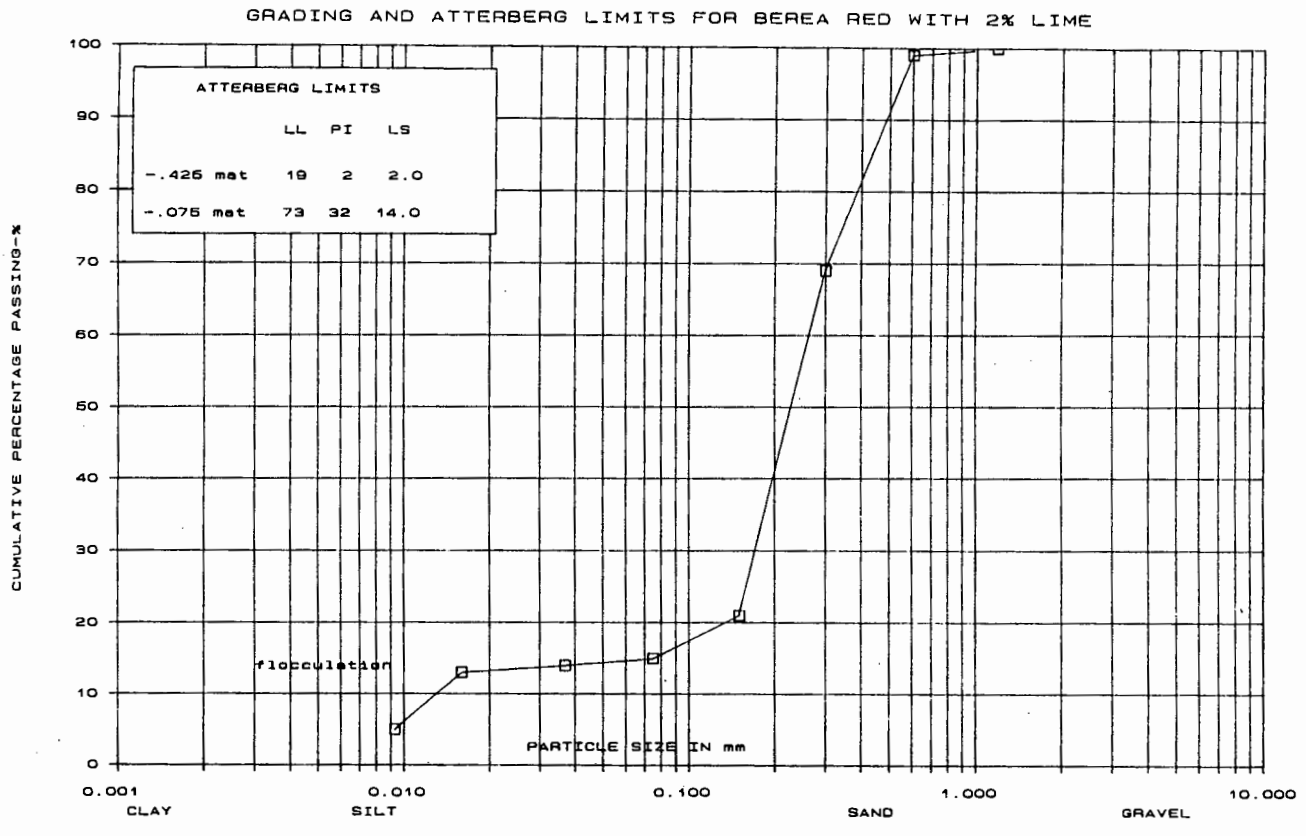

Grading curve and Atterberg limits of Berea Red soil modified with 4% lime

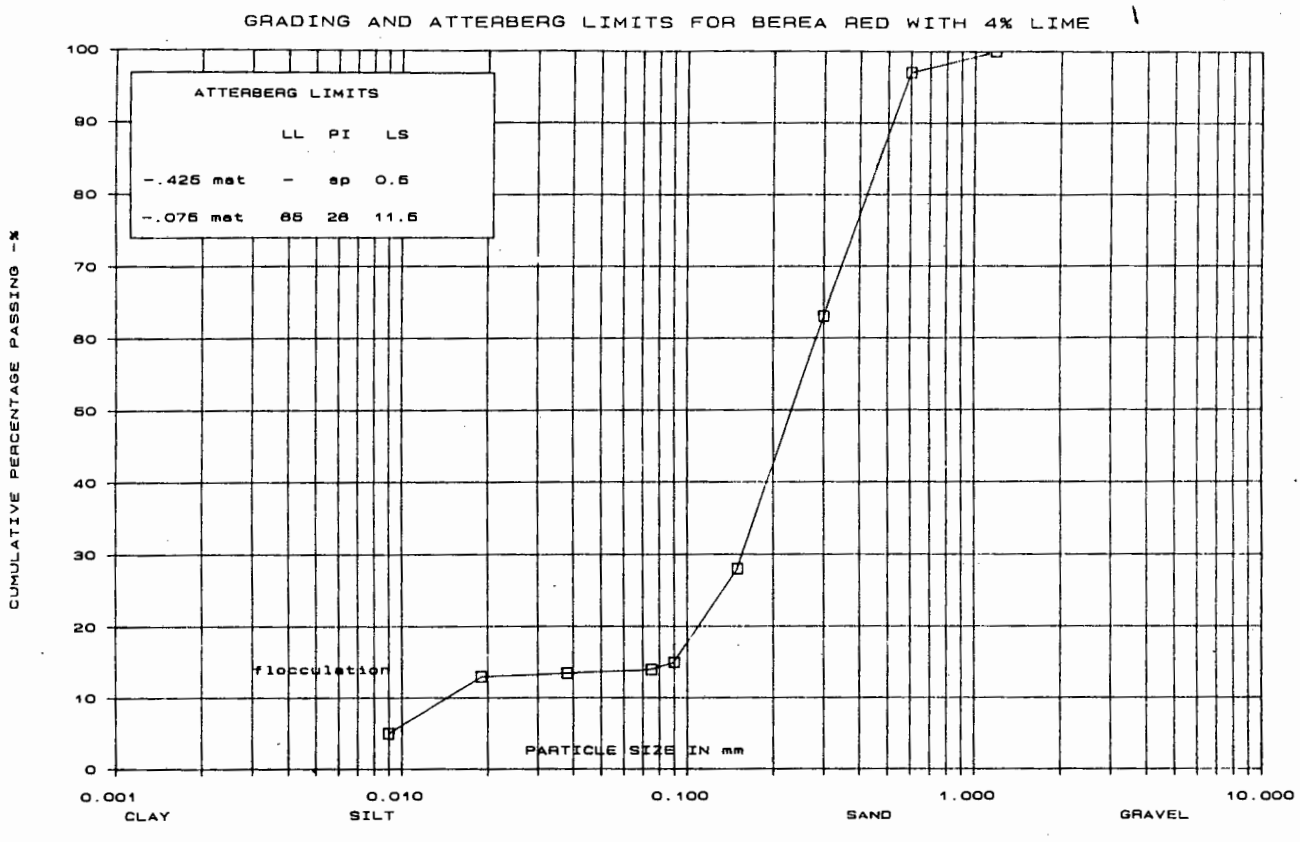

OBSERVED RELATIVE DENSITIES	
Lime only	2,227
Berea Red with 0% Lime	2,680
Berea Red with 2% Lime	2,677
Berea Red with 4% Lime	2,647

c) Oedometer tests

Number of tests	% lime	% mod AASHTO density	% w	curing days	Remarks
4	0	100	10,4	-	
2	0	95	10,4	-	
2	0	90	10,4	-	
1	2	100	10,4	10	
2	4	100	10,4	10	
1	2	100	10,4	18	
2	4	100	10,4	18	
2	0	90	10,4	-	Collapse potential

d) California Bearing Ratio tests

PERCENTAGE ADDITIVE	CBR RATIO			
	DAYS CURING			
	0	3	7	28
0	94	-	-	-
2	-	160	135	160
4	-	185	128	180

CBR's expressed for material moulded at 100% mod AASHTO density.

e) Unconfined Compression tests

STABILIZER %	UNCONFINED COMPRESSION STRENGTH (MPa)		
	DAYS CURING		
	7	28	Rapid Cured
2% lime	0,86	0,91	3,47
4% lime	1,01	1,27	4,40
1% lime + 1% slag	0,79	1,11	0,84
2% lime + 2% slag	0,92	1,06	4,05
2% cement	1,4	1,55	1,83
4% cement	3,23	2,74	3,47

Each result is an average of two test specimens.

APPENDIX B

a) Tensile testing results of Berea Red soil

0% lime at 95% mod AASHTO density

SAMPLE	ν	E [MPa]	X_{tf} 10E-4 [mm]	ε_{tf} [%]	σ_t [kPa]
BR18	0,195	33	6,0	0,032	41,0
BR19	0,287	54	5,5	0,029	44,2
BR20	0,304	47	6,2	0,032	36,7
BR21	0,287	46	6,0	0,032	44,2

0% lime at 100% mod AASHTO density

SAMPLE	ν	E [MPa]	X_{tf} 10E-4 [mm]	ε_{tf} [%]	σ_t [kPa]
BR14	0,311	71	6,1	0,031	59,3
BR15	0,146	62	7,5	0,041	66,9
BR16	0,160	30	6,6	0,036	62,0
BR17	0,214	67	5,4	0,029	61,5

0% lime at 100% mod AASHTO density

SAMPLE	ν	E [MPa]	X_{tf} 10E-4 [mm]	ε_{tf} [%]	σ_t [kPa]
BR01	0,036	48	6,0	0,034	56,6
BR02	0,049	40	-	0,034	55,0
BR03	0,202	66	6,2	0,033	54,0
BR04	0,169	61	5,0	0,027	49,1

2% lime at 100% mod AASHTO density
cured at 7 days

SAMPLE	γ	E [MPa]	X_{tf} 10E-4 [mm]	ε_{tf} [%]	σ_t [kPa]
2L1	0,213	78	2,6	0,015	55,0
2L2	*(1)	121	3,0	0,015	92,3
2L3	0,190	89	3,2	0,017	72,8
2L4	0,379	94	4,5	0,023	67,4

4% lime at 100% mod AASHTO density
cured at 7 days

SAMPLE	γ	E [MPa]	X_{tf} 10E-4 [mm]	ε_{tf} [%]	σ_t [kPa]
4L1	-	*(2)	1,4	0,008	89,6
4L2	0,195	129	1,6	0,009	78,2
4L3	0,025	122	0,6	0,003	70,1
4L4	0,116	107	1,5	0,008	87,4

2% lime at 100% mod AASHTO density
cured at 28 days

SAMPLE	γ	E [MPa]	X_{tf} 10E-4 [mm]	ε_{tf} [%]	σ_t [kPa]
2L5	-	-	-	-	97,1
2L6	-	42	0,9	0,005	87,9
2L7	-	152	0,8	0,005	91,7
2L8	*(1)	94	1,7	0,010	94,4

4% lime at 100% mod AASHTO density
cured at 28 days

SAMPLE	γ	E [MPa]	X_{tf} 10E-4 [mm]	ε_{tf} [%]	σ_t [kPa]
4L5	-	0,344	1,0	0,006	128,9
4L6	-	0,345	2,0	0,012	124,1
4L7	-	0,241	1,0	0,006	115,8
4L8	-	-	1,0	0,006	144,1

*(1) Poisson's ratio is not always readily obtained due to bad deformation ratio values.

*(2) When unrealistic Poisson's ratios were obtained, a value of 0,24 was used to calculate Elastic modulus values.

6% lime at 100% mod AASHTO density
cured at 28 days

SAMPLE	γ	E [MPa]	X_{tf} 10E-4 [mm]	ε_{tf} [%]	σ_t [kPa]
1L6	-	120	2,5	0,013	91,7
2L6	-	140	10,0	0,052	107,9
3L6	-	150	2,0	0,010	80,9
4L6	-	-	-	-	91,7

8% lime at 100% mod AASHTO density
cured for 28 days

SAMPLE	γ	E [MPa]	X_{tf} 10E-4 [mm]	ε_{tf} [%]	σ_t [kPa]
1L8	0,138	308	2,0	0,011	92,8
2L8	-	121	2,2	0,012	183,4
3L8	-	868	1,0	0,005	156,5
4L8	-	388	1,0	0,005	172,6

6% cement at 100% Mod AASHTO density
cured at 28 days

SAMPLE	ν	E [MPa]	X_{tf} 10-E4 [mm]	ε_{tf} [%]	σ_t [kPa]
1/6C	,364	794	9,0	0,047	809,3
2/6C	,167	657	7,0	0,037	701,4
3/6C	-	-	-	-	733,1
4/6C	,198	730	8,0	0,043	809,3

LESOTHO CLAY - DRY DENSITY 1454 kg/m at w = 27%
PI = 40 LL = 65,0 PL = 15,5

SAMPLE	ν	E [MPa]	X_{tf} 10E-4 [mm]	ε_{tf} [%]	σ_t [kPa]
LC1	-	51	0,102	0,054	69,1
LC2	-	47	5,3	0,028	60,4
LC3	-	91	5,1	0,027	72,8

CAPE FLATS SAND MOULDED WITH A POLYMER BINDER

SAMPLE	ν	E [MPa]	X_{tf} 10-E4 [mm]	ε_{tf} [%]	σ_t [kPa]	MOULDING DESCRIPTION
L8	0,019	589	-	-	194,2	Material poured into Mould and levelled
L7	0,048	573	-	-	221,2	
P7	0,755	502	-	-	766,1	Material packed in and levelled
P8	0,908	468	-	-	728,3	
T8	0,116	302	-	-	501,7	Material lightly tamped and levelled
T7	-	-	-	-	463,9	

ν = Poisson's Ratio
E = Elastic Modulus (MPa)
X_{tf} = Total Horizontal Deformation (mm)
$\%\varepsilon_{tf}$ = Total % Tensile Strain at Failure

THE FOLLOWING EQUATIONS WERE USED FOR THE DERIVATION OF THE ITS TEST DERIVED MATERIAL PROPERTIES

TENSILE FAILURE STRESS: σ_t

$$\sigma_t = 2F(i)/\pi t L_o \times (\sin 2\alpha - t/D_o) \quad [1]$$

t = width of load platten [mm]
D_o = diameter of specimen [mm]
L_o = height of specimen [mm]
2α = the angle subtended by the load platten and the centre [rad]
$F(i)$ = applied load at reading number (i) [N]

POISSON'S RATIO (for 100 diameter specimens)

$$\gamma = \frac{0,0673D_R - 0,8954}{-0,2494D_R - 0,0156} \quad [2]$$

D_R = deformation ratio (vertical strain/horizontal strain) slope of the best fit line by linear regression from 0 to point of failure.

ELASTIC MODULUS (Mpa):(for 100 diameter specimens)

$$E = S_H/H\,[0,9976\,\gamma + 0,2692] \quad [3]$$

S_H = horizontal tangent modulus [applied load (N)/horizontal deformation(mm)] up to the point of failure.

H= height of the specimens [mm].

TOTAL TENSILE STRAIN:at the point of failure

$$\varepsilon_{TF} = X_{TF}(0,1185\gamma+0,03896)/(0,2494\gamma+0,0673) \quad [4]$$

X_{TF} = total horizontal deformation at the point of failure [mm].

Typical Plots of (a) vertical strain vs horizontal strain and (b) vertical load vs horizontal displacement

(a)

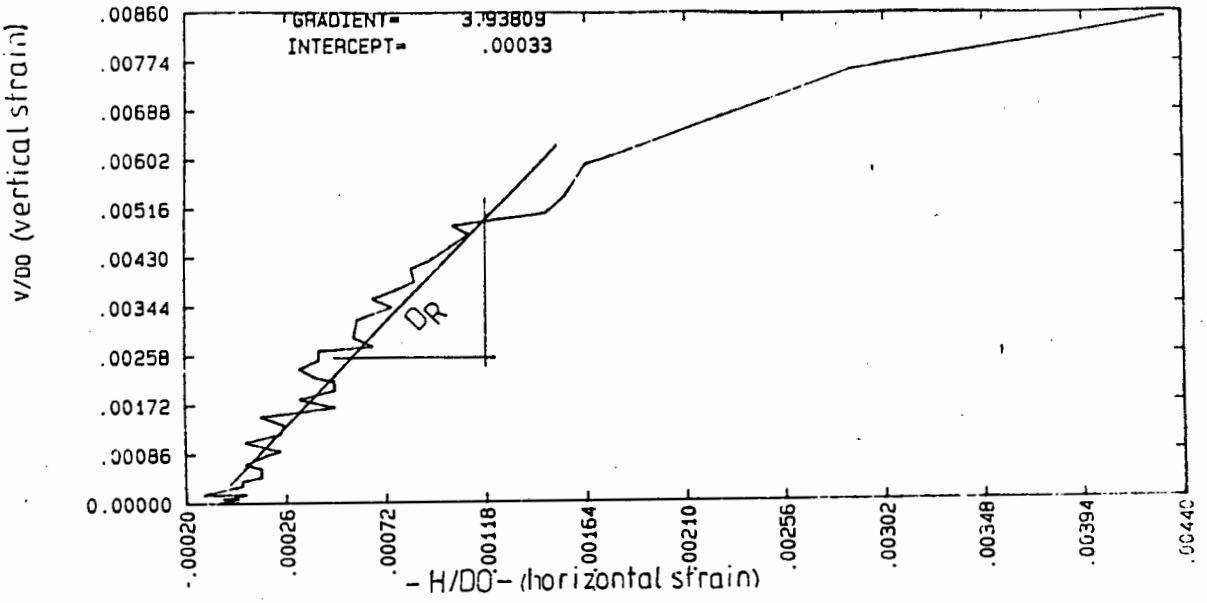

(b)

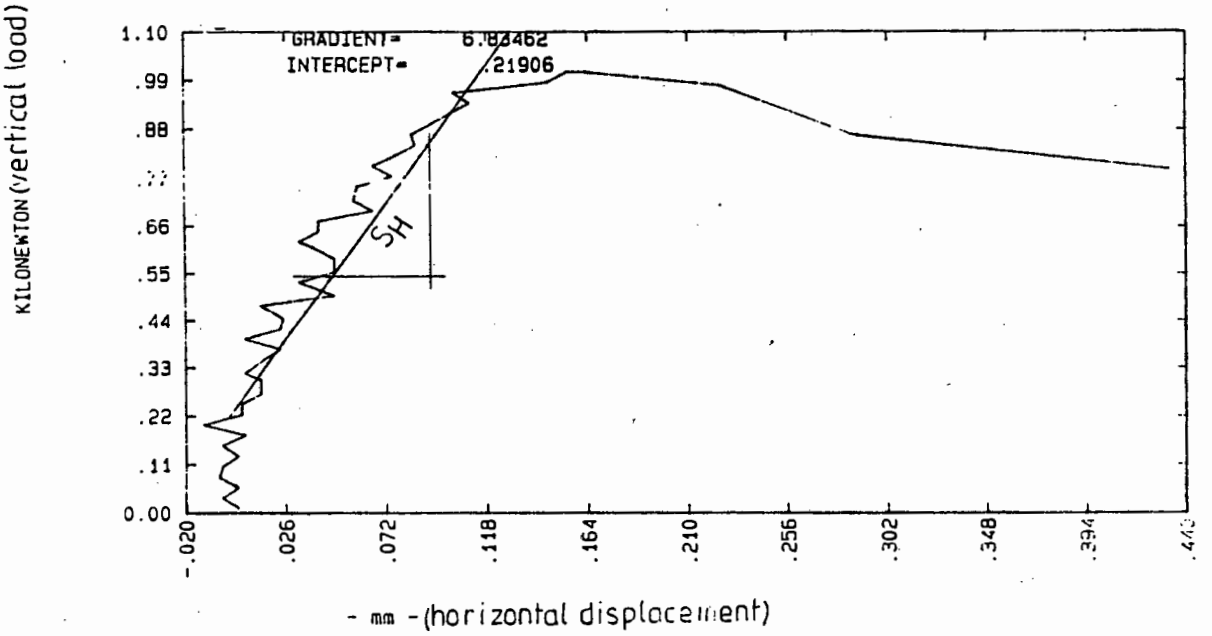

The determination of the above equations (1 to 4) to determine the stresses and strains at the centre of a diametrically loaded disc i.e. r/R=0

reveals:

The tensile stress at the center:

$$\sigma_{\theta x} = \sigma_{rx} = \frac{2P}{\pi.D.t}$$

And the compressive stress at the center:

$$\sigma_{\theta y} = \sigma_{ry} = \frac{-6P}{\pi.D.t}$$

where D=diameter of the specimen
and all other variables as before.

Tensile stresses positive
Compressive stresses negative

The above agrees with Hadley et al's(20) formulation of the stresses.

Some authors have expressed concern about the stress condition at the points of loading. It was thought that high compressive forces in this area were firstly causing failure locally and therefore resulting in a tensile crack due to the wedge action at the top and bottom in the area of the loading platten.

The stress distribution in the region of the load, reveals that biaxial compression takes place, which implies that the material can resist much greater compressive strength in an unconfined situation. In the ITS test, the ratio of tensile stress at the center to rim compressive stress is 18 to 1. Therefore end crushing is unlikely to precede tensile failure of the soil specimen.

Prior to the development of LVDT's (Linear variable displacement transducers) strain rosettes set at 120 degrees to each other were used to measure strain during ITS tests by bonding them to the ends of the specimen with adhesive thus allowing strain to be measured. This procedure is quite unsatisfactory for testing soil as the strain gauges can not be succesfully bonded to the soil. Measuring strain at the ends of a specimen has a number of short-falls and is illustrated by Wijk(15).

Wijk(15) used three dimensional elasticity to highlight the uneven tensile stress distibution that occurs along the failure plane of an ITS specimen. Fig.81 was produced using his equations to highlight the variation if a tensile stress of unity is assumed at the center of the specimen. Using the same theory he produced a relationship for determining the maximum length of the specimen t(max). If the tensile stresses in the vicinity of the loads shall not exceed those of the central part of the specimen, then for Wijk's(15) example $|Z| < 0.17R$ and a subtended angle $\alpha = 7.5$ (the angle between the loading platten and the center of the cylindrical sample) and a Poisson's ratio ν of 0,3. (which implies that the thickness should not be greater than 17 percent of the specimen diameter.)

In the case of this research, a proctor mould has been chosen in which the size is 115mm x 100mm diameter which satisfies the above requirement of t>1,17xradius.

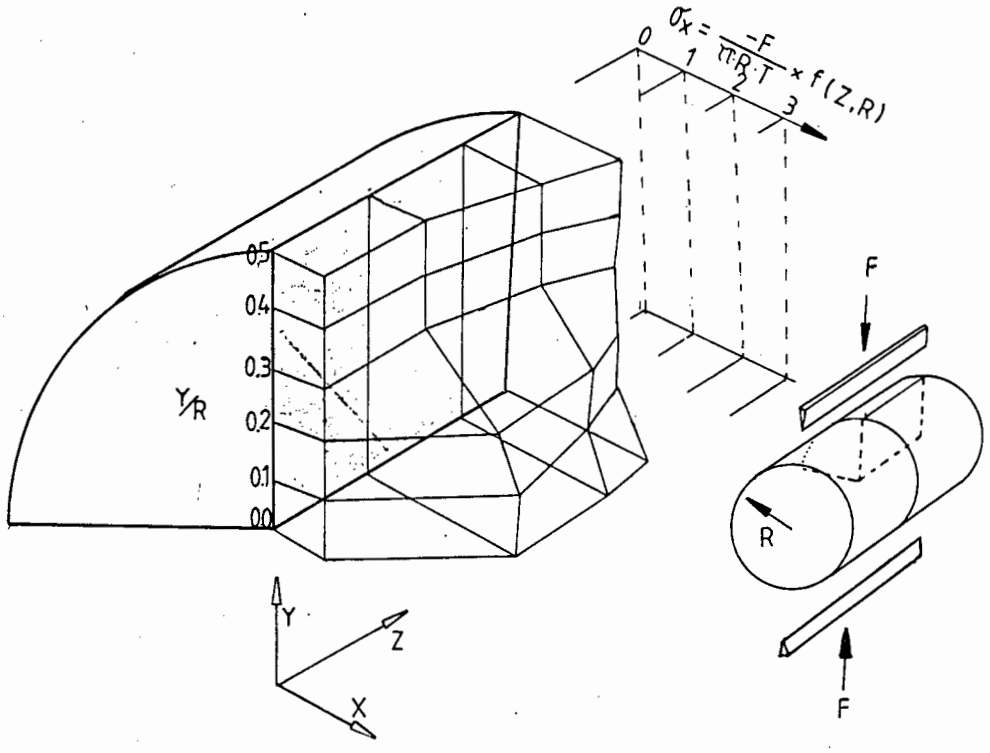

Fig. B1 σ_x distribution along half length of a quarter cylinder (after Wijk(15))

The rather complicated combination of normal and shear surface loads necessary to produce a plane stress field within a specimen can never be applied in practice in a controlled manner. Thus, one is left with considerable uncertainty about stress in the vicinity of the loads. This implies in the ITS tests, attention should not be directed to the theoretically calculated stresses at points in the specimen which are close to the loaded areas. From this it can be concluded that the tensile stress at the center of the specimen is the most reliable location to determine stresses and strains.

Having identified the equation for stress distribution within a diametrically loaded specimen assuming the "knife edge" width a<0,1D, (where (a) is the knife width and (D) is the diameter) a relationship between the ratio of Tensile/Applied stress can be calculated and plotted against the ratio of Y-ordinate/Radius if t=12mm or 19mm and R=50mm.

The results in Fig. 5.3 show that the 12mm knife edge produces a larger, though lower tensile stress distribution along the specimen diameter. Therefore based on the above a 12mm platten was adopted.

If the tensile stress distribution is integrated across the limits ±0.84 Y/R (which are the limits of the tensile stress, then the tensile force (Ft) is

$$Ft(X) = \int_{40.19}^{-40.19} \sigma_{\theta} \quad \delta x$$

knowing the relationship between jack pressure P(I) and the loading strip pressure Ps(i).

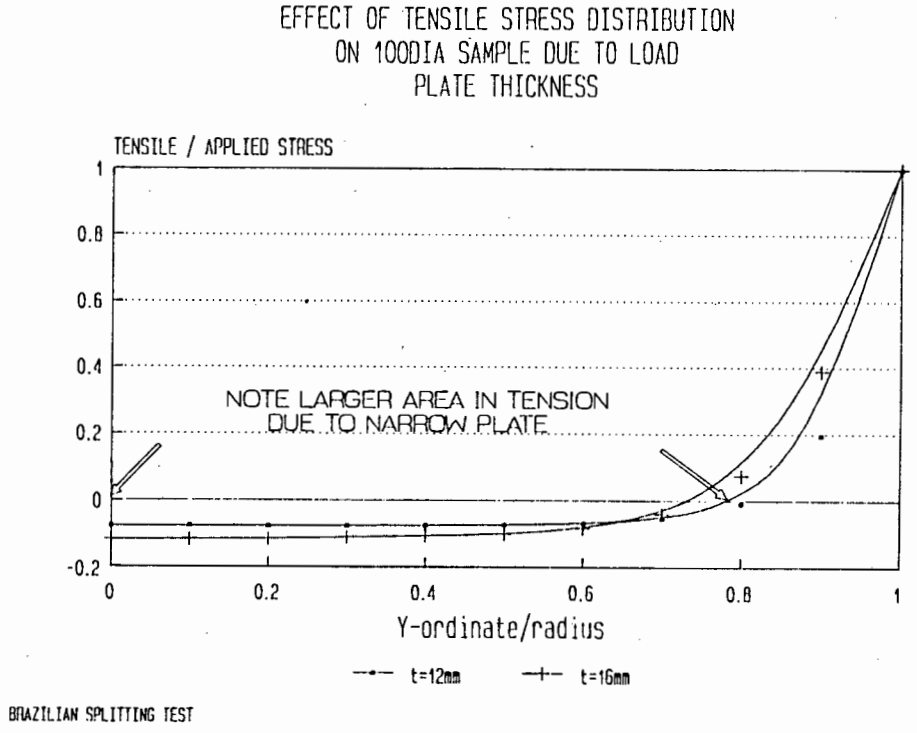

Fig. B2 Stress distribution due to load platten thickness on the ITS test

It follows that the tensile stress in the specimen with a 100mm diameter jack and a jack pressure of P(I)kPa

$$\tilde{\sigma}t = \frac{Ft(I)}{A} = \frac{4.33P(I)}{Lo\,Do} MPa$$ Lo&Do in mm

If, however, the thickness of the bar is ignored, then

$$lim\tilde{\sigma}t(r, \theta = 0) = \frac{F(I)}{\pi Rt} = \frac{5.0P(I)}{Lo\,Do} MPa$$

Davies & Stagg(14) and TMH1(56) ignore the width of the loading strip which results in an error of 13 percent.

Hadley et al(20) use another modification of the same equation to determine $\tilde{\sigma}t$ in which they do not reveal the origin or source.

$$\tilde{\sigma}t = \frac{2F(I)}{\pi tLo}(\sin 2\alpha - \frac{t}{Do})$$ MPa - [1]

where:
t=plate width; Lo=height of specimen; Do=diameter of specimen; x=half the angle subtended by the origin of the load plate (in mm or radians).

Which if related to the jack pressure reveals

$$\tilde{\sigma}t = \frac{4.928}{Lo\,Do}\ P(I)$$ MPa for t=12mm

This implies a 1.4 percent error when compared to the equation for the uncorrected t.

Wright(3) used basic geometry to derive a correction factor c and applied the previous equation.

$$\tilde{\sigma}t = \frac{2F(I)}{\pi Do\, Lo} \bullet C$$

In conclusion, a correction in the order of 0.99 appears to be satisfactory if a 12mm loading bar is used on 100mm diameter specimens and was adopted for this research.

5.2.1 Strain measurement for soils

As previously mentioned, most work done on the Brazilian test was for obtaining properties of concrete hence it was necessary to devise a means of measuring strain on the extremes of the diameter of the specimen and to derive equations to determine the material properties from the measurements.

Hadley et al(20) have produced equations for the determination of the soil properties, but the origin and derivation was not presented. Further investigation revealed that the radial plane stress equations for strain were the basis of his work. Using the preceeding assumptions and derivations, LVDT's were the ideal means of determining external diametrical strain in two planes at the mid length of the specimen.

Determination of Poisson's ratio from an ITS test may be derived from a plane stress analysis using equations from Timoshenko et al(2)

$$\epsilon_\theta = \frac{1}{E}(\sigma_\theta - \nu\sigma_r) \qquad \epsilon_r = \frac{1}{E}(\sigma_r - \nu\sigma_\theta)$$

Combining these equations and eliminating Young's modulus,

$$\frac{\epsilon_r}{\epsilon_\theta} = \frac{(\sigma_r - \nu\sigma_\theta)}{(\sigma_\theta - \nu\sigma_r}$$

solving for Poisson's ratio v, and making $\frac{\epsilon_r}{\epsilon_\theta} = Dr$

$$\nu = \frac{(\sigma_r - \sigma_\theta Dr)}{(\sigma_\theta - \sigma_r Dr)}$$

Analysing the ITS test and taking signs into consideration (i.e. tension positive and compression negative), then

$$\nu = \frac{(\sigma_{ry} + \sigma_{rx} Dr)}{(\sigma_{\theta x} Dr + \sigma_{\theta y})}$$

As the equations are derived from an incremental element dr, then the stresses have to be integrated across the radius r, therefore

$$\nu = \frac{\left\{\int_{-r}^{+r} \sigma_{ry} + Dr \int_{-r}^{+r} \sigma_{rx}\right\}}{\left\{Dr \int_{-r}^{+r} \sigma_{\theta x} + \int_{-r}^{+r} \sigma_{\theta y}\right\}} \, dr$$

If this expression is fully expanded by inserting the equations for σ_{ry}, σ_{rx}, $\sigma_{\theta x}$, $\sigma_{\theta y}$ reveal an ungainly equation to be simplified and integrated, by numerical intergration. Hadley et al(20) used a programme MODELAS to perform the numerical integration and to simplify the problem further yet, they chose values for t-load plate width, R-radius of specimen which revealed the subtended angle α.

The simplified version for Poisson's ratio v for a 100 mm specimen is:

$$\nu = \frac{0.0673Dr - 0.8954}{-.2494Dr - 0.0156} \qquad - [2]$$

Young's modulus E may be determined using the same plane stress theory, hence:

$$\epsilon_r = \frac{1}{E}(\sigma_r - \nu\sigma_\theta)$$

$$E = \frac{1}{\epsilon_r}(\sigma_r - \nu\sigma_\theta)$$

$$E = \frac{P}{\epsilon_r}\left(\frac{\sigma_r}{P} \cdot \nu\frac{\sigma_\theta}{P}\right)$$

Again, as before, integrating the stresses over the radius r reveals:

$$E = \frac{P}{\epsilon_r}\left\{\int_{-r}^{+r}\frac{\sigma_{rx}}{P} - \nu\int_{-r}^{+r}\frac{\sigma_{\theta y}}{P}\right\}dr$$

set $\frac{P}{Xt} = S_H$ the best fit line between load P and horizontal deformation Xt and using a 100 mm specimen,

then $$E = \frac{S_H}{H}(0.9976\nu + 0.2692) \qquad \text{- [3]}$$

The tensile strain at failure ϵ_{tf} may be calculated using the equation:

$$\epsilon_\theta = \frac{(\sigma_r - \nu\sigma_\theta)}{E}$$

Using the same derivation procedure for Young's modulus above

$$\epsilon_\theta = \frac{\sigma_r - \nu\sigma_\theta}{\frac{P}{Xt}\left\{\frac{\sigma_r}{P} - \nu\frac{\sigma_\theta}{P}\right\}}$$

Again, the above is for an incremental element of strain across the complete specimen until first failure, then

$$\epsilon_{tf} = X_T\frac{\left[\int_{-l/2}^{+l/2}\frac{\sigma_{rx}}{P} - \nu\int_{-l/2}^{+l/2}\frac{\sigma_{\theta x}}{P}\right]dl}{\left[\int_{-r}^{+r}\frac{\sigma_{rx}}{P} - \nu\int_{-r}^{+r}\frac{\sigma_{\theta x}}{P}\right]dr}$$

which when simplified for a 100 mm specimen is

$$\epsilon_{tf} = X_{TF}\left[\frac{0.1185\nu + 0.03896}{0.2494\nu + 0.0673}\right] \qquad \text{- [4]}$$

Equations (1-4) were used for the derivation of the natural properties of Berea Red soil using ITS techniques.

b) Physical problems encountered while developing the strain measuring equipment

The ratio of vertical to horizontal strain should have been in the order of 6 to 7 i.e. (6 <vertical strain/horizontal strain> 7), but many of the tests were of the order of 10, which indicated that something was functioning incorrectly.

In order to discover which LVDT's were faulty it was decided to produce a `no go' situation, i.e. apply pressure but close the valve to the jack so no strain actually took place. It was found that when vertical strain was plotted against vertical stress a zero vertical strain was experienced. However, when horizontal strain vs vertical stress were plotted, positive and negative displacements in the order -0,01 to +0,1 mm were obtained.

To fully understand how the strains were measured, a study of the section on software should be made. However, at initialization of the test, fifteen readings at 100 micro-seconds delay were taken and averaged, and that average was considered E1(0). Any additional strain was equal to E1(n)-E1(0) (were (n)=reading set number).

It was found that two problems existed.

(a) The two ANI1 microlink channels were creating a scatter on the initialisation sub-routine of up to 10 digital units on the 4095 digital scale. This mystery was resolved when it was found that the channels had had the noise filters removed, as it was expected they should have been consistent. This was not the case. To rectify the problem all three channels were operated off the AN16-32 module with complete success.

(b) There was no scatter on the digital readings of the AN16-32 module in a no-strain situation which allowed the resolutions to be confidently stated as 2 microns.

A pause statement of 50 milliseconds had to be incorporated in between the talk and listen instructions to the A-D converter, as there was found to be a finite delay which caused erroneous readings to appear occassionally.

The vertical strain vs horizontal strain ratio was still not correct and after recalibration it was discovered that an LVDT was not functioning correctly. It was also found that if a calibration reading was taken and then the gauge head was moved and returned to the same position, the digital reading was out by 100 units, which amounted to 0,15 mm. A new LVDT was acquired and all horizontal strain problems were solved.

To measure the vertical strain a 400mm x 8mm x 100mm cantilever bar was attached to the jack shaft. The LVDT gauge head measured strain at the end of the cantilever when the jack moved. As the LVDT's were spring loaded and operate close to the limit in the compressed position a small load was applied to the cantilever which apparently moved downwards during testing, hence exagerating the vertical strain and thus causing the vert.str/hrz.str ratio to increase. A new thicker cantilever was made and the problem was solved.

During testing of the stiffer materials, it was found that negative strains were initially being recorded. These negative strains although small were, however, present (-0,01 mm max).

On inspection the digital LVDT readings revealed that one LVDT was sending values with increasing magnitude and the other with decreasing magnitude. This indicated that the specimen was moving laterally while being loaded. Further investigation revealed that the top platten rotated and forced the guides apart, causing the nett movement to be lateral and rotational. This problem was overcome by stiffening the guides and joining the pairs of guides together at the top to alleviate the problem of separation.

It was found that this occurred primarily on the lower density specimens. For example Lesotho clay, which was moulded to 100% mod. AASHTO density and OMC resulted in a dry density of 1454 kg/m3 at 27% moisture content. The specimen felt firm when pressed with the thumb and forefinger. It's Atterberg limits were PI=40, LL=65.0, PL=15.5. However when loaded between the knife edges on the ITS apparatus, the vertical strain was observed to be excessively high where the horizontal strain was normal. Closer inspection of a plot of vertical load versus horizontal strain revealed no movement for the first 30% of the failure load. This was thought to be consolidation and stress redistribution taking place.

It should be noted that clay specimens in the ITS test do not fail due to brittle fracture but rather fail plastically.

As stated earlier in the stress analysis of the knife loaded disc analysis Section 5.2 for brittle materials, compression failure of the wedge under the load plattens is highly unlikely because the horizontal and vertical stress in those areas are in compression, which enhances the failure strength in that area.

However, highly plastic materials like the Lesotho clay which were unstabilized pose the problem that the compression wedges appear to compress into the specimen considerably before the rest of the specimen begins to strain in the vertical direction. This generally appears to be the problem with lightly stabilized materials or materials moulded with no stabilization. To see if the same problem occurred, a series of tests was done on Cape Flats sand, which is a cohesionless single sized wind blown sand with shell fragments present. The specimens were moulded in a proctor sized mould and modified with a patented polymer at 2% by mass. The sand was poured into the mould and levelled. No compactive effort was applied, and therefore a high void ratio was produced. The specimens were cured in the mould for 7 days.

Similar hand tamped specimens tested at 10 days revealed a failure strength of 2600 kPa and had not failed as the maximum limit of the apparatus had been reached, where the loose specimens failed at 230 kPa.

Testing of the loosely moulded specimens at 7 days revealed that local crushing of the sample in the vicinity of the support had taken place.

Local crushing of ITS specimens illustrates that the ITS test is not the solution to all tensile testing, as the brittle theory only holds for "stiff" brittle materials and not plastic materials.

APPENDIX C

a) Standard triaxial compression specimen moulding properties

Sample Name	Lime [%]	% w Before	% w After	Moulded Density kg/m^3	Target Density % w	Failure Mode
TR33	0	10,0	17,8	1878	95% mod	Barrelling
TR34	0	11,1	18,3	1860	AASHTO	Barrelling
TR35	0	11,1	17,8	1860	1872 kg/m^3 %w=10,4	Barrelling
TR8	0	10,4	14,0	1970	100% mod	Barrelling
TR17	0	10,4	15,6	1969	AASHTO	Barrelling
TR18	0	10,4	14,7	1980	1970 kg %w=10	Barrelling
TR24	2	10,0	15,4	1995	100% mod	Barrelling
TR25	2	10,0	13,6	1991	AASHTO	and shear plane
TR26	2	10,0	14,1	1996	2000 kg	Barrelling
TR30	2	9,9	14,3	2001	%W=9,9	Barrelling
TR31	2	10,3	14,8	1991		Barrelling
TR32	2	10,0	15,4	1998		Barrelling
TR27	4	11,0	14,0	1986	100% mod	Barrelling
TR28	4	10,7	13,7	1991	AASHTO	Barrelling
TR29	4	10,7	13,5	1992	2006 kg %w=10,1	Barrelling

b) **Deviator stress vs strain representation of natural Berea Red soil**

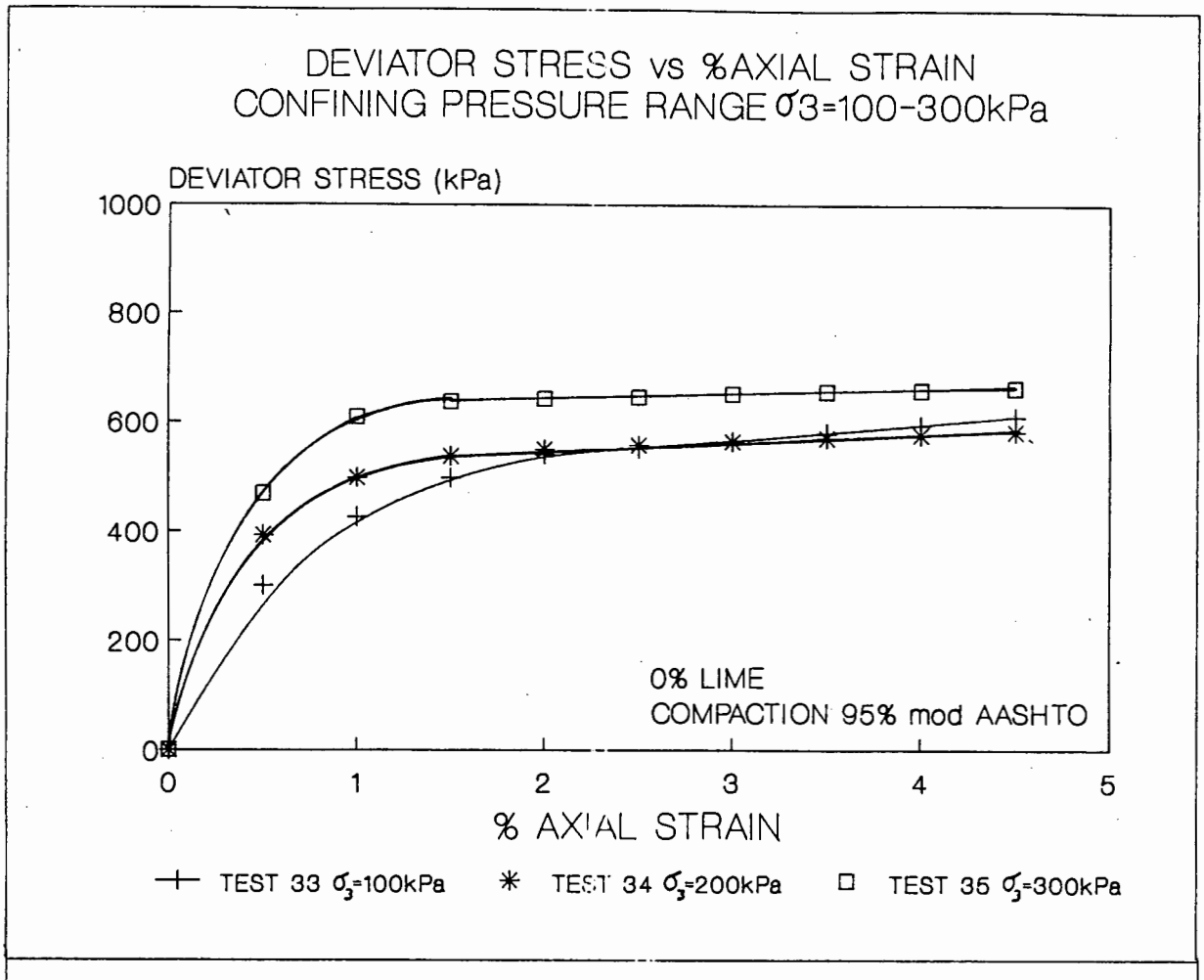

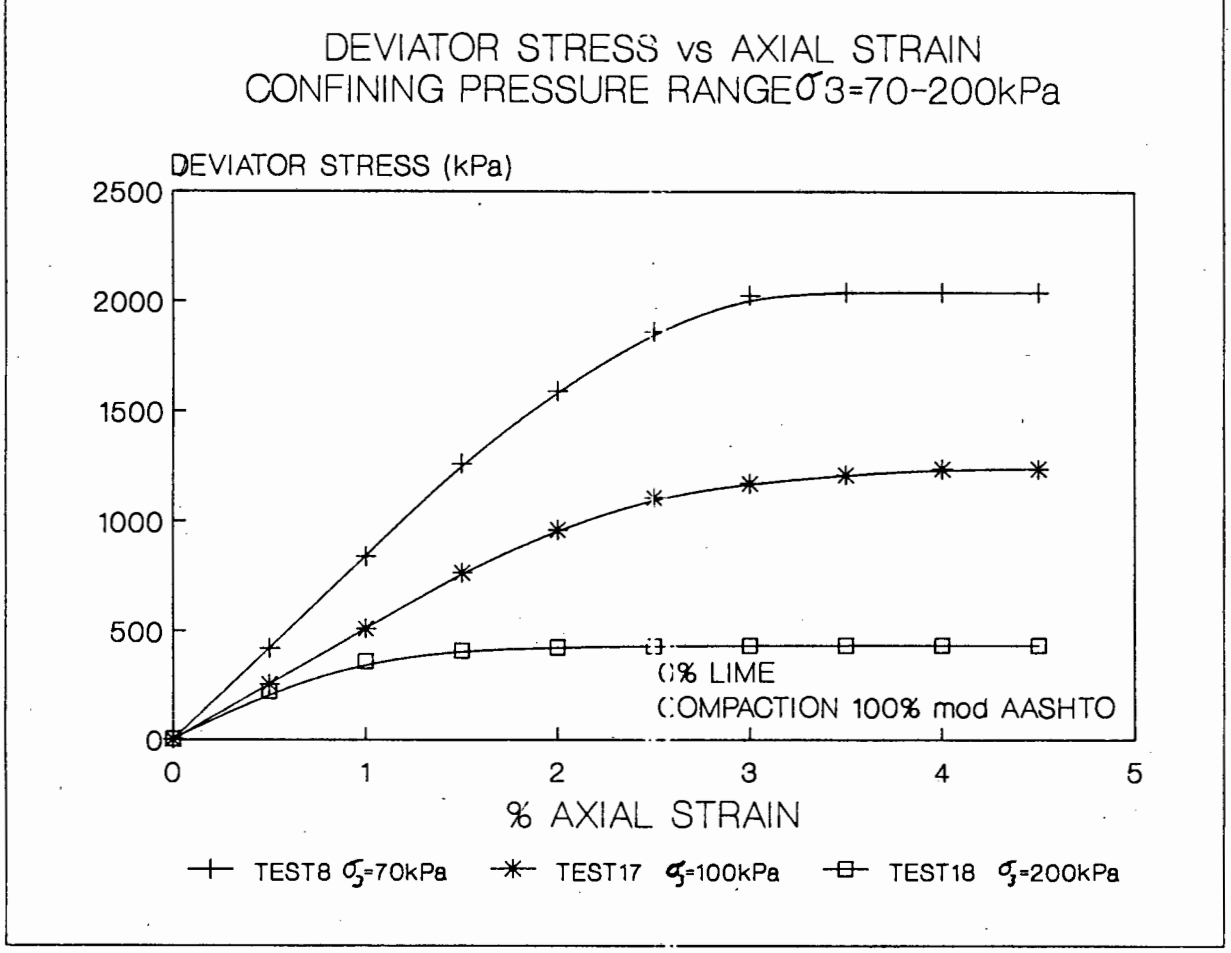

c) **Deviator stress vs strain representation of lime modified soil**

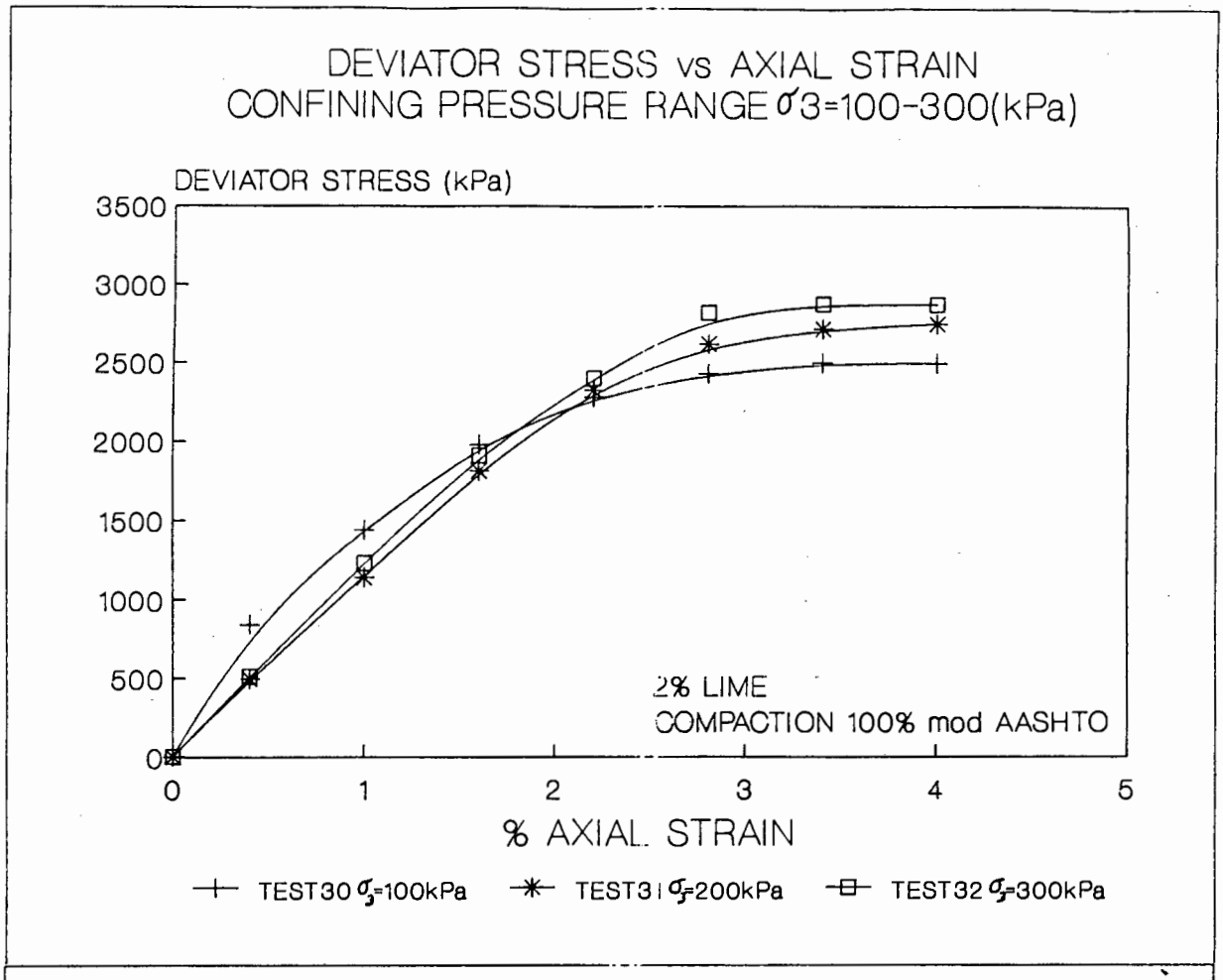

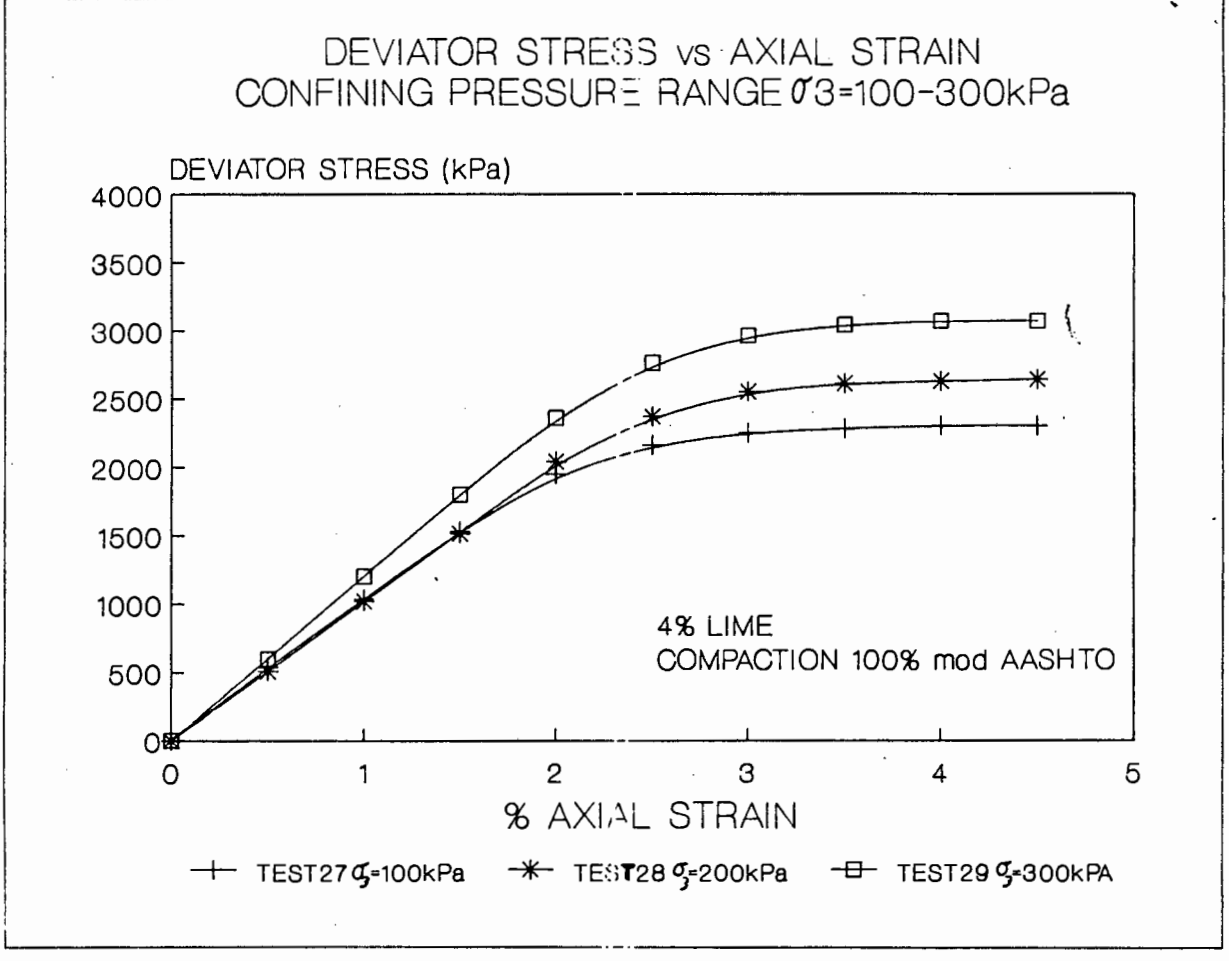

d) Young's modulus derived from standard triaxial compression tests

MATERIAL	CONFINING STRESS	YOUNG MODULUS
	$\sigma 3'$(kPa)	E(MPa)
0% Lime 95% mod AASHTO density	100 200 300	46 54 61
0% Lime 100% mod AASHTO density	70 100 200	54 52 81
2% Lime @ 28 days 100% mod AASHTO density	100 200 300	127 112 119
4% Lime @ 28 days 100% mod AASHTO density	100 200 300	100 100 117

The following information is given in the specification for the Activator by G.D.S. Instruments.

MEASURAND	CHARACTERISTIC ERROR	ENVIRONMENTAL FACTOR	RESOLUTION	
			DISPLAY	LOGGING CONTROL
Pressure	0,1% full range(1) + 0,05% measured value (2) +	0,025%/C measured value (3)	1 kPa	1 in 4096 (7)
Volume Change	0,25% measured value(4)	0,02%/(5) + 0,2% MPa (6) volume of water in cylinder	1 mm^3	1 mm^3 (8)

(1) Combined non-linerety and hysteresis of pressure transducer

(2) Certified by manufacturers of dead weight pressure tester used for calibration.

(3) Manufacturers specified thermal drift of 10,000 volt power supply to transducer.

(4) Based on accuracy of machine bore of pressure cylinder

(5) Thermal cubic expansion of water

(6) Bulk modulus of water.

(7) 12 Bit A-D converter

(8) Volume change resolution set in firmware.

Maximum rate at which stress can be applied is 60 kPa/sec.

Saturation Procedure of Berea Red soil for Effective Stress Triaxial Testing

Effective stress testing requires the specimen to be fully saturated, i.e. no air is present in the soil voids. It was envisaged to perform all the tests in an undrained condition at low effective confining stresses. The following Section discusses the difficulties encountered and the reported procedures employed to overcome the problems.

In order to calculate the undrained shear strength of soils, the determination of the change in pore water pressure has to be known. Skempton(86) produced an equation for a change in pore water pressure based on two variables and the two principal stresses in isotropic conditions.

$$\Delta u = B[\Delta\sigma_3 + A(\Delta\sigma_1 - \Delta\sigma_3)]$$

where Δu = change in pore water pressure
$\Delta\sigma_1$ $\Delta\sigma_3$ = change in the two principal stresses
A and B = Pore pressure co-efficients
For a partially saturated soil, the change in effective stress is $\sigma_1' = \Delta\sigma_1 - u_a$

If C_c is the compressibility of the soil structure, and the porosity $n=e/(1+e)$

then $V_c = -C_c\ V(\Delta\sigma_3 - \Delta u_a)$

Where V_c and V are the volume change and the original volumes of the specimen. If C_v is the compressibility of the fluid (air & water).

It follows that the change in volume of the soil space (V_v) is

$$V_v = -C_v \cdot nV \cdot \Delta ua$$

Skempton(86) proved by experimentation that the two changes in volume were equal.

Therefore $\Delta ua/\Delta\sigma 3 = 1/(1+nC_v/C_c) = B$

However, if a soil is fully saturated there will be no free air present.

Then: $C_v/C_c=0$ as water is incompressible, in comparison to the soil structure.

It becomes clear that a fully saturated soil has a B value of one and a completely dry specimen having no pore water pressure, will have a B value equal to zero as the ratio of Cv/Cc approaches infinity.

Hence $B = \Delta u/\Delta\sigma 3$

Skempton(86) noted that materials moulded under Proctor compaction at optimum moisture content revealed B values from 0,1 to 0,5. This has been verified, as the B value of Berea Red soil, compacted at OMC under modified AASHTO compaction energy is 0,4. In order to achieve a 100% saturation or a B parameter equal to one, it is essential

to establish the increases needed to either the cell or back pressure or both to achieve full saturation. An explanation of the solubility of air in water in a soil specimen is discussed in the following section.

Disolution of air in the pore water of a soil specimen by the application of back pressure

The introduction of additional air free water under pressure into the voids of a partially saturated soil specimen which is commonly known as backpressure increases the degree of saturation after equilibrium has been reached within the specimen. Back pressure is best defined as an external water pressure applied to the specimen, but should never exceed the cell pressure which is confining the specimen. Pressure increases cause some of the air to be absorbed into solution, and the theoretical additional of back pressure U_b required to increase the degree of saturation from an initial saturation S_o to a final value S is given by Lowe & Johnson(82) by the equation

$$\Delta U_b = [P_o]\,[(S-S_o)(1-H)]/[1-S(1-H)] \quad \text{in kPa}$$

Where P_o is the initial absolute pressure, usually atmospheric i.e., 101,325kPa. H is the Henry coefficient, approximately 0,02 cm^3 of air per cm^3 of water at 20°c. If a final saturation of S=1 is envisaged, then the required pressure is

$$U_b = 4965(1-S_o) \quad \text{in kPa}$$

This relationship can be plotted as back pressure vs initial saturation and is illustrated in Fig.C1. If it is undesirable to increase the water content of the specimen, then the application of additional confining pressure may be applied.

Bishop and Henkel(69) proposed the following equation for determining the cell pressure increase to achieve a theoretical increase in air pressure (Ua) to reach full saturation.

$$\Delta Ua=[Po] \cdot (1-So)/(So \cdot H) \text{ in kPa}$$

where the variables are the same as those previously mentioned.

Again, $Sr=1$ the required pressure

$$\Delta Ua=5066\ (1-So)/So \text{ in kPa}$$

This relationship is also plotted on Fig. C1 as curve b.

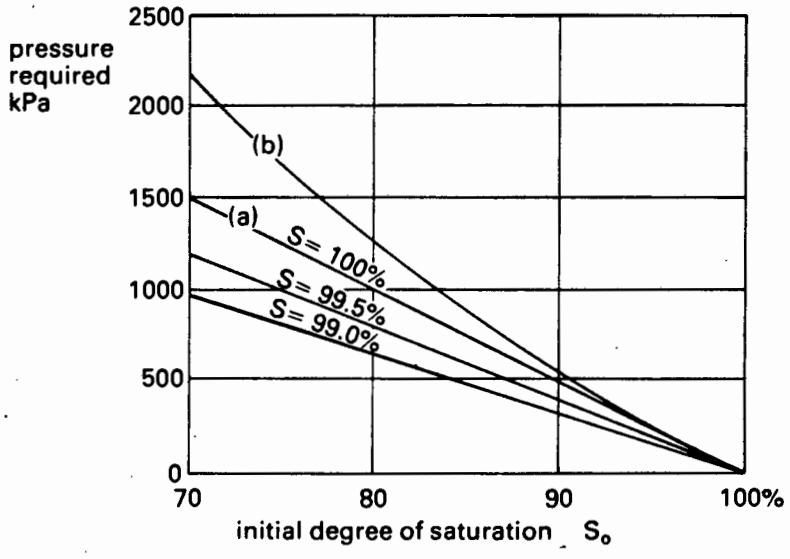

Fig.C1 Pressure required for saturation of soil that is initially partially saturated (Head(67))

The curve (a) illustrates the back pressure required to obtain the desired saturation of a soil which is partly saturated and curve (b) shows the increase in confining pressure required to reach full saturation. It is evident that an increase of air pressure alone, without the introduction of additional water requires appreciably higher pressures to give full saturation if $So > 95\%$.

When a partly saturated specimen is subjected to an increase in confining pressure only, the increase in pore air pressure will be less than the confining pressure increment. Head(67) notes that this saturation procedure is only practicable for soft uncemented soils.

Saturation Procedures Investigated and Applied to Berea Red soil

The reluctance of Berea Red soil to saturate while moulded at 100% mod AASHTO, presented difficulties because of the time period required to achieve full saturation.

The grading curve of the Berea Red soil revealed that 89% was sand, 4% silt, and 7% was clay (by mass). It would have been expected that a material with this grading would saturate with ease. This material did not saturate with such ease for apparently the following reasons:

a) The void ratio of the material (e=0.38) was quite low. With a sandy material with such a high percentage of sand, it would be reasonable to expect a higher void ratio. On closer inspection of the soil, it appears that any voids created by the sand are well packed by the finer material forming a dense homogeneous material, when compacted to 100% mod AASHTO density. Having such a low void ratio, implied the permeability was low, hence not allowing any trapped air to escape.

b) The initial saturation at moulding was not particularly high (S_r=0.77) so trapped air had to be removed or dissolved.

The following Section discusses the saturation procedures investigated and the results obtained on Berea Red soil.

Procedure 1: Percolation of deaired water through the specimen to dissolve and remove the free air

Knowing that the specimen had a high sand content, it was thought that by applying a low back pressure via the pedestal into the specimen and opening the top drain to atmospheric pressure while the specimen was supported by a low confining pressure saturation may have been obtained.

It was reasoned that the deaired water that entered the specimen would readily absorb the free air as it passed through the specimen. However, a small text from Bishop & Henkel(69) revealed that " even if deaired water was passed through a partly saturated specimen under a small hydraulic gradient for a month or more, full saturation would not be achieved..."

Procedure 2: Application of back pressure

Application of back pressure has a number of advantages and is summarized below:

a) All the air in the void spaces within the specimen is forced into solution under the applied pressure when full saturation is reached.

b) Any air entrapped between the membrane and within the pore or back pressure systems and the specimen pores is also dissolved.

c) In a specimen which dilates during shear, water can be freely sucked in during a drained test without the movement being impeded by an air lock due to air bubbles.

d) For a similar specimen in an undrained test, initial application of a high enough back pressure can prevent the pore pressure falling below atmospheric pressure which could cause cavitation as it tries to dilate.

Procedure 3: Applying high back pressure (500kPa)

Although the application of back pressure has been theoretically verified, experience is still required to determine the rate of back pressure application, time required between increments, and an acceptable B value. A B value of 0,95 chosen based on observations made by Head(67) which are discussed in the following paragraph.

Instead of using the traditional arbitrary B value of about 0,97 as a criterion for saturation in all instances, it was more realistic to relate the required B value to the properties of the soil. The most important factor is whether the degree of saturation of less than 100% would have a significant effect on the pore water response or whether 99% saturation could affect the specimen behaviour. For example a soft specimen at 98% saturation has a B value of 0,97 where as a very stiff specimen at 100% saturation produces a B value equal to 0,90 (Head(67)).

On the same topic, Head(67) states that 100% saturation is near impossible to achieve on certain soils as the pore pressure response due to an increment in cell pressure is shielded by the materials stiffness. Black & Lee(70) illustrates the B values to expect on soils with varying stiffnesses (illustrated below).

VALUES OF B FOR TYPICAL SOILS AT AND NEAR FULL SATURATION

SOIL CATEGORY	DEGREE OF SATURATION (S_r%)		
	100%	99,5%	99,0%
Soft	0,9998	0,992	0,986
Medium	0,9988	0,963	0,93
Stiff	0,9877	0,69	0,51
Very Stiff	0,913	0,20	0,10

After Black & Lee(70)

The incremented back and cell pressures were applied with the G.D.S. activators by instructing them to target to predetermined maximum pressures.

The increments of pressure were made in steps of 90 sec/ kPa with a 20kPa difference between the cell pressure and back pressure, the latter being the higher pressure. Saturation was achieved after 5 days with a cell pressure of 550kPa (B=0,95). After consolidation had been completed to achieve the initial $\sigma 3'$, the specimens were sheared at a strain rate of 1mm/hour i.e., (1%/hour on a 100mm specimen based on the standard time to failure described by Head(67) and Bishop & Henkel(69)).

It was found that the pore water pressure would increase by approximately 3% up to an axial strain of about 0,6%, thereafter a sharp increase of 20% of the original pore water pressure would occur, reaching a peak at 1,1% axial strain, then it would drop off to a zero or slightly negative pressure. The ramifications of this were that the confining stress $\sigma 3'$ started at a desired pressure and increased steadily to a very high value.

Variation in effective confining stress during standard triaxial testing of Berea Red soil

	INITIAL STRESS (BEFORE LOADING) (kPa)	FINAL STRESS (AT FAILURE) (kPa)
Cell Pressure σ_3	550	550
Back Pressure U_b	350	0
$\sigma_3' = \sigma_3 - U_b$	200	550

During the evaluation of stresses within a pavement, it was clear that the range of σ_3' using high back pressures would be contravened as the pore pressure decreased. The requirements of the testing programme required saturated specimens to be tested at low confining pressures. This behaviour is attributed to the dilatant properties of the Berea Red soil compacted to high densities. It was clear that the application of high back pressure was not the solution to achieving satisfactory saturation.

Procedure 4: Application of low back pressure (200kPa)

Black & Lee(70) did a study on the time effects of air being dissolved into solution in water in small bore pipes and found that air dissolves into water at the same rate within the pressure range 140-560kPa. Based on the above, attempts were made to saturate the specimens at low back pressures which revealed a B parameter increase from 0,4 to 0,5 after a week which was considered unsatisfactory.

Procedure 5: Saturating sand by vacuum methods and low back pressures

Having found that high and low back pressures (procedures 4 & 5) were unsatisfactory for saturation, a compromise procedure was investigated which required the use of an initial vacuum, followed by the application of low back pressures.

Rad & Clough(71) performed research on the liquifaction effects on sands and found that undesirably high back pressures had to be used to saturate the specimens using conventional methods. Rad & clough(71), Bishop and Henkel(69) and Head(67) have proposed a procedure that was considered but could not be applied.

The method involved moulding the specimen in carbon dioxide so the gas that was trapped in the soil voids would be readily dissolved when the pore water pressure was applied. The above references have all heeded warning that unwanted chemical reactions between the carbon dioxide and lime cause carbonation in lime stablized specimens which would be the case with stabilized Berea Red soil.

Rad & Clough(71) and Domaschuk et al(72) proposed methods whereby a combination of a vacuum and a low back pressure could be applied to a specimen in order to achieve full saturation. They suggest that the vacuum should only be applied for +-5 minutes. They indicated that the process was very successful with cemented materials which normally create vast problems with saturation as experienced with stabilized Berea Red soil.

Rad & Clough(71) methods were modified and applied to Berea Red soil. The customized procedure is discussed below.

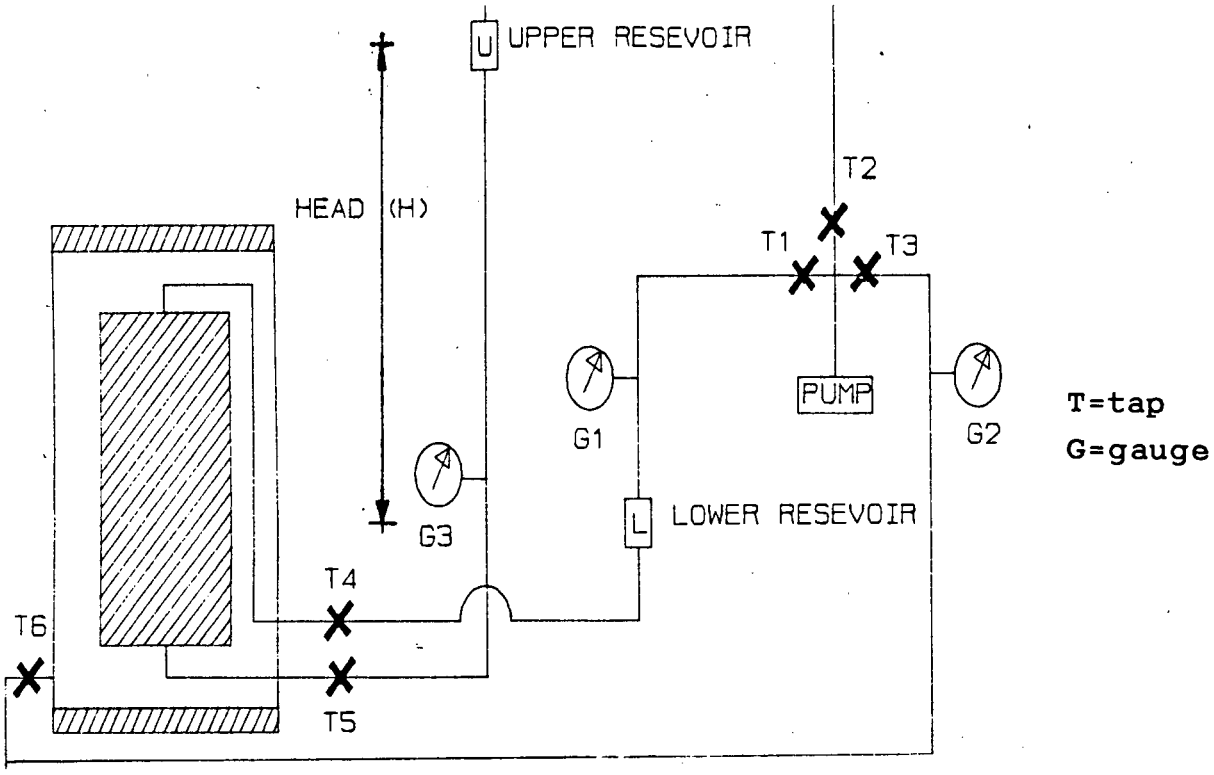

Fig.C3 Schematic Diagram of the vacuum saturation technique employed on Berea Red soil.

The following vacuum saturation test procedure was employed.

1) Place the specimen in the triaxial cell. Fill the cell with water.

2) Fill the upper reservoir(U) with deaired water, while keeping the lower reservoir empty(L).

3) Open valves T4 and T1 and apply an incremental vacuum of 20kPa. Valves T5 and T2 should be closed.

4) Apply an increment of vacuum of 10kPa to the inside of the cell.

The effective confining stress is now equal to the cell minus the back pressure i.e. [(-10)-(-20)=10kPa] were the negative value indicates a vacuum. Therefore, a negative back pressure is set up.

5) Increase the vacuum inside and outside the specimen at the same desired effective stress.

Due to the nature of the Berea Red grain structure the vacuum period was best applied for a minimum of six hours, especially in the case of the unstabilized soil. A good indication of sufficient time spent on applying the vacuum was when the lower pressure gauge (G3) read 10% less than the upper gauge (G1).

6) The opening of T2 and T5 and elevating the upper reservoir (U) H metres above the sample, resulted in a vacuum gradient of 9,81*H kPa across the sample.

7) It was found that percolation of the deaired water for +-4 hours was sufficient on the Berea Red soil.

8) After completion of the vacuuming the cell pressure and back pressure had to be ramped down. This was done in exactly the same way as the ramping up the vacuum. During ramping down a stage was reached when the pore pressure was still negative. Thereafter for every decrease in pore pressure vacuum there should be an equuivalent increase in positive cell pressure, thus maintaining the hydrostatic state of stress.As soon as the pore pressure was zero, normal back pressure procedures should be applied.

Application of low back pressures and a vacume, facilitated the full saturation to be achieved. The application of the back pressure and cell pressures was done simultaneously over a period of 24 hours to achieve the required positive pressures.

Conclusion to saturation techniques

The use of high cell and back pressures is the most convenient and easiest procedure to saturate soil specimens but some difficulties do arise when the specimen is tested as in the case of Berea Red soil which readily dilates when sheared.

It was found that the use of vacuuming techniques along with low back pressures, satisfied the needs of this testing programme.

APPENDIX D

Testing constraints of cyclic triaxial tests on natural and stabilized Berea Red soil

Additive	%	Test Description	No of cycles	Min. l cycle	Curing (days)	Test Duration (days)
Lime	0	drained sat	2260	2,5	-	4,0
	0	undrained sat	2500	2,0	-	3,5
	0	undrained part. sat	2858	2,5	-	5,0
	2	undrained sat	5241	2,0	28	7,5
	2	undrained part. sat	2814	2,5	28	7,5
	2	drained sat	7854	1,0	*Rc	5,5
	2	undrained sat	41475	1,0	120	30,0
	4	undrained sat	4929	2,0	28	7,0
	4	undrained part. sat	2716	2,5	28	5,0
	4	drained sat	7759	1,0	*Rc	5,5
Cement	2	undrained sat	4189	1,1	28	3,5
	4	undrained sat	4203	1,1	28	3,5

*Rc rapid cured (45 hrs at 60°C)

All specimens moulded at 100% AASHTO density at OMC

Cyclic deviator stress 25-465kPa with a 100kPa confining stress

APPENDIX E

Recommendations on methods of enhancing the cyclic speed of the G.D.S. triaxial apparatus.

The G.D.S. triaxial apparatus was not capable of applying a cyclic deviator stress greater than 1 cycle/2 minutes. The following section discusses methods which could be implemented to improve the equipment's cyclic speed capability.

As water is a compressible material (bulk modulus 0,2MPa/%) it is obvious that to reach a target pressure, a volume change is required.

It was found that less than 2 seconds was needed to alter the volume in the pump to achieve the same pressure change as described above.

The activator can ramp a volume faster, because the control algorithms are built into the programmable memory to cause the motor to step to a target volume change by only counting the number of steps in the stepper motor. While ramping, the pressure has to be checked by means of an integral solid state pressure transducer and then corrected so that the activator does not hunt.

As the software was coded, the fastest speed at which cyclic testing could occur depended on the following factors:

i) The inherent maximum volume change characteristics speed at which the controller could operate.

ii) The speed of data transfer through the interface bus.

iii) The processing time within the computer which is a function of the subroutines systematic order

iv) The analogue to digital conversion rate (50 times/second)

v) The stiffness of the soil specimen for the case of cyclic loading (as compared cyclic deformation)

vi) Amplitude of the load pattern.

Generally if amplitude is increased, so is minimum period, and if amplitude is decreased so is minimum period. In the case of stress controlled cyclic loading of soft soils where load amplitudes will require larger deformations, minimum required periods will increase. For cyclic loading of stiff soils where load amplitudes will require smaller deformations, minimum required periods will decrease.

Using standard HP BASIC it is possible to update target pressures or volume changes and to log data once a second. To define a complex wave form like a sinusoid may require more than 60 co-ordinate points and therefore a minimum period of 60 seconds would be required.

With the new firm-ware version of the controller installed, the processing time of the computer is the limiting factor. One reason for the above is due to the manner in which the software was written.

Proposals which have been made include:

1. Removing the standard Bishop Wesley Cell with the fixed top reaction rod and replacing it with the standard large diameter triaxial cell with the standard sliding reaction rod and applying a cyclic load from above by using a pneumatic, hydraulic or mechanical method. Using an air space at the top of the cell to absorb the shock in the cell pressure due to the increased volume of the cycling reaction rod.

2. Rewriting the software for the G.D.S and simplifying the loading wave shape.

   An example of the above would be to perform the first 20 cycles under pressure control, during which volume changes were monitored to achieve the required pressure envelope, thereafter using volume control to apply the first 80% of the upward ramp and then seeking the final stresses in pressure control. The ramping down to the lower value could also be done in volume control with pressure control seeking the lower value over the last 20% of the unloading cycle.

3. As resilient modulus is determined from the maximum and minimum deviator stress, accurate results would still be achieved. However, the loading shape would not be very well defined, but higher cyclic speeds would be achieved and rest periods could also be allowed for.

4. The activator could be computer instructed using four programming lines to cause it to cycle the axial pressure in a triangular shape in a stand alone mode. Thereafter the controller would need no additional computer control, allowing the computer all its processing time for data acquisition. This control method was adopted for the cyclic I.T S apparatus.

An example of the four programming lines follows:

```
10 SEND 7;UNT UNL MTA LISTEN A1 DATA CHR$ (1) & VAL 4 (SL)
& CHR $ (255)
20 SEND 7;UNT UNL MTS LISTEN A1 DATA CHR$ (3) & VAL 4 (LL)
& CHR $ (255)
30 SEND 7;UNT UNL MTA LISTEN A1 DATA CHR$ (5) & VAL 4 (UL)
& CHR $ (255)
40 SEND 7;UNT UNL MTA LISTEN A1 DATA CHR$ (31)& CHR$ (255)
```

KEY: (1) Slope Code (SL) Slope Variable (Millisecond/kPa)
(3) Lower Limit Code (LL) Lower Limit Variable (kPa)
(5) Upper Limit Code (UL) Upper Limit Variable (kPa)
(31) Cycle Code
(255) End message.

A deviator stress had to be cycled from 25 to 465 and back

to 25kPa on 100 x 50 4% lime stabilized Berea Red sample with a cell pressure of 550 kPa and a back pressure of 450kPa. That implied that the lower chamber had to be cycled from 552,4kPa - 596,9kPa. A pressure range of 44.4kPa. The diameter of the lower chamber was 160mm.

The only variable which had to be changed was (SL) Milliseconds/kPa

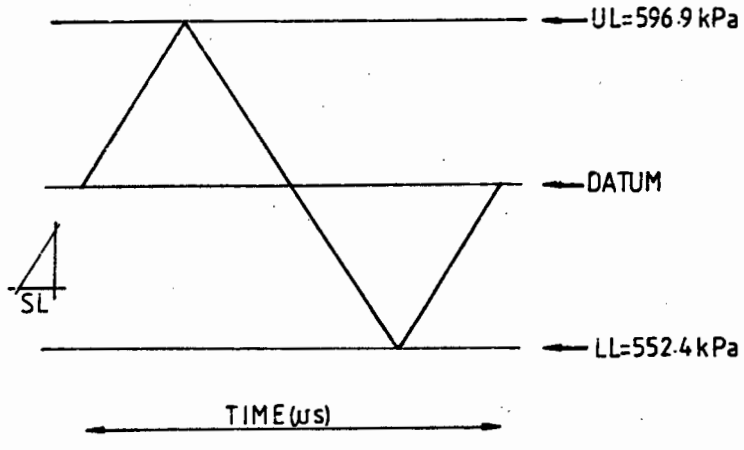

Schematic diagram of digital controller vs time

The steepest slope which produced meaningful upper and lower limits was 200 S/kPa which implied a cycle speed of 200 x 44.4 = 8,9 seconds which is 0,113hz. This frequency is considered reasonable by Silver and Seed (39), Pumphery (24) and others (19).